The effect of Medial Septum Stimulation on Hippocampal Electrophysiology and Behaviour of Freely Moving Rats

A Thesis Submitted to the University of Dublin for the Degree of

Doctor of Philosophy

by

Matheus Cafalchio de Oliveira

2020

Under the Supervision of
Professor Shane O'Mara and
co-supervision of Professor Marian Tsanov
School of Psychology, Institute of Neuroscience
Trinity College Dublin
Ireland

Declaration

I declare that this thesis has not been submitted as an exercise for a degree at this or any other university and it is entirely my own work.

_____

Matheus Cafalchio de Oliveira

Summary

This study focuses on the interaction between the medial septum and hippocampus in freely moving animals. To investigate this circuit, we used electrophysiological techniques combined with behavioural tasks.

The medial septum exerts a modulatory effect on the entire hippocampal and parahippocampal formation. However, the role of the medial septum in spatial processing is still poorly understood. Here, we explore the septohippocampal circuit, focusing on electrophysiology, spatial processing and behaviour.

Our results suggest that nonselective optogenetic stimulation of the medial septum induces inhibition of intra-septal neurons and consequently, disinhibition of hippocampal CA1 interneurons. We also demonstrated that firing rate of medial septal neurons is inversely proportional to the animal's speed.

Transgenic models were used to investigate the contribution of septal GABAergic and cholinergic neurons in reward-related behaviour. We showed for the first time that the firing of medial septal GABAergic neurons can mediate place preference behaviour.

To investigate if medial septum neurons can modulate hippocampal spatial processing, we recorded CA1 place cells during septal stimulation. We showed that medial septum stimulation induces place field remapping. We also showed that the medial septum stimulation restricted to a region of the arena was able to induced place preference and shifted the place field assembly towards this region.

Permission

I agree to deposit this thesis in the University's open access institutional repository or allow the library to do so on my behalf, subject to Irish Copyright Legislation and Trinity College Library conditions of use and acknowledgement.

_____

Matheus Cafalchio de Oliveira

Acknowledgements

First and foremost, I would like to express my sincerest gratitude to my supervisor, Professor Shane O'Mara and my co-supervisor Dr. Marian Tsanov, whose expert knowledge guided me from the initial to the final stages of this thesis. I want to express my gratitude to my fellow lab and office mate Dr. Omar Mamad for his invaluable assistance with all my work. I also would like to thank Dr. Christopher Dillingham for his support during my hard times and all good ideas and discussions which were essential to complete this work.

I also owe a very important thank you to my friend Dr. Bibiana Mota for many de-stressing lunch chats. For all the students that I had the pleasure to meet during these years, in special to Caoimhe Tyndall and Cristina Gil for the immense help and friendship. To my friends Flávia e Eoghan to have the patience to read my thesis, and to Prof Dr. Marina Lynch for the trust and guidance during my first year. I would like to thank my two friends and colleagues Ham Gao Xiang and Sean Martin for reading and correcting my English mistakes. A special thanks to my mother Elza Cafalchio and my father João de Oliveira who believed and supported me during my all my studies. Also, to my beloved brother Glaucio and my beloved sister Luiza. Lastly and importantly, I want to express my profound thanks to the person who assisted me to keep my mental health during my Ph.D. and helped me in everything I needed, my beloved wife, Petrya do Nascimento Brito, love you.

My studies were financed via the Brazilian Federal Agency for Support and Evaluation of Graduate Education - CAPES.

Table of Contents

Declaration ..... *II*
Summary ..... *III*
Permission ..... *IV*
Acknowledgements ..... *V*
List of Figures ..... *IX*
List of Tables ..... *XI*
List of Abbreviations ..... *XII*
1. Introduction *1*
1.1. Memory **1**
1.1.1. Types of Memory 1
1.1.2. Hippocampus as a place for memory 3
1.1.3. Place cells in the hippocampus 4
1.1.4. Memory formation 6
1.2. The hippocampus **9**
1.2.1. Hippocampus anatomy 9
1.2.2. The entorhinal cortex 10
1.2.3. The tri-synaptic circuit 10
1.2.4. Neuronal subtypes 13
1.3. Spatial processing in the hippocampus **14**
1.3.3. Place cells and reward 18
1.1. Hippocampal theta oscillation 22
1.1.2. Origins of hippocampal theta 26
1.4. The septohippocampal system **27**
1.4.1. The Lateral septum 29
1.4.2. Medial septum 31
1.4.3. Septal projections to the hippocampus 33
1.4.4. Septal stimulation 37
1.5. Objectives 38
2. Chapter General Methods *40*
2.1. Housing conditions **41**
2.1.1. Electrodes and Microdrives 42
2.1.2. Electrodes implantation and viral injection 42
2.1.3. Stereotaxic coordinates 44
2.1.4. Virus construction 45
2.1.5. Laser stimulation 45
2.2. Experimental apparatus **46**
2.2.1. Open field 46
2.2.2. Rectangular linear track 48
2.3. Data acquisition **49**
2.3.1. Spike recording 49
2.3.2. Position tracker 50
2.3.3. Referencing 50
2.4. Data analysis **50**
2.4.1. Spike sorting 50
2.4.2. Data exclusion criteria 53
2.4.3. Spike properties 53
2.4.4. Place fields definition 54
2.4.5. Units classification 54
2.4.6. Autocorrelation histograms 55
2.4.7. Theta index 55
2.4.8. Spatial Information 56

2.4.9. Bursting units 56
2.4.10. Grand Rate 57
2.4.11. Phase-Locking Value 57
2.4.12. Passes score 58
2.4.13. Firing rate analysis 58
2.4.14. Field size analysis 59
2.4.15. Running speed and spike frequency correlation 59
2.4.16. Real-time place preference 59
2.4.17. Classification of Photo-Responsive Cells 60
2.4.18. Centre of mass 61
2.4.19. Symmetric COM distance 62
2.4.20. COM angle 64
2.4.21. Spatial Population Vector 64
2.5. Post-mortem verification 65
2.5.1. Transcardial perfusion and tissue fixation 65
2.5.2. Tissue preparation 66
2.5.3. Verification of the virus expression and electrodes position 66
2.6. Statistical analysis 67
3. Chapter The Effect of Nonselective Optogenetic Stimulation of The Medial Septum on Hippocampus Interneurons 68
3.1. Introduction 69
3.2. Methods 72
3.2.1. Animals 72
3.2.2. Surgery 73
3.2.3. Protocol 73
3.2.4. Data analysis 74
3.2.5. Unit classification 74
3.2.6. Post-mortem verification 76
3.2.7. Statistical analysis 76
3.3. Results 77
3.3.1. Theta modulated medial septal units 77
3.3.2. Medial septum unit classification 78
3.3.3. MS units with firing correlated with running speed 85
3.3.4. Nonselective optogenetic stimulation of the MS 88
3.3.5. Classification of hippocampal CA1 interneurons 90
3.3.6. CA1 interneurons with firing frequency correlated with speed 93
3.3.7. The effect of nonselective MS optogenetic stimulation on CA1 interneurons 96
3.3.8. Medial septal stimulation induced strong theta activity on hippocampal LFP 97
3.4. Discussion 100
Chapter 4 Optogenetic Stimulation of the Medial Septum Induce Real-Time Place Preference 107
4.1. Introduction 108
4.2. Methods 111
4.2.1. Animals 111
4.2.2. Stereotaxic surgeries and viral injections 112
4.2.3. Viral constructions 113
4.2.4. Phase-Locking Value 113
4.2.5. Open field 114
4.2.6. Real-time place preference 114
4.2.7. Passes score 116
4.2.8. Spike sorting 117
4.2.9. Post-mortem verification 117
4.2.10. Statistical analysis 118
4.3. Results 119
4.3.1. Viral expression in the MS of non-transgenic rats 119

4.3.2. Initial place preference test 120
4.3.3. Stimulation of non-specific MS neurons induce real-time place preference 122
4.3.4. Viral expression of Cre-dependent virus on Gad1-Cre rats 124
4.3.5. Initial place preference test for Gad1 rats 125
4.3.6. Stimulation of GABAergic neurons induced real-time place preference 127
4.3.7. Stimulation of MS GABAergic fibres in the lateral hypothalamus 129
4.3.8. No place preference was observed during stimulation of MS cholinergic neurons 130
4.3.9. Phase-locking value comparison 132
4.4. Discussion 135
4.4.1. Real-time place preference pathways 135
4.4.2. Real-time place preference pathways 136
4.4.3. Glutamatergic neurons 137
4.4.4. GABAergic neurons 138
4.4.5. MS cholinergic neurons 140
5. Chapter Manipulating Hippocampal Spatial Representation by nonselective Optogenetic Stimulation of The Medial Septum in Freely Moving Rats 142
5.1. Introduction 143
5.2. Methods 146
5.2.1. Animals 146
5.3. Data analysis 148
5.3.1. Place fields properties 148
5.3.2. Spatial population vector 149
5.3.3. Statistical analysis 150
5.4. Results 151
5.4.1. Effect of the MS stimulation on the hippocampal place cells 151
5.4.2. Medial septum stimulation does not affect place fields properties 155
5.4.3. Medial septum stimulation induces place field remapping 157
5.4.4. Firing rate analysis 159
5.4.5. MS stimulation did not affect place field properties during recordings on the linear squared maze 160
5.4.6. MS stimulation induce changing on the place fields assembly 163
5.5. Discussion 167
5.5.1. Nonselective MS stimulation can induce both inhibition and disinhibition of CA1 pyramidal neurons 167
5.5.2. Analysis of place field properties in the open field 169
5.5.3. MS stimulation induced place fields remapping 170
5.5.4. Analysis of place fields properties in the linear squared maze 171
5.5.5. Hippocampal place fields assembly encode reward 172
Chapter 6 General Discussion and Conclusion 174
6.1. Introduction 175
6.2. Stimulation of MS neurons and its effect on hippocampal interneurons 175
6.3. Stimulation of the medial septum induced place preference 177
6.4. Medial septum modulates hippocampal place cells 179
6.5. Future directions 180
6.6. Conclusion 182
7. Bibliography 183

List of Figures

Figure 1. Types of Memory. 3
Figure 2. Tolman mazes. 5
Figure 3. Basic anatomy of the hippocampus. 12
Figure 4. Hippocampal place cell. 16
Figure 5. Spatially sensitive neurons. 22
Figure 6. Theta precession of CA1 place cells. 25
Figure 7. Pellet chasing task. 47
Figure 8. Rectangular-shaped linear track. 48
Figure 9 Single cell isolation 52
Figure 10. Track of the electrodes. 78
Figure 11. Electrophysiological differences between groups 81
Figure 12. Theta Burst unit ISI histogram and autocorrelogram. 82
Figure 13. Theta Non-Burst unit ISI histogram and autocorrelogram. 83
Figure 14. Regular spiking unit ISI histogram and autocorrelogram. 84
Figure 15. Theta burst unit with firing rate negatively correlated with speed. 85
Figure 16. Theta non-burst unit with firing rate positively correlated with speed. 86
Figure 17. Regular spiking unit with firing rate negatively correlated with speed. 87
Figure 18. Effect of the light stimulation. 89
Figure 19. Electrophysiological differences between groups. 92
Figure 20. Theta burst showing firing positively correlate with speed. 93
Figure 21. Theta non-burst unit showing firing positively correlate with speed. 94
Figure 22. Regular unit showing firing positively correlate with speed. (A) ISI of a theta non-bursting interneuron with a mean frequency of 1.01 Hz. (B) A spike waveform average from the same unit, showing a width of 172.23 ± 29.25 μs. (C) The autocorrelogram without theta modulation, the theta index for this unit was 0.13. (D) Autocorrelation (±10) used to verify the unit isolation. (E) Firing rate positively correlated with speed (Pearson r = 0.80). 95
Figure 23. Evoked theta power before and after stimulus. To confirm that MS stimulation affects the CA1 LFP, we calculated the difference of the evoked power between 4-12Hz (theta band). A paired t-test showed that the evoked power was significative higher after the laser stimulation $p < 0.001$). 97
Figure 24. Power spectrogram of CA1 LFP. Example of two color-coded power spectrograms of hippocampal 4-20Hz oscillations before and after MS stimulation. The blue arrow indicates the time of the stimulus. The black arrows indicate the peak of the power around 8 Hz. 98
Figure 25. Theta bursting units affected by MS stimulation. 99
Figure 26 Schematic of the linear square arena. 116
Figure 27. Viral expression in MS. 120
Figure 28. Rats had no place preference during baseline recordings. 121
Figure 29. Effect of non-specific MS stimulation on real-time place preference. 123
Figure 30. Non-specific MS stimulation induce place preference. 124
Figure 31. Viral expression in Gad1-Cre transgenic rats 125
Figure 32. Transgenic GAD1 rats had no place preference during baseline recordings. 126
Figure 33. Effect of GABAergic MS stimulation on real-time place preference. 127
Figure 34. GABAergic stimulation induces place preference. 128
Figure 35. Stimulation of GABAergic fibres to LH. 130
Figure 36. Stimulation of MS cholinergic neurons. 132
Figure 37. The phase-locking value between groups. 134
Figure 38. Inhibited place cells. 152
Figure 39. MS stimulation affect place cells firing. 153
Figure 40. Firing rate index before and after MS stimulation. 154
Figure 41. Disinhibited units' spatial information and field size. 156
Figure 42. Inhibited units' spatial information and field size. 157
Figure 43. MS stimulation degrades the stability of the place fields. 158

FIGURE 44. GRAND RATE INDEX BETWEEN GROUPS. 160
FIGURE 45. PLACE FIELD SIZE COMPARISON BETWEEN BASELINE AND MS STIMULATION. 161
FIGURE 46. MEAN FIRING RATE BETWEEN BASELINE AND MS STIMULATION. 162
FIGURE 47. PEAK FIRING RATE BETWEEN BASELINE AND STIMULATION. 163
FIGURE 48. MS STIMULATION INDUCED A CHANGE IN THE PLACE FIELD ASSEMBLY MEASURED BY WEIGHTED COM ANGLE. 165
FIGURE 49. MS STIMULATION INDUCED A CHANGE IN THE PLACE FIELD ASSEMBLY DISTRIBUTION MEASURED BY THE AVERAGED COM ANGLE 166

List of Tables

TABLE 1 NUMBER OF ANIMALS USED FOR EACH EXPERIMENT/CHAPTER 44
TABLE 2: STEREOTAXIC COORDINATES 45
TABLE 3 VIRAL CONSTRUCTION 45
TABLE 4. ELECTROPHYSIOLOGICAL CHARACTERIZATION OF THE MEDIAL SEPTUM IN FREELY BEHAVING RATS 79
TABLE 5. MS UNITS WHICH HAD FIRING RATE CORRELATE WITH SPEED 88
TABLE 6. EFFECT OF NON-SELECTIVE OPTOGENETIC STIMULATION OF MS UNITS 88
TABLE 7. CHARACTERIZATION OF THE CA1 INTERNEURONS AFFECTED BY MS STIMULATION 90
TABLE 8. CA1 INTERNEURONS WHICH HAD FIRING RATE CORRELATE WITH SPEED 96
TABLE 9. EFFECT OF NONSELECTIVE OPTOGENETIC STIMULATION OF MS ON CA1 INTERNEURONS 96

List of Abbreviations

ACh	**acetylcholine**
AChE	**acetylcholinesterase**
AD	**Alzheimer's disease**
ANOVA	**analysis of variance**
CA1	**field CA1 of the hippocampus**
CA3	**field CA3 of the hippocampus**
ChAT	**choline acetyltransferase**
ChR2	**channelrhodopsin 2**
DB	**diagonal band of Broca**
DG	**dentate gyrus**
EEG	**electroencephalogram**
EPSP	**excitatory postsynaptic potential**
FFT	**fast Fourier Transform**
g	**gram**
GABA	**gamma aminobutyric acid**
GAD	**glutamic acid decarboxylase**
Hz	**hertz**
ICSS	**intracranial self-stimulation**

LFP	**local field potential**
LS	**lateral septum**
LTD	**long-term depotentiation**
LTP	**long-term potentiation**
µl	**microliter**
µm	**micrometre**
mA	**milliampere**
mg	**milligram**
ml	**millilitre**
ms	**millisecond**
MPP	**medial perforant path**
MS	**medial septum**
mV	**millivolt**
nm	**nanometre**
NMDA	**N-methyl-D-aspartate**
PB	**phosphate buffer**
REM	**rapid eye movement**
s	**second**
SEM	**standard error of the mean**
VDB	**vertical limb of Broca**

1. Introduction

1.1. Memory

1.1.1. Types of Memory

'I think, therefore I am'. The most famous philosophical proposition of René Descartes was related to the capacity of thinking and questioning. However, neither thinking nor questioning would be possible without memory. Memory is the capacity of learning and retrieval of information, and it can be considered the brain's most intriguing faculty and is undoubtedly crucial to life itself. The model of memory, as we understand today, is relatively recent. It is derived mostly from studies in amnesic patients and lesioned animals and has been broadly classified into two distinct systems: 1. short-term memory, i.e., information that amnesic patients could keep for a short period, and 2. long-term memory, which could be stored for decades.

Long-term memory can be further subdivided into non-declarative (implicit) and declarative (explicit). Non-declarative memory refers to unconscious information stored in the long-term memory, which is difficult to articulate, e.g., riding a bike or tying a shoelace. While declarative memory, including both episodic (contextual) and semantic (non-contextual), can be articulated (retrieved) in an understandable way.

Semantic memories are not bound to a specific time or place. Instead, it is a general type of information, e.g., knowing what the definition of a word is, or how a computer works. Episodic memories refer to specific personal experiences, including information about when and where it occurred (Squire and Zola, 1998).

The model of memory was defined to describe only human memory, but a large amount of neuronal data related to memory have been derived from animal studies. Episodic memory is a type of declarative memory, i.e., can be explicitly described, and includes information relating to time and context. It is usually described as "what," "where" and "when" memory (Ergorul and Eichenbaum, 2004). Animals cannot describe their memories as humans can, so "episodic-like" memory was suggested as the capacity to remember where and when specific events occurred (Clayton and Dickinson, 1998). Although episodic memory is not easily assessed in animals, an enormous collection of data suggest that animals can encode and retrieve episodic memories. In both animals and humans, the hippocampus has been the locus of memory research (Morris, 2001, Crystal, 2009, Templer and Hampton, 2013, Sluka et al., 2018).

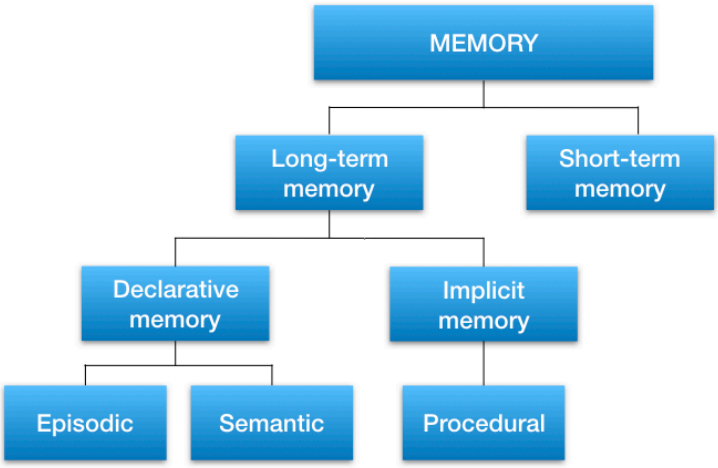

Figure 1. Types of Memory.

Schematic diagram of the classification of memory based on (Squire, 1986).

1.1.2. The hippocampus as a place for memory

In the early 1950s, memory was considered to be regularly distributed throughout the brain, mainly by the influence of the pioneering neuropsychologist Carl Lashley (1890-1958) who published his work called: 'In Search of the Engram the neural representation of a memory trace' (Lashley, 1950). The work summarized thirty-three years of his research in the theory of memory, searching for the brain area where specific memories were stored. To search for memory areas, Lashley did a series of lesion studies in rats. First, he trained the rats in a maze, and once the rats could solve the maze, he systematically removed parts of their cortex. The objective was to remove the area of the brain which contained the memory of the maze. If he succeeded, the rats would show a deficit in the task by exploring the maze as it was its first time. However, the results showed that independent of the

area removed, the lesioned rats could do better than control rats in solving the maze, suggesting that the lesion failed to remove the memory. Based on an extended series of similar experiments, he introduced the principle of "mass action," which attested that the memory is equally distributed in the brain rather than being restricted within a single area, and the degree of impairment is proportional to the brain damage.

However, seven years later, a case study published by (Scoville and Milner, 1957) of a patient who underwent surgery in an attempt to cure severe drug-resistant epilepsy, shined a light in the field. After the surgery, the patient known as H.M. developed profound anterograde amnesia as well as semantic and spatial deficits (Corkin et al., 1997, Corkin, 2002). The surgery removed parts of the hippocampus and amygdala from both sides of the brain. Despite the tragic side effect of his surgery, the studies on H.M. changed the view of how memory is distributed in the brain and placed the hippocampus at the centre of memory studies.

1.1.3. Place cells in the hippocampus

In 1971, O'Keefe and Dostrovsky observed that some hippocampal CA1 pyramidal neurons had a distinct preference for a discrete region of the arena. Outside of this region, the firing rate of the neuron was close to zero, and as the animal approached a specific region, the firing rate increased significantly. They named these cells as 'place cells' (O'Keefe and Dostrovsky, 1971). In the following years studying properties of place cells, O'Keefe and Nadel published a the book titled

"Hippocampus as a Cognitive Map". In this book, the authors proposed that the place cells are the essential elements of a cognitive map of the environment, and the hippocampus would provide the spatial and temporal context to support memory formation (O'Keefe and Nadel, 1978). Although the discovery of place cells revolutionized how we understand the hippocampus and earned O'Keefe the Nobel Prize in physiology, the idea of a cognitive map was first described by Edward Tolman in 1948. By observing how rats used spatial cues to solve complex problems, Tolman concluded that rats could encode an allocentric, e.g., based on relations between external objects, map-like representation of the environment, which he described as 'cognitive map' (Tolman, 1948).

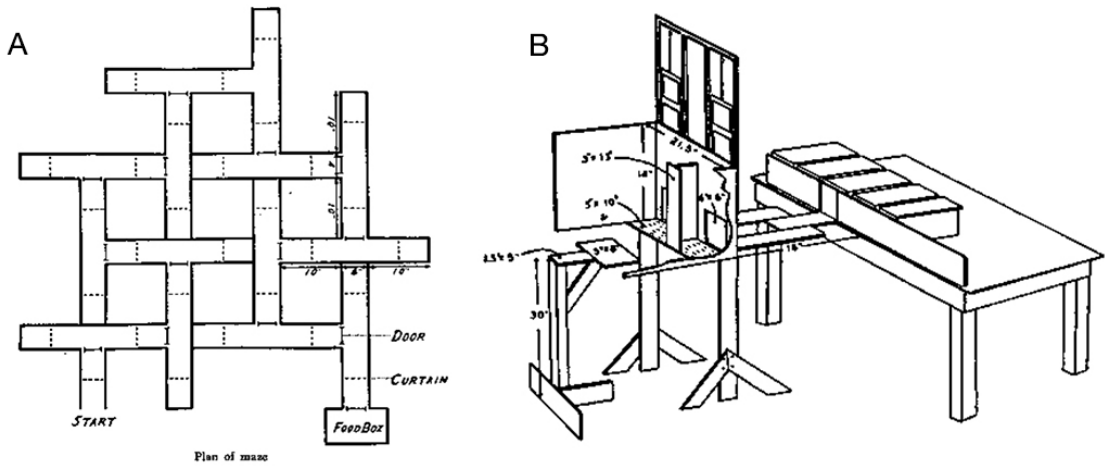

Figure 2. Tolman mazes.

Two examples of mazes used by Edward Toman. A) T-alley maze, food-deprived rats were allowed to “solve” the maze where error and time were accounted. B) A complex apparatus to measure “Vicarius”, a term used to describe the time that rats take looking back and forth before making a choice.

Since the discovery of the place cells, many other components of the spatial processing system have been described, supporting the idea of a cognitive map. Furthermore, the neural encoding of spatial location has been found in the hippocampus and parahippocampal regions of many different species (Yoder and Taube, 2009, Taube et al., 1990, Finkelstein et al., 2015, Tollin and Yin, 2002, Robertson et al., 1999, Ekstrom et al., 2003). In fact, the integrity of the hippocampus is crucial to encoding spatial memory i.e., the ability to encode information about the environment and use this information for navigation and orientation (Kessels et al., 2001, Eichenbaum, 2013). Spatial memory involves aspects of declarative and non-declarative, short-term and long-term memories (Moscovitch et al., 2006, Preston and Eichenbaum, 2013). Before understanding how place cells are related to memory and spatial processing, a brief description of the hippocampal anatomy will be given (1.2.1.) to anchor cell types with their circuits.

1.1.4. Memory formation

The mechanism by which memory could be formed in the brain was proposed by Donald Hebb in 1949 as a postulate: "When an axon of cell A is near enough to excite cell B and repeatedly or persistently takes part in firing it, some growth process or metabolic change takes place in one or both cells such that A's efficiency, as one of the cells firing B, is increased". His postulate is widely famous as the Hebbian rule which was simplified as: "Neurons that fire together wire together" (Hebb, 1938). The Hebbian rule was complemented latter based on

experimental results which considered the decrease of synaptic efficiency when the presynaptic axon fails to excite the postsynaptic dendrite. The "increase" (potentiation) or "decrease" (depotentiation) of the synaptic connection can last for seconds or minutes ("short-term"), or last for hours or days ("long-term") (Bliss and Lomo, 1973, Wiesel and Hubel, 1965, Stent, 1973).

The two phases of the potentiation of synapse efficacy are commonly described as early phase potentiation, also called short-term potentiation (STP), and late phase potentiation, also referred to as long-term potentiation (LTP). Plasticity between synapses depends on many factors, and the most studied type of LTP is N-methyl-D-aspartate (NMDA) receptor-dependent. In the CA1, the short-term potentiation is induced by glutamate neurotransmitters on the presynaptic terminal of the NMDA receptor, which depolarises the membrane potential of the postsynaptic neuron inducing an increase in postsynaptic levels of Ca2+. Consequently, the increase of Ca2+ induce a cascade of reactions which result in phosphorylation of the NMDA receptor, making the receptor more sensitive to glutamate (Sweatt, 2001, Lynch, 2004). The LTP requires the activation of intracellular signalling and synthesis of new proteins including AMPA receptor. Consequently, the sensitivity to glutamate will last for several hours (Linden and Routtenberg, 1989, Kelleher et al., 2004). The decrease in the efficacy of neuronal synapses is commonly named as long-term depotentiation (LTD), and it can also occur on the NDMA receptor (Fitzjohn et al., 2010). However, to contribute to memory, both LTP and LTD have to be balanced in a coordinated fashion across remote networks. Although the mechanism of how such large-scale coordination occurs is not yet understood,

several theories suggest neural oscillations as a strong candidate for coordinating networks, due to its ability to travel to remote brain regions.

Oscillations are voltage fluctuations which are mainly caused by neuronal activity. They occur at different frequencies and can precisely synchronize local and remote neuronal populations. The ionic movement across synaptic membranes generates electric differences which are referred to as local field potential (LFP). In the hippocampus, the two main frequency bands present in the LFP are the theta (4-12 Hz) and gamma (25-140 Hz) (Buzsaki and Wang, 2012). In the hippocampal CA1 of anesthetized rats, stimulation bursts delivered at the peak of the theta cycle can induce LTP, in contrast, the same bursts delivered at the trough can induce LTD (Hyman et al., 2003). Moreover, just a single burst of 4 pulses at 100 Hz could induce LTP in CA1 neurons (Huerta and Lisman, 1995). In humans, a recent study showed that episodic memory formation is increased when the video and audio of a movie were flickering at theta frequency (4 Hz) compared with slower frequency (1.7 Hz), faster frequency (10.5 Hz) and non-flickering movies (Clouter et al., 2017). Showing how human episodic memory may rely on a theta-specific synchronization mechanism.

1.2. The hippocampus

1.2.1. Anatomy of the hippocampus

The hippocampal formation comprises three primary structures: the dentate gyrus (DG), subiculum (SUB) and the cornus ammonis subfields (CA). The cornus ammonis is subdivided into four subfields named CA1 to CA4, and this region is usually referred to as the hippocampus proper (to avoid misperception, in this thesis only the term cornus ammonis (CA) will be used) (Afifi and Bergman, 2005). The dentate gyrus, cornu ammonis, and subiculum all have a common anatomical arrangement and are organized in three different layers. The nomenclature of these layers depends on the area where they are found (Andersen et al., 1971). The intermediate layer is densely formed by cell bodies of hippocampal glutamatergic neurons and interneurons. In the CA region, this layer is referred to as the pyramidal layer, due to the morphology of neurons present in this region. In the DG it is named the granule layer, again in reference to the granule cells present in the DG. The hilus in the DG and stratum oriens in the CA are layers formed by fibres and interneurons. Lastly, in the DG and SUB, the most superficial layer is called the molecular layer. In the CA area, this layer is further subdivided into multiple sublayers and houses most of the dendrites of the pyramidal cells. The sub layers are; the stratum lacunosum-moleculare, formed by the dendrite's termination of the pyramidal cells; the stratum radiatum, formed by the apical dendrites of the pyramidal cells; and the stratum lucidum, which receives afferents from the DG.

1.2.2. The entorhinal cortex

The entorhinal cortex (EC) is the primary input of the hippocampal formation, and it receives projections from many areas related to sensory processing. Regarding cytoarchitecture distribution, it is divided into two main subdivisions: lateral EC (LEC) and medial EC (MEC). The MEC has a defined laminar distribution in six layers. In contrast, in the LEC the laminar distribution is less characterized (Burwell and Amaral, 1998b, Burwell and Amaral, 1998a, Witter et al., 2000). Both MEC and LEC project to the hippocampus, DG and other regions through the perforant pathway. It is generally accepted that the EC processes both spatial and contextual information. Indeed, in layer II of the MEC, cells that encode spatial information of the environment can be found (Sargolini et al., 2006). Curiously, these cells show a regular spaced triangular or hexagonal grid firing pattern during navigation. They are called "grid cells" and will be described further in this chapter (Deshmukh and Knierim, 2011, Yoganarasimha et al., 2011, Hafting et al., 2005, Sargolini et al., 2006).

1.2.3. The tri-synaptic circuit

Information flow in the hippocampus generally follows a single direction through the primary circuit named the trisynaptic pathway, which is required for learning and pattern-completion (Nakashiba et al., 2008, Nakashiba et al., 2009). The axons from layers II and III of the EC constitute the perforant path, which links the EC to the granule cells of the DG. From the DG, the granule cells project to CA3 forming

the so-called mossy fibres, and from there, the CA3 then projects to CA1 via the Schaffer collaterals.

These connections are topographically organized along the transverse axis. The distal portion of the CA3 neurons targets proximal portions of the CA1 and vice versa (Ishizuka et al., 1990, Steward, 1976, Witter et al., 1988). CA1 neurons project back to the EC where the fibres terminate mostly in the deep layers (V and VI), closing the loop. Axons from CA1 also project to the subiculum (Amaral et al., 1991, Berger et al., 1980). Pyramidal neurons of layer III of the EC project directly to CA1 via the temporoammonic pathway (Speed and Dobrunz, 2009). Although the tri-synaptic path is where most of the information is processed in the hippocampus, back-projections exist, i.e., CA3 neurons project to each other (Witter and Amaral, 1991), DG granule cells target mossy cells dendrites in the polymorphous layer which back project to other granule cells in the molecular layer (figure 3).

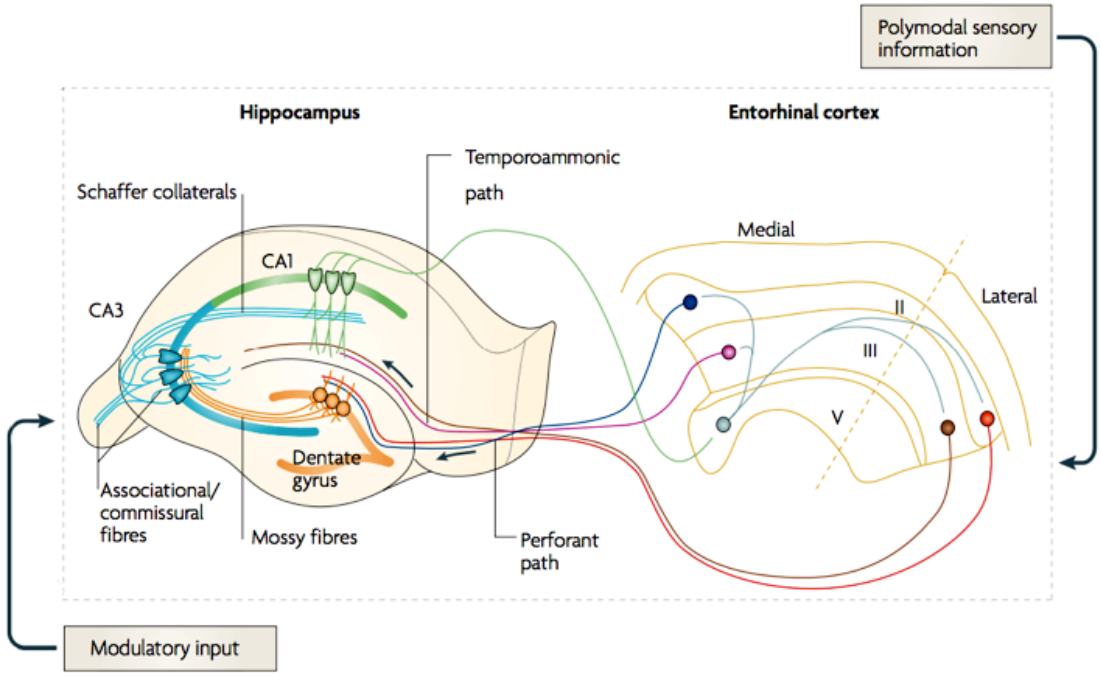

Figure 3. Basic anatomy of the hippocampus.

On the left side of the figure, the trisynaptic pathway and dentate gyrus are represented. The trisynaptic circuit consists of projections from layers II and III of both medial and lateral entorhinal cortex to dentate gyrus through the perforant path. From dentate gyrus to CA3 via mossy fibres, and from CA3 to CA1 via Schaffer collaterals. Pyramidal neurons of the layer III of the EC can also project directly to CA1 via the temporoammonic pathway, and CA1 neurons project back to the EC to close the loop. The entorhinal cortex receives polymodal sensory information from perirhinal and postrhinal cortices (Hartley et al., 2014). The CA area receives modulatory input, mostly in the theta band from the medial septum (figure adapted from (Neves et al., 2008)).

1.2.4. Neuronal subtypes

Hippocampal neurons that compose the trisynaptic circuit consist mostly of excitatory glutamatergic cells. In the intermediate layers in the CA area and subiculum, these were termed pyramidal cells by Ramon y Cajal due to their bipolar dendritic arborisation. The principal layer of the DG is also composed of glutamatergic cells which have elliptical cell bodies, and for this reason, they are called granule cells (Amaral, 1978, Spruston, 2008, Amaral et al., 1990).

The hippocampal interneurons comprise a heterogeneous group of cells, and many studies have attempted to characterize the vast subtypes, which are outside the scope of this introduction. However, a basic description of interneuron subtypes is presented (Freund and Buzsaki, 1996, Freund, 2003, Klausberger et al., 2003). It is estimated that ~10-15% of the hippocampal interneurons are GABAergic, these cells populate all hippocampus layers and establish inhibitory synapses via $GABA_A$ and $GABA_B$ receptors (Fritschy and Panzanelli, 2014, Benarroch, 2012, Lewis, 2010, Pelkey et al., 2017). The GABAergic synapses cover almost the entire membrane surface of pyramidal neurons and have a pivotal role in controlling pyramidal neurons output (Toth et al., 1997).

The most studied interneuron type is the basket cell, it can be found either inside/adjacent to the pyramidal layer or inside the dentate gyrus granule layer. Their axons form basket-like structures (Toth et al., 1997). The hippocampal basket cells can express parvalbumin (PV+) or cholecystokinin (CCK+). Studies suggest that PV+ basket cells act as timekeepers for cortical oscillations, while CCK+ interneurons may act to fine-tune synchronous activities related with motivation,

emotions and autonomic state of the animal (Buzsáki, 1996). Although these cells have few receptors for subcortical modulatory inputs that carry this type of information, PV+ cells are driven by local principal cells (Toth et al., 1993, Freund, 2003). Fast spiking GABAergic interneurons, including parvalbumin-positive interneurons, have heterogeneous firing patterns and are classified as bursting or regular spiking neurons (Kawaguchi and Kubota, 1996). These neurons can act as modulators of CA1 pyramidal cells and silencing these neurons result in increase in firing rate of pyramidal cells (Royer et al., 2012).

Another type of interneurons are the dendritic inhibitory neurons, which target dendrites of principal neurons and control the excitatory input of pyramidal neurons, these neurons can receive inputs from the same pyramidal neuron, resulting in feedback inhibition (Wozny and Williams, 2011, Lacaille et al., 1987, Tremblay et al., 2016). Some interneurons innervate other interneurons, they are located in all layers of the hippocampus and can be characterized by the expression of calretinin (Freund and Buzsaki, 1996, Acsady et al., 1996, Gulyas et al., 1996, Gulyas et al., 2003).

1.3. Spatial processing in the hippocampus

The understanding of navigation in rodents opened a window towards the understanding of spatial processing in general. Since the discovery of place cells, many other spatially modulated cells were also described in different areas of the brain. Furthermore, many studies were designed to understand the features of

these cells, and how they are related to navigation and formation of spatial and episodic memories. This work focused mainly on the hippocampal CA1 place cells. However, it is essential to understand that spatial processing is spread over many brain regions (for review (Grieves and Jeffery, 2017)).

1.3.1. Place cells

Place cells are CA1 and CA3 pyramidal cells that show a location-specific firing preference (O'Keefe and Dostrovsky, 1971). These cells display a maximum firing rate when the rat is in a discrete region of the environment, which is called the "place field" of a place cell. It has been proposed that a sufficient number of place cells would cover all of the environment with their place fields (O'Keefe, 1979, O'Keefe and Conway, 1978). Place cells fire in intermittent bursts of several action potentials which decrease in amplitude within a burst, for this reason, they are referred to as complex-spikes (Ranck, 1973, Muller et al., 1987). Place cell bursting activity shows an increase in firing rate towards its maximum peak (5 - 30 Hz) when approximating to its place field (O'Keefe and Burgess, 1996).

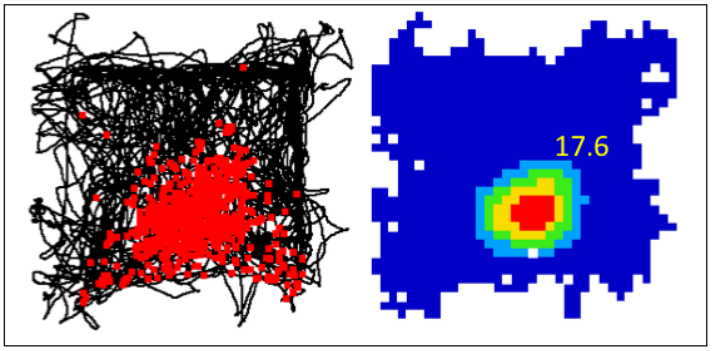

Figure 4. Hippocampal place cell.

Above is an example of a typical hippocampal place cell. On the left, the black trace represents the rat's movement on the arena, the red dots on the left are spikes recorded. On the right, the smoothed map of firing rate showing 17.6 spikes per second peak frequency.

The specific position preference with which a place cell will fires seems to be randomly defined during the first moments of the animal's exploration of a new environment (Hill, 1978, Wilson and McNaughton, 1993, Frank et al., 2004, Cohen et al., 2017). Once a place field is formed, it can be stable for days or weeks, i.e., during recordings in the same environment, place cells fire in the same sub region that they were firing before (Lever et al., 2002, Muller and Kubie, 1987, Ranck, 1973). Place cells can also form in entirely dark environments and remain stable when the light is turned on (Quirk et al., 1990). Since its discovery in 1971, many additional proprieties of place cells have been described. Position stability refers to the capacity of place cells to reorganize in relation to each other, and it is one of the most intriguing properties of these cells due to the similarity to memory formation (O'Keefe and Conway, 1978, Muller and Kubie, 1987).

1.3.2. Place cell remapping

The term remapping was first introduced by studies describing how place fields changed when spatial cues were altered. If surrounding landmarks or distal cues of the environment are rotated, the place cell firing fields rotate correspondingly (O'Keefe and Conway, 1978, Muller and Kubie, 1987). Although place cells can reorganize, there are distinct types of rearrangements. The terms 'global remapping', 'partial remapping' and 'rate remapping' were introduced to describe different levels in the place fields' reorganization (Knierim and McNaughton, 2001, Leutgeb et al., 2005b).

Global remapping refers to when a set of place cells that were active in a defined environment change position to each other. In this case, cells that were active in one environment can become silent in a new environment. Equally, cells that were silent in the first environment could be active in another. These changes are known as the all-or-none phenomenon (Colgin et al., 2008). Aged rats with memory impairment can form place fields when they visit the environment for the first time; however, their place fields are not stable and global remapping can occur in subsequent sessions without changes in the environment, showing the close relationship between place cells and memory (Barnes et al., 1997).

Partial remapping, as the name suggests, is used to describe when some place cells change their firing patterns or positions, and other place cells stay unaltered in response to spatial or non-spatial changing in the environment (Bostock et al., 1991, Leutgeb et al., 2005b, Leutgeb and Leutgeb, 2007).

The term 'rate remapping' is used to describe changes in the firing frequency of the place cell but not in the position which the set of place cells are active (Leutgeb and Leutgeb, 2007). As the location and population of place cells remain the same, the rate remapping suggests that non-spatial information can be encoded by the pyramidal cells. Indeed, accumulating data indicate that place cells can encode contextual information. For example, changing the reward location within a single session can induce place field reorganization (Breese et al., 1989, Smith and Mizumori, 2006b, Smith and Mizumori, 2006a).

1.3.3. Place cells and reward

There is no doubt regarding the encoding of spatial information by the place cells. However, in addition to spatial features, motivational factors can also induce reorganization of place fields. This line of research suggests that place cells could encode contextual information. In an experiment where rats had to recognize different odours to retrieve a reward, a statistically significant number of place cells were not correlated with the position, but with the odour (Wood et al., 1999). In another study, place cells were recorded stable during a random foraging task and partially remapped when the food pellets were solely available at discrete regions of the maze (Markus et al., 1995).

Place fields have been observed to fire closer to reward areas (Dupret et al., 2010). A study showed that on an annular water maze, the number of place cells near the hidden platform was more than twice that of the rest of the arena, independently

of where the maze was positioned in the room (Hollup et al., 2001). Another study suggested that place cells tend to accumulate in an area where the VTA, a brain area related to reward processing, has been stimulated using optogenetics (Mamad et al., 2017). A very recent study described that small populations of CA1, and subicular neurons are specialized for encoding reward location. In this experiment, mice navigated in a linear track in a virtual environment with rewards provided at fixed positions. Accumulation of place fields was observed near reward locations. In addition, exposing the animals to different virtual environments, resulted in a majority of the cells being remapped randomly as expected, but the reward cells were consistently encoding the reward positions (Gauthier and Tank, 2018).

1.3.4. Grid Cells

In 2004, Moser's group published their data from recordings in the medial entorhinal cortex. They found that allocentric spatial information was encoded by neurons close to the border with the postrhinal cortex, an area that receives projections from visual and parietal cortices. These cells were later named grid cells because of their pattern of firing (Fyhn et al., 2004).

In contrast to place cells in the hippocampus, grid cells in the MEC fire in multiple discrete and regularly spaced locations (figure 6). Some studies proposed that grid fields serve as periodic functions that could be combined to result in place fields in the hippocampus (O'Keefe and Burgess, 2005, Fuhs and Touretzky, 2006, McNaughton, 2006). Interestingly, the firing of grid cells are also associated to the

theta frequency oscillations (Mizuseki et al., 2009), and inactivation of the medial septum (MS) abolishes theta oscillation and a grid pattern of firing (Koenig et al., 2011).

1.3.5. Head direction cells

Head direction cells are essential to the understanding of the ability of encoding self-motion. First described in the rodent post subiculum by Ranck, Jr. (1984) and found in other brain areas including lateral mammillary nuclei (Stackman and Taube, 1998), retrosplenial cortex (Chen et al., 1994, Jacob et al., 2017), MEC (Sargolini et al., 2006) and dorsal thalamic nuclei (Taube, 1995). These cells fire at the maximum frequency when the animal faces a particular direction in the horizontal plane. The firing frequency is independent of the animal's behaviour, and different cells fire in different directions (Taube et al., 1990). Data suggests that head direction cells can rely on visual cues. Recordings in the dark showed that cells kept a preferred direction which was less precise, and the direction caused drift over time. Moreover, the rotation of external cues induced the head direction firing to rotate in the same proportion (Goodridge et al., 1998, Zugaro et al., 2003).

1.3.6. Other spatial modulated neurons

Place cells, head direction cells, and grid cells are the most studied spatially modulated types of cells and together they are considered the neuronal basis of the cognitive map. However, many other less understood cells are related to spatial information. Boundary vector cells for instance, were first proposed as a model to explain how place cells kept a relative distance from the borders of the maze. It was observed that when elongating a maze from squared to rectangular, the cells kept the distance from the border (O'Keefe and Burgess, 1996). In this model, hippocampal inputs should provide information about the distance and directions of boundaries. The model previewed a type of cell called "Boundary Vector Cell" (Barry et al., 2006, Jeffery et al., 1997). Years later the boundary vector cells were found in the dorsocaudal region of the MEC, approximately 10% of the pyramidal cells had the firing close to selected geometric borders of the environment (Solstad et al., 2008). Additionally, cells with the same properties were also found in another regions including subiculum and parasubiculum (Boccara et al., 2010, Bjerknes et al., 2014, Solstad et al., 2008). Another example of cells that have activity closely related to the environment features is the object cells. These are cells that respond to object locations (Lenck-Santini et al., 2005). In the claustrum, about 5.5% of the cells fired while the animal was exploring an object and stopped to firing when the object was removed. Firing of these cells persisted in the darkness or if the object was replaced by another, indicating that it does not represent the object itself, but the position of the object in the space (Jankowski and O'Mara, 2015).

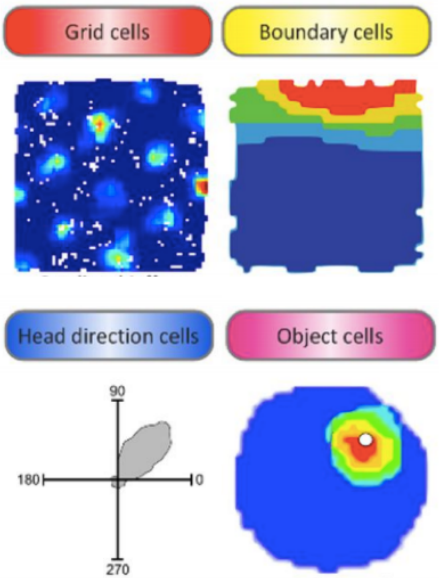

Figure 5. Spatially sensitive neurons.

The figure shows the firing rate maps of a grid cell, a boundary vector cell, and an object cell. The polar plot shows the firing rate depends on the direction of the animal head (adapted from (Grieves and Jeffery, 2017)).

1.1. Hippocampal theta oscillation

Theta band oscillations (5 - 12 Hz) are high amplitude voltage fluctuations that are tightly related with memory processing and spatial cognition in rodents (Gordon et al., 2005, Brandon et al., 2011, Buzsaki, 2002). These oscillations can be detected from extracellular local field potential (LFP) in the hippocampal formation while the animal performs locomotor behaviour (translational movement) and also during rapid eye movement sleep (REM) (Vanderwolf, 1969, Oddie and Bland, 1998, Jouvet, 1969). It is additionally present outside the hippocampus, in areas

related to sensory processing, spatial processing, and memory. For example, the perirhinal cortex, entorhinal cortex, cingulate cortex and amygdala (Buzsaki, 2002). Moreover, recordings of freely-moving rodents showed an approximately linear relationship between theta frequency and running speed (Bouwman et al., 2005, McNaughton et al., 1983a). It still not clear if theta oscillations from different areas are related. One hypothesis suggests that theta waves may be integrating information between distinct areas. Indeed, coordination of theta signals between the hippocampus and connected structures increases with learning (Brandon et al., 2011, Burgess and O'Keefe, 2005, Kleen et al., 2011, Backus et al., 2016, Benchenane et al., 2010). In the hippocampus, theta oscillation can be detected before the locomotion begins and continues during movement (Fuhrmann et al., 2015) These theta oscillations travel in waves and gradually shift their phase moving from septal to ventral pole, potentially coordinating neuronal activity in a synchronized fashion (Lubenov and Siapas, 2009, Patel et al., 2012).

Although specific theta-frequency firing neurons have been found in slices of the hippocampus (Manseau et al., 2008, Goutagny et al., 2009, Amilhon et al., 2015), it is well accepted that the MS is the hippocampal theta generator (Kocsis et al., 1999, Kang et al., 2015, Tsanov, 2017, Brazhnik and Fox, 1999). The septal area and hippocampal formation can be considered a unique formation connected by the fimbria-fornix which is referred to as the septohippocampal system (Risold and Swanson, 1997b, Sheehan et al., 2004).

1.1.1. Place cells and theta

Recordings of CA1 pyramidal cells during navigation showed that place cells have an interesting relationship with the phase of the theta frequency present in the LFP. As the animal enters a place field, the burst firing of a given cell occurs in later phases of the theta cycle, as the animal crosses the place field, a regular phase shift progressively occurs towards to early phases of successive theta cycles (figure 6). In this manner, when the animal is exiting the place field, the firing of the place cell is at earlier phases of the theta cycle. This phenomenon is referred to as 'phase precession' (O'Keefe and Recce, 1993, Skaggs et al., 1996, Foster and Wilson, 2007, Gupta et al., 2012).

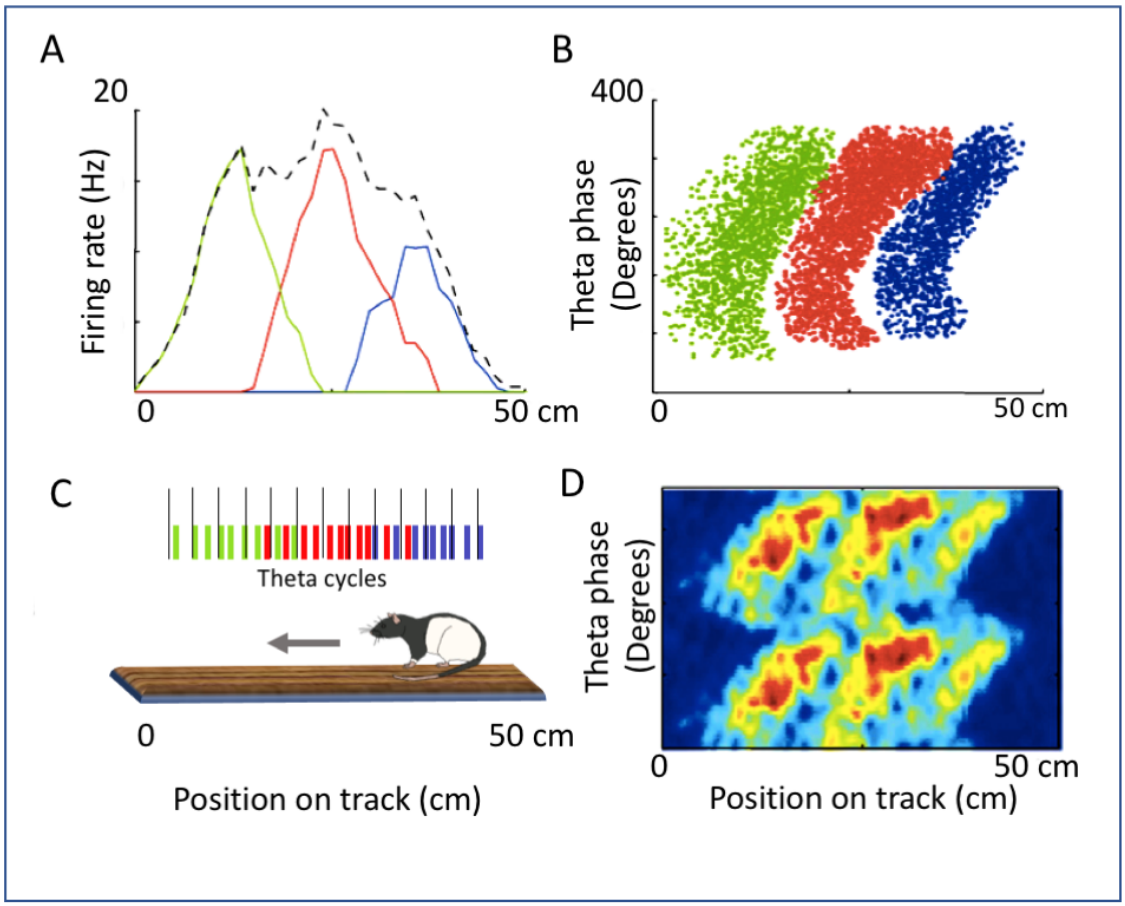

Figure 6. Theta precession of CA1 place cells.

Place cells in the CA1 region are considered to cover all the extents of the environment. During navigation, sequences of place cells overlap with each other concerning the environment position. Moreover, the firing starts at later phases of theta when the animal enters the place field and successively moves towards earlier phases as the animal moves out of the place field. **(A)** Firing rate of neighbour place fields plotted in function of the space. **(B)** Each colour represents a place cell, and each point represents the phase of the cell about the position. **(C)** The representation of the rat moving on a linear track and cells sharing the same theta cycle as the rat moves. **(D)** The firing rate for the neuron plotted as a function of position and phase. Figure adapted from (Maurer et al., 2006a).

Theta precession is clearly observed when rodents run along linear tracks, but it can also be apparent in 2D environments during repeated movement (Skaggs et al., 1996, Huxter et al., 2008). Although it was first described in pyramidal CA1 cells, this phenomenon can be observed on hippocampal interneurons (Maurer et al., 2006b, Ego-Stengel and Wilson, 2007), other hippocampal areas (Skaggs et al., 1996, Johnson and Redish, 2007, Hafting et al., 2008, Kjelstrup et al., 2008, Royer et al., 2010), medial prefrontal cortex (Jones and Wilson, 2005) and ventral striatum (van der Meer and Redish, 2010). Interestingly, as the theta frequency is proportional to speed, at faster speeds, firing phase can better describe location than firing rate of the place cell (Jensen and Lisman, 2000, Jones, 2003).

1.1.2. Origins of hippocampal theta

The MS has been considered the theta generator of the hippocampus since temporary inhibition or lesion of the MS virtually eliminate hippocampal theta oscillations. Moreover, disconnection of these areas by fimbria-fornix is also sufficient to suppress theta in the hippocampus (Andersen et al., 1979, Gray, 1971, Oddie and Bland, 1998, Sainsbury and Bland, 1981).

Neurons in the MS have been identified to fire in bursts phase-locked in theta frequency within the hippocampus and entorhinal cortex (Stewart and Fox, 1990). Moreover, a neuronal subpopulation found in MS have shown tight phase coupling to hippocampal theta, these GABAergic neurons express hyperpolarization-activated, cyclic nucleotide-gated non-selective cation (HCN) channels and its

population partly overlaps with GABAergic parvalbumin-positive neurons. All neurons expressing (HCN) were found to fire in theta range (Varga et al., 2008).

Apart from the hippocampus, MS projects to several distinct brain areas including the subiculum, the entorhinal cortex, the amygdala, the lateral hypothalamus, the mediodorsal thalamus, the habenular nuclei, the mammillary complex, the supramammillary area, the ventral tegmental area and the raphe nuclei (Swanson and Cowan, 1979, Meibach and Siegel, 1977, Montagnese et al., 2004). The MS also receives afferent inputs from diverse brain structures in addition to the hippocampal formation. These areas include the amygdala, the ventral pallidum, the lateral septum, the lateral hypothalamus, the supramammillary area, the dorsal thalamus and from several brainstem nuclei (ventral tegmental area, substantia nigra, raphe nuclei, locus coeruleus (Swanson and Cowan, 1979, Montagnese et al., 2004).

1.4. The septohippocampal system

The septum has extensive connections with the hippocampus via the fimbria-fornix pathway. While the MS has reciprocal projections, the lateral septum (LS) mostly receives projections from the hippocampus (Raisman, 1966, Risold and Swanson, 1997b). For this reason, these regions are referred to as the septohippocampal system (Dutar et al., 1995, Khakpai et al., 2013).

The septohippocampal system has been extensively studied concerning spatial memory since septal lesions cause learning and memory deficits in both humans

(Gaffan et al., 1991, Botez-Marquard and Botez, 1992) and animals (Rawlins and Olton, 1982, Numan and Quaranta, 1990).

The septum area is a subcortical forebrain region located rostrodorsal to the hypothalamus, situated between the lateral ventricles in rodents. It is functionally and anatomically divided into two major areas: the lateral septum (LS) and the medial septal-diagonal band of Broca (MS), each having different function and cell populations (Leranth and Frotscher, 1989). The MS sends cholinergic, glutamatergic and GABAergic projections to the hippocampus while receiving mostly GABAergic fibres. On the other hand, the LS is the main subcortical target of the hippocampal CA1, CA3 and subicular pyramidal neurons (Swanson and Cowan, 1979, Risold and Swanson, 1997b). Due to its close anatomical connection with the hippocampus and areas related to emotions and behaviour response, e.g., ventral tegmental area, hypothalamus, and basolateral amygdala, the septum is a strong candidate for theintegration of spatial and non-spatial information processed in the hippocampus and these areas. Indeed, the LS has been shown to have a crucial role in emotional processes and stress responses. It is also related with feeding suppression and modulation of several cognitive and emotional processes including learning, memory, anxiety and autonomic responses (Sheehan et al., 2004, Reis et al., 2010, Singewald et al., 2011).

1.4.1. The Lateral septum

The LS is the most substantial nucleus of the septum and was historically anatomically divided into dorsal, intermediated and ventral areas. It is the primary output of the hippocampus, receiving massive projections from CA and subiculum. It is also interconnected with motivation centres, which are known to translate motivational values into motor outputs e.g., lateral hypothalamus, periaqueductal grey and thalamus (Swanson and Cowan, 1979, Risold and Swanson, 1997b, Valenstein et al., 1970, Sheehan et al., 2004). It is composed of small and medium-sized glutamic acid decarboxylase (GAD) positive GABAergic neurons. Double fluorescence in situ hybridization and immunohistochemistry of calcium-binding proteins showed that GABAergic neurons in the LS displayed immunoreactivity for calbindin or calretinin, but not parvalbumin (Colom et al., 2005). There are two subtypes of GAD enzymes: GAD 65 and GAD 67, consequently GABAergic GAD 65+ and GABAergic GAD 67+ neurons, suggesting two different GABAergic circuits in the septum (Zhao et al., 2014).

Risold and Swanson's group did an extensive study on the connections and chemoarchitecture of the LS. They redefined LS subdivisions related to neurochemical expression and neuroanatomical data and observed that the rostral area of the LS contains dense enkephalinergic and neurotensinergic neurons. These neurons receive massive projections from CA1 and are interconnected with the medial hypothalamic area. The caudal region of the LS expresses somatostatin and receives projections from CA3 of the hippocampus (Risold and Swanson, 1997b). Furthermore, the hippocampal projections to the LS are topographically

organized, suggesting a functional pathway between these areas (Risold and Swanson, 1997a).

Regarding neurotransmitters, the LS receives inputs from monoaminergic and cholinergic cell groups in the midbrain, including dopaminergic information from the VTA, serotonergic inputs from the raphe nuclei, adrenergic inputs from the locus ceruleus, cholinergic inputs from the laterodorsal tegmentum, and glutamatergic inputs from the hippocampus (Meibach and Siegel, 1977, Sheehan et al., 2004). Projections from the LS are topographically organized to the hypothalamus, arranged in dorsoventral to rostrocaudal gradients (Risold and Swanson, 1997b). Some authors have described a GABAergic connection between the LS and the MS (Leranth and Frotscher, 1989, Risold and Swanson, 1997b). However, others have argued against the existence of this connection, suggesting that LS and MS connections are very sparse (Jakab and Leranth, 1995). Additional anatomical studies revealed that the hypothesized projection from the LS to the MS is either very weak or non-existent (Staiger and Nurnberger, 1991, Gulyas et al., 1991, Leranth et al., 1992).

The LS is also involved in theta-rhythmic regulation of locomotion through projections from the hippocampus to the lateral hypothalamus, via the dorsal LS (Bender et al., 2015). Moreover, infusion of muscimol in the dorsal LS increased theta frequency in the hippocampus. Conversely, infusion of the competitive $GABA_A$ receptor antagonist GABAzine in the dorsal LS abolished theta, suggesting a relationship with the MS (Chee et al., 2015).

1.4.1.1. Electrophysiological recordings of the LS

As the main forebrain output of the hippocampus, the LS receives direct projections from pyramidal cells of CA3 and CA1 which are known by their spatial firing. Indeed, electrophysiological recordings in freely moving rats have shown that LS cells encode spatial information. However, the place-related activity described in the LS is unstable and less representative compared with spatial hippocampal place cells (Zhou et al., 1999, Leutgeb and Mizumori, 2002, Takamura et al., 2006). It is well accepted that septal area contributes to memory, and damage in the septal area can impair memory and spatial learning (Rawlins and Olton, 1982, Numan and Quaranta, 1990, Fraser et al., 1991). Nevertheless, lesions restricted to LS does not produce severe deficits in goal spatial solving task, a kind of spatial working memory task (Fraser et al., 1991).

1.4.2. Medial septum

The medial septum is composed of two main areas: the medial septal nucleus and the nucleus of the diagonal band of Broca, these regions are intimately interconnected, and for simplification purposes, they will be considered as a single region called MS for this thesis (Colom, 2006, Dragoi et al., 1999). In terms of neuronal structure the MS is formed predominantly by three distinct interconnected neuronal populations which form a dense and complex local network: GABAergic which are immunopositive for glutamic acid decarboxylase (GAD), cholinergic which are immunopositive for choline acetyltransferase

(ChAT) and glutamatergic, which are immunopositive for vesicular glutamate transporter (VGluT) type 1 or/and type 2 (Sotty et al., 2003, Colom et al., 2005, Leão et al., 2015, Frotscher and Leranth, 1985, Hajszan et al., 2004, Kiss et al., 1990). Furthermore, the complexity of the circuit is increased by a subpopulation of neurons which were described to be immunopositive for both GAD and ChAT (Sotty et al., 2003).

The MS is interconnected with the hippocampus, receiving most GABAergic projections from hippocampal interneurons (Freund and Antal, 1988, Risold and Swanson, 1997b, Takacs et al., 2008, Alonso and Köhler, 1982). On the other hand, projections from MS to the hippocampus are composed of the three different subpopulations present in MS and innervate all areas of the hippocampus and entorhinal cortex (Risold and Swanson, 1997a, Risold and Swanson, 1997b).

The hippocampal GABAergic projections to MS are found in all regions of the hippocampus: from the CA1 area, they are located in the stratum oriens; in the dentate gyrus, they are found in the hilar area and the CA3 area they are distributed in all layers (Jinno and Kosaka, 2002, Totterdell and Hayes, 1987). These projections mostly target MS parvalbumin GABAergic expressing neurons and cholinergic neurons in a much less proportion (Toth et al., 1993). These inputs mediate fast inhibitory response in MS GABAergic neurons (Mattis et al., 2014). Although the hippocampal to MS projections are not crucial for theta oscillations, they are believed to have a regulatory function in the network (Tóth and Freund, 1992). Back projections from the hippocampus have been identified to project to the same GABAergic MS neurons from which they receive inputs (Takacs et al., 2008).

Although the majority of the MS studies are related to its relation to the hippocampus, the MS is connected to another region related to reward and memory processing as described before. The privileged anatomical position suggests that the MS can be a strong candidate to integrate these processes (Swanson and Cowan, 1979, Woolf, 1996, Yamano and Luiten, 1989, Vertes, 1992, Chiba and Murata, 1985).

1.4.3. Septal projections to the hippocampus

1.4.3.1. MS cholinergic neurons

About 66% of the MS fibres to the hippocampus are cholinergic, and it is the primary source of acetylcholine in the hippocampus (Sun et al., 2014). The septo-hippocampal cholinergic fibres are widespread in the hippocampal and can modulate distinct population of neurons which express ionotropic nicotinergic and metabotropic muscarinic receptors (Cobb and Davies, 2005). The decrease of cholinergic modulation of the hippocampus has been described in patients who have Alzheimer's disease (Bartus et al., 1982, Whitehouse et al., 1982). Furthermore, the strength of cholinergic post-synaptic responses in the hippocampus is diminished during aging, which increased the interest of MS cholinergic as a target for Alzheimer's treatment (Chouinard et al., 1995, Shen et al., 1996).

The acetylcholine levels in the hippocampus are highly correlated with the frequency of low-firing rate neurons of MS, these neurons fire at frequencies below 4 Hz in vitro and in vivo (Simon et al., 2006, Sotty et al., 2003, Zhang et al., 2010). Although cholinergic neurons do not show phase coupling with the hippocampal oscillations, they increase their activity during hippocampal theta oscillations (Simon et al., 2006, Zhang et al., 2010). Since the cholinergic neurons fire at low frequencies, acetylcholine release might increase the general network excitability and sensory-related drive to the hippocampus, rather than setting the pace of theta rhythm (Buzsaki, 2002, Vandecasteele et al., 2014).

In the hippocampal CA1, the primary targets of cholinergic terminals are the proximal dendrites and soma of pyramidal neurons (Frotscher and Leranth, 1985, Kiss et al., 1990, Sun et al., 2014). The cholinergic fibres also induce different timing responses in the hippocampal interneurons, which express different cholinergic receptors to the muscarinic and nicotinergic. The muscarinic receptors have a slower transient response compared with the nicotinergic receptors. The high diversity of interneurons increases the complexity of cholinergic actions in the hippocampus, as described in section (1.2.4), interneurons can innervate different compartment of pyramidal cells and other interneurons, forming complex networks (McQuiston, 2014, Müller and Remy, 2014). Furthermore, selective lesions of MS cholinergic projections to the hippocampus can impair the formation of place fields in a novel environment (Wilson et al., 2005) and auditory fear memory (Staib et al., 2018). Suggesting that MS cholinergic neurons are potent modulators of memory formation (Maurer and Williams, 2017).

1.4.3.2. MS glutamatergic neurons

The glutamatergic medial septum neurons are estimated to constitute 25% of the MS population and to provide 4% of the septohippocampal projections in mice (Colom et al., 2005, Henderson et al., 2010). In the hippocampal CA1, glutamatergic projections terminate in both pyramidal cells and inhibitory interneurons; however, pyramidal cells receive three-fold more glutamatergic projections compared to interneurons (Sun et al., 2014). Glutamatergic neurons are mutually connected with cholinergic and GABAergic neurons within the MS (Manseau et al., 2005, Leão et al., 2015). Moreover, they form a heterogenic population in the MS concerning size and firing patterns, including fast-spiking, slow-spiking, cluster and burst spike patterns (Huh et al., 2010). They are characterized by the expression of vesicular glutamate transporters (VGluT) type 1 or VGluT type 2 and by the lack of expression of either ChAT or GAD (Sotty et al., 2003).

The activity of MS VGluT2 is related to movement in rodents, the frequency of these neurons increases before the movement starts and get higher during running compared to resting states. Optogenetic activation of MS VGluT2 neurons in the theta band induces movement. The higher the frequency of the stimulated theta, the shorter is the time lag between the beginning of stimulation and the resulting running initiation. Subsequent running speed is also positively correlated to the stimulation frequency. Furthermore, optogenetic activation of glutamatergic septal (VGluT2+) neurons in the theta frequency band induced frequency-lock oscillations in CA1 by regulating feedforward inhibition via septohippocampal projections onto alveus/oriens interneurons (Fuhrmann et al., 2015, Robinson et

al., 2016). Even a short stimulation of septal glutamatergic neurons could entrain self-sustaining hippocampal theta with subsequent running initiation (Fuhrmann et al., 2015).

1.4.3.3. MS GABAergic neurons

The GABAergic projections from the medial septum target predominately hippocampal GABAergic interneurons expressing parvalbumin (Freund, 1989, Freund and Antal, 1988, Sun et al., 2014, Unal et al., 2015). In contrast, hippocampal projections to MS are predominantly somatostatin-expressing neurons which form synapses mostly with MS GABAergic parvalbumin, and in smaller proportion with MS cholinergic neurons (Jinno and Kosaka, 2002). As described before, a subpopulation of hippocampal projections ends in the same neurons that projects back to the hippocampus, forming a septo-hippocampal loop (Toth et al., 1993, Elvander-Tottie et al., 2006). Parvalbumin-expressing MS neurons show hippocampus theta-related firing at different patterns, e.g., theta bursting and non-bursting, theta modulated and independent theta firing (Gogolak et al., 1968, Gaztelu and Buno, 1982). Moreover, a subpopulation of parvalbumin neurons expresses hyperpolarization-activated cyclic nucleotide-gated channels (HCN). These neurons are likely to induce local theta synchronization in the MS and provide theta rhythmic drive to the hippocampus since they produce theta rhythmic activity in the lack of hippocampal theta (Borhegyi et al., 2004, Petsche and Stumpf, 1962, Wang, 2002, Varga et al., 2008).

1.4.4. Septal stimulation

The septum was the first area to be associated with intracranial self-stimulation (ICSS), rats implanted with an electrode into the septal area could learn to press a lever to receive electric stimulation (Olds and Milner, 1954). In addition, subsequent studies showed that rodents could press the lever until exhaustion to receive electrical stimulation in the septum (Ball and Gray, 1971, Cazala et al., 1988). Since the discovery of the ICSS in the septum, many areas have been described to induce self-stimulation. Olds experiments showed that stimulation on the lateral hypothalamic medial forebrain bundle, which is a pathway containing fibres from the septum, lateral hypothalamus, and tegmentum of the midbrain (including the ventral tegmental area), induced fast and persistent self-stimulation (Olds, 1958b).

MS self-stimulation has been reported to be phase-locked with hippocampal theta cycles (Buno and Velluti, 1977). GABAergic septohippocampal projections have been associated with learning of lever pressing to receive ICSS (Vega-Flores et al., 2014, Mitoma et al., 2003). Mice have been reported to self-administrate $GABA_A$ receptor agonist muscimol and not $GABA_A$ receptor antagonist bicuculline in the septum. Moreover, injection of halobenzazepine in the ventral tegmental area prevented self-administration of muscimol, suggesting that dopamine release in the VTA may be involved in the acquisition of this behaviour (Gavello-Baudy et al., 2008). The septum complex also supports the self-administration of α-amino-3-hydroxyl-5-methyl-4-isoxazole-propionate (AMPA), an agonist for AMPA receptors which mimics the effect of glutamate, suggesting that MS glutamatergic neurons could be involved in self-stimulation behaviour (Liu et al., 2008).

1.5. Objectives

The medial septum is a vital component of the subcortical network which synchronizes hippocampal oscillations during activity states. This interaction is required for memory formation and spatial processing. Moreover, the MS has been associated to reward for over fifty years. Considering the importance of understanding how the medial septum modulates hippocampus and reward processing, the work presented in this thesis aims to:

- Determine how the expression of ChR2 by AAV controlled by nonselective Hsyn promoter affects medial septal theta modulated neurons, which has been described to control hippocampal oscillations.
- Assess how hippocampal theta and non-theta modulated interneurons are affected by MS nonselective stimulation.
- Determine if nonselective optogenetic stimulation of the MS could induce reward-related behaviour, by assessing the place preference during MS stimulation.
- Investigate the role of MS GABAergic and cholinergic neurons on place preference behaviour using transgenic animals.
- Examine if medial septal stimulation could exert a modulatory effect on hippocampal place cells properties and stability
- Investigate if hippocampal place cells can encode MS stimulation.

Together these results will contribute to furthering our understanding of reward processing and improving our understanding of medial septum function on the hippocampal electrophysiology, oscillations and spatial processing.

2. Chapter

General Methods

"All animal work has been carried out in the Health Products Regulatory Authority (HPRA) authorised establishment, Trinity College Dublin (establishment authorisation number: AE19136) ensuring compliance with the requirements of Directive 2010/63/EU and S.I. No. 543 of 2012. This work has also been approved by the TCD Animal Research Ethics Committee (AREC) which is a Level 2 ethics committee responsible for reviewing the proposed use of animals in teaching and research in line with the Research Ethics Policies in operation in TCD".

2.1. Housing conditions

Before any experimental procedures, the rats were allowed to acclimatize to their housing for at least five days, during this time they were handled and habituated to the laboratory environment and experimenter. They had ad libitum access to food and water in a temperature-controlled (18-22 °C) laminar airflow unit, maintained on a 12-hour light (8 a.m. - 8 p.m.) and 12-hour dark cycle. After surgery, animals recovered at least for seven days having access to food and water ad libitum. During recording sessions, rats received 10-25g of food as standard each day and 15-20 mg of food pellets (TestDiet, Formula 5TUL, USA) during each trial. The recording sessions were conducted during the light phase (10 a.m. – 18 p.m.) and, in between session the rats were kept in the conditions described above.

2.1.1. Electrodes and Microdrives

We used platinum-iridium wires which are inert and resistant to corrosion. The low impedance of these materials results in an excellent signal to noise ratio when recording. The recordings microdrivers were constructed using eight bundles of four platinum-iridium wires (total of 32 channels) (90% platinum, 10% iridium; HM-L insulated, 25µm bare wire diameter, (California fine wire Ltd., California, USA) twisted together. The microdrive (Axona Ltd., UK) was constructed using moveable screw allowing tetrode advancements in steps of as little as 25 µm. The wires were carefully inserted into the microdrive 25-gauge guide cannula and protected by a 21-gauge outer cover. Each wire was manually connected to the corresponding wire of the microdrive and soldered. To protect and isolate the wires, the microdrive was covered with several layers of nail polish. On the day of surgery, the electrodes were measured and cut at an angle of about 10 degrees.

2.1.2. Electrodes implantation and viral injection

Male adult rats (Lister Hooded, 350-450 gr) were anesthetized using isoflurane via a gas anesthesia system with an average flow rate of 1.0 ± 0.3 litres per minute inside an anaesthetic chamber. The animal's head was shaved and returned to the chamber for 5 min. The anaesthetic gas was then switched to the mask of the stereotaxic frame, and the animal was fixed by ear bars. Iodine was placed on the animal's head and eyes protected with eye cream. The animal's breathing was monitored, and isoflurane level was adjusted throughout the surgery to ensure the

correct anaesthetic state. An incision (about 2 cm) was made, followed by cleaning in order to expose lambda and bregma. Measurements were made to ensure that the skull was horizontally aligned. Coordinates for injection and electrodes were marked with a pen for further drilling. Animals were injected with a recombinant adeno associated virus (AAV) to express channelrhodopsin-YFP. The virus was injected with a volume of 2 µL at the rate of 0.2 µL/min using a Hamilton syringe. After injection, the needle was left in place for ten additional minutes, to allow the virus to disperse inside the brain before it was withdrawn slowly. After virus injection, an optic fibre (200 µm core diameter, Thorlabs Inc.) was chronically implanted. For neural recordings, the tetrodes were inserted into the target area. The scalp was scratched to remove all blood vessels and to create a rough surface for better adhesion of the dental cement. For stabilization of the microdrive on the animal's head, five to six stainless steel screws were inserted on the skull. To reduce noise, a ground wire was soldered on a screw and connected to the microdrive ground. The assembly was permanently attached to the skull using dental cement. Implanted animals were housed individually with ad libitum access to water in a food controlled stated to keep animals 85-90% their weight at surgery day. Animals recovered for at least seven days before any experiment.

The table below shows the animals used in the experiment and chapters.

Table 1 Number of animals used for each experiment/chapter

Rats	Tetrodes	Virus injection	Procedures	Chapters
MS1	32 in MS	2 µL in MS	open field	3
MS2	32 in MS	2 µL in MS	open field	3
MS3	32 in MS	2 µL in MS	open field	3
MSCA1	32 in CA1	2 µL in MS	open / square	3
MSCA2	32 in CA1	2 µL in MS	open / square	3/4/5
MSCA3	32 in CA1	2 µL in MS	open / square	3/4/5
MSCA4	32 in CA1	2 µL in MS	open / square	3/4/5
MSCA5	32 in CA1	2 µL in MS	open / square	3/4/5
MSCA6	32 in CA1	2 µL in MS	open / square	3/4/5
MSCA7	32 in CA1	2 µL in MS	open / square	3/4/5
MSCA8	32 in CA1	2 µL in MS	open / square	3/4/5
MSCA9	32 in CA1	2 µL in MS	open / square	3/4/5
Chat1	32 in CA1	2 µL in MS	squared	4
Chat2	32 in CA1	2 µL in MS	squared	4
Chat3	32 in CA1	2 µL in MS	squared	4
Chat4	32 in CA1	2 µL in MS	squared	4
Gad1	32 in CA1	2 µL in MS	squared	4
Gad2	32 in CA1	2 µL in MS	squared	4
Gad3	32 in CA1	2 µL in MS	squared	4
Gad4	32 in CA1	2 µL in MS	squared	4
Gad5	32 in CA1	2 µL in MS	squared	4
Gad6	32 in CA1	2 µL in MS	squared	4

2.1.3. Stereotaxic coordinates

The table below describes the stereotaxic coordinates in relation to bregma. The table contains the anterior-posterior (AP), mediolateral (ML), dorsoventral (DV) and angle used for each target area. All implants were unilateral.

Table 2: Stereotaxic Coordinates

CA1	**-3.8 AP**	**-2.5 ML**	**1.4 DV**	**0 ML**
MS	+0.8 AP	-1.4 ML	5.5 - 6.5 DV	10 º ML
LH	-2.4 AP	+2.6 ML	8.8 - 9.0 DV	-25 º ML

2.1.4. Virus construction

All the viral constructions were serotyped with AAV5 coat proteins which were demonstrated to express in the MS. Both viral constructions were packaged by Vector Core at the University of North Carolina. Viral titers ranged from 1.5 to 1.8 x 10^{12} particles per mL.

Table 3 Viral construction

Viral construction	Adgene code
AAV5.EF1a-DIO.hChR2-(E123T/T159C).EYFP.WPRE.hGH	35509
AAV5.hSyn.hChR2(H134R)-eYFP.WPRE.hGH	26973P

2.1.5. Laser stimulation

Blue laser light was provided by a 473nm multimode fibre-coupled diode laser source (model S1FC473MM, Thorlabs, USA), the laser module was modulated by a direct digital synthesizer (JYETech, China). The synthesizer generated squared waves from 20 – 50 Hz, the power in the tip of the optic fibre was set to 10-12 mW,

and the stimulation protocols were generated by an internal Basic script on the recording system. Before stimulation, an optic cable was connected to the cannula implanted in the animal. To avoid light leakage, two heat shrinkable sleeves covered the connection. Two laser stimulation protocols were used; during open arena recordings, the laser was active every 6s using a sequence of 12 pulses of 5 ms duration and during linear squared recordings, the laser was constantly flashing 5 ms pulses while the animal was on the south west corner of the arena.

2.2. Experimental apparatus

All electrophysiological recordings were conducted in awake rats in two different environments (open field and linear square maze). Open field was used for screening of cells and establishing baseline photostimulation responses. Once the tetrodes were at the pyramidal layer of the hippocampus, the linear squared maze was used to evaluate the effect of the photostimulation on the animal's behaviour (real-time place preference, chapter 5). After the end of the behaviour protocol, interneurons (chapter 4) and place cells were recorded during MS stimulation (chapter 6).

2.2.1. Open field

To assess the effect of the photostimulation on the cells, rats were placed on an open field arena which consisted of a square (60 cm x 60 cm) made of plywood,

painted black arena, elevated 30cm from the floor. During sessions, the animals were placed on the arena and food pellets (TestDiet, Formula 5TUL) were thrown in every 20 seconds to pseudo-random locations within the open field ("random foraging" task); in this way, animals moved continuously, allowing for a complete spatial sampling of the environment (Muller et al., 1987). Each recording sessions consisted of two back to back 12 min recording (baseline followed by stimulation). For the stimulation sessions, the laser was controlled by the recording system software through DACBASIC scripts (Axona Ltd.), the laser was switched on every 6 seconds using the following laser protocol: 12 pulses of 5 ms pulse duration of blue light 473 nm. During sessions, the rat's trajectory path was also recorded using a LED tracking system.

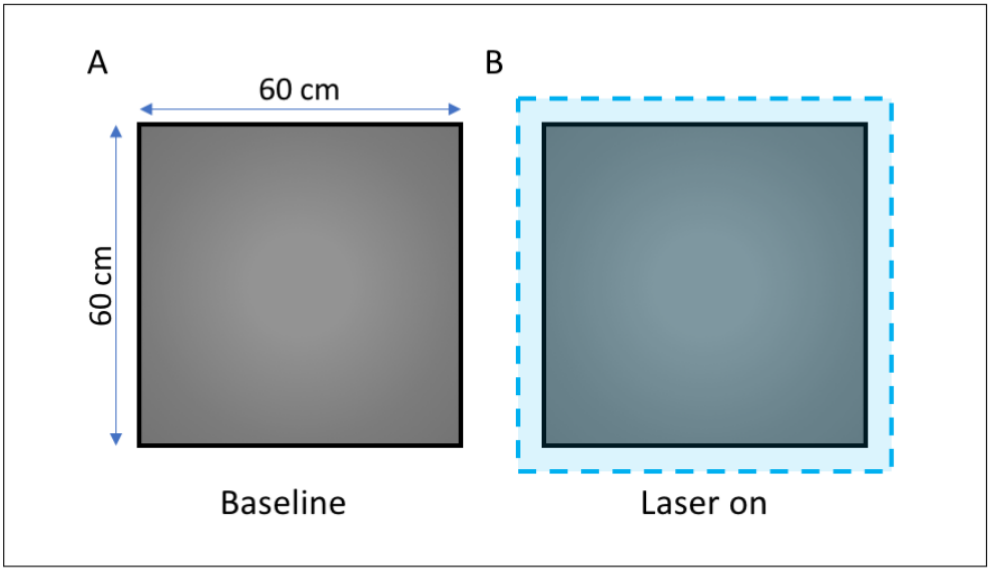

Figure 7. Pellet chasing task.

A (60 x 60 cm) plywood arena elevated 30 cm from the floor. **(A)** The rats were recorded for 12 min without laser stimulation while sugar pellets were thrown on the arena. **(B)** The animals were recorded for another 12 min in the same conditions as A, but the laser was automatically turned on every 6 s.

2.2.2. Rectangular linear track

A squared arena, 85cm x 85 cm and 10 cm wide made of plywood painted black and elevated 30 cm above the floor was used for place preference discrimination and place field comparison. During training sessions, animals were free to navigate between the SW and NE corners, where two food pellets (TestDiet, Formula 5TUL) were alternated placed on the corners. The animals could navigate in both clockwise and anticlockwise directions. For place preference assessment, the experiment was divided into a baseline session, followed by a laser stimulation session.

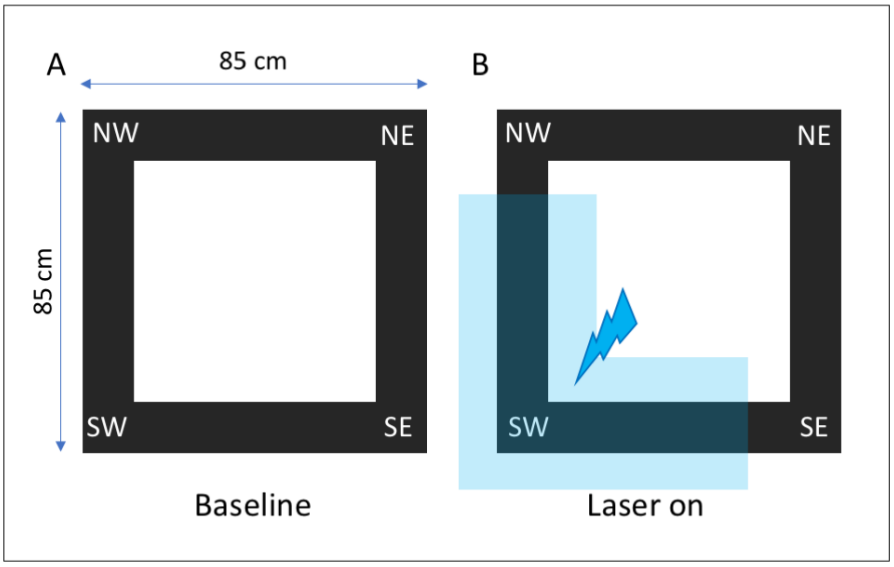

Figure 8. Rectangular-shaped linear track.

The (85 x 85 x 10 cm) arena made of plywood was used to test for place preference and to record place cells. **(A)** During the baseline recordings, sugar pellets were presented on southeast (SE) and northwest (NW) corners. The rats were running towards both sides of the arena. Both the time and passes on the SW and NE corners were measured. **(B)** During the laser on recordings, the conditions were the same as in baseline, except that the laser was turned on while the rat was positioned on the SE-SW-NW side (blue area).

For the stimulation sessions, the laser was controlled by the recording system software through DACBASIC scripts (Axona Ltd.), the laser was switched on while the animal was on the north arm or the west arm of the maze, with continuous photo-stimulation trains. The stimulation trains were composed of 12 pulses of 5 ms pulse duration of blue light 473nm followed by 500 ms inter-train interval. Intercalated sessions were recorded, i.e., baseline followed by photo-stimulation. The session length was 12 minutes for both baselines and photo-stimulation, the cells were recorded as well as rat's trajectory path by a LED tracking system.

2.3. Data acquisition

2.3.1. Spike recording

Recording sessions started at least seven days after surgery. During sessions, a 32-channels head stage amplifier was connected between the microdrive and the data acquisition system (Axona Ltd., UK). Tetrodes were lowered 50µm three times a day until cells were detected. Once waveforms were detected, the lowering was reduced to 10µm steps in order to improve the signal/noise relation. Signals were amplified 5000 – 10000 times and bandpass filtered (380 Hz - 6 KHz). To reduce the amount of data collected, a threshold was set up in relation to the noise and only waveforms three times bigger than the threshold were captured. Spikes were stored to disk at 44.1 KHz (50 samples per waveform at 8 bits per sample), with a

timestamp vector recorded at the same sample. Electroencephalograms (EEGs) were recorded 32 times, one for each electrode at a sampling frequency of 250 Hz and stored to disk for offline analysis.

2.3.2. Position tracker

A camera positioned on the room ceiling was coupled with the recording system to track the position of the infrared LED attached to the head stage, while the animal moved on the arena. The LED position was converted into X and Y coordinates at a sampling of 50 Hz and post-hoc synchronized with the neural signal.

2.3.3. Referencing

Due to the high amplification of relatively low amplitude waveforms, noise poses a major problem for these types of recordings. In order to minimize noise, each tetrode with minimal background signal and no cellular activity. The signal from both tetrodes was then subtracted to eliminate common waveforms.

2.4. Data analysis

2.4.1. Spike sorting

Implanted tetrodes pick up extracellular neural activity from all neurons in close proximity to electrode recording tip. The distance between the source of the signal (neuron) to each of the four tetrodes wires results in minor differences in the recorded waveform and was used for cell identification (figure 9.a). To separate the waveforms recorded from different cells, the neural signal was clustered by the k-means algorithm, using graphical software (Tint, Axona Limited). Waveforms were separated based on spike amplitude, duration, maximum and minimum spike voltages and duration of the peaks In addition, autocorrelation was plotted for inspection of the clustering quality (figure 9).

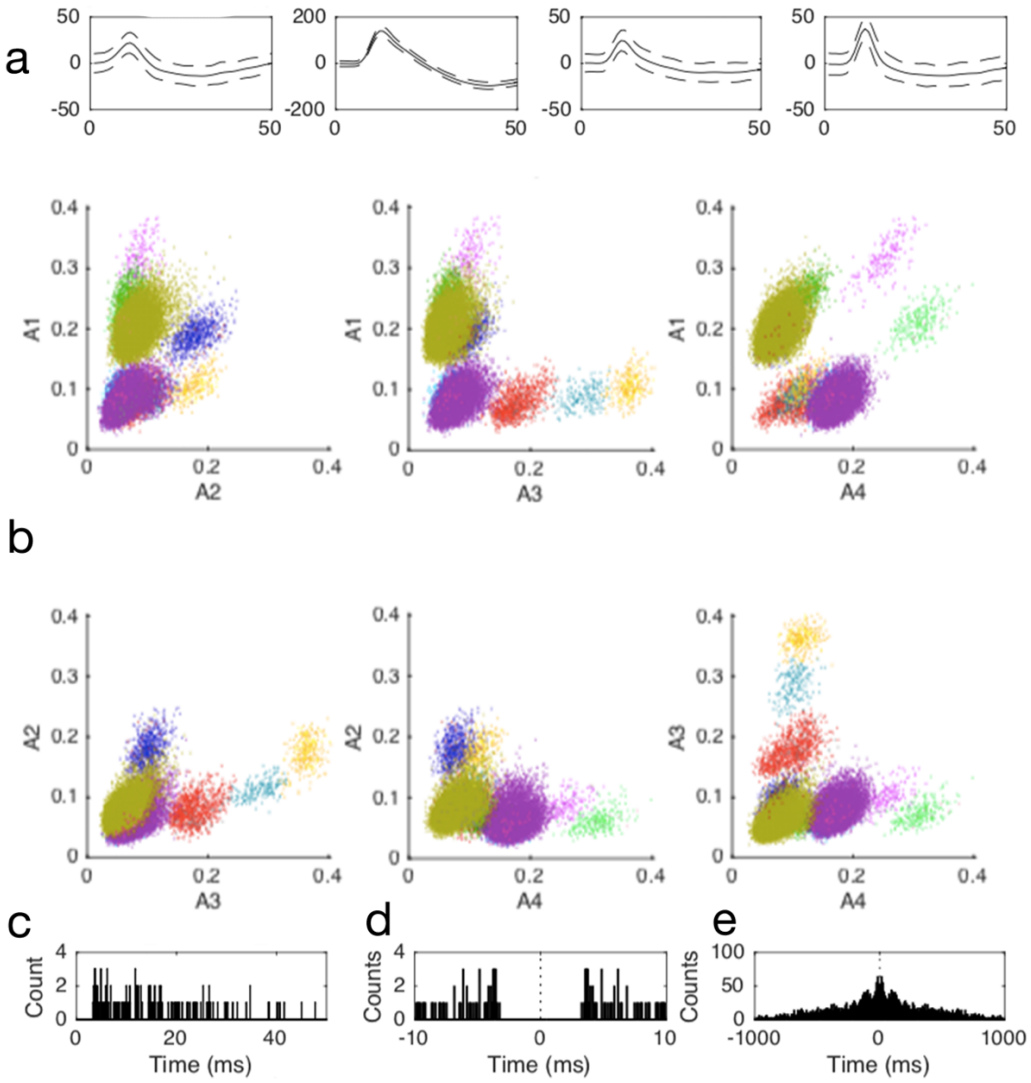

Figure 9 Single-cell isolation.

(a) Examples of waveforms of a neuron recorded in one tetrode. Each waveform is a copy of the same cell detected by different electrodes. **(b)** Example of clustered spikes from different neurons. Spikes were separate in clusters based on spike amplitude, duration, maximum and minimum spike voltages and duration of the peaks. **(c)** Autocorrelation histograms plotted in different times used to check unit isolation and to evaluate oscillatory properties of the neuron.

2.4.2. Data exclusion criteria

Following spike sorting, each spike of a given cluster was compared with all other spikes of the same cluster in a -10 to 10 ms time window and plotted as a histogram (figure 9.d). This process produces an autocorrelation histogram. The resulting histogram displays the most frequently occurring spike intervals. Based on the refractory period of hippocampal pyramidal cells, clusters that presented intervals less than 2 ms after cell isolation, were excluded from further analysis. Units that had less than 50 spikes per 12 min session (0.07 Hz) were also excluded. Lastly, clusters were plotted for a subjective visual examination of the similarity between sessions. To ensure the same cell was recorded in more than one session, spike cluster distribution, spike amplitudes, and waveforms were compared in subsequent sessions.

2.4.3. Spike properties

To ensure that the same cell was recorded between sessions, for each isolated cell, the mean and standard deviation of the spike width, height and amplitude were calculated. Cells with significant changes in these properties were excluded from the intersession analysis.

2.4.4. Place fields definition

The place fields were calculated by synchronizing the information from the animal's position (camera) with the spike times of an isolated cell. The resulting firing map was divided into 2 cm^2 square bins. Time spent within the bin was normalized by the number of spikes in each bin. The rate map was smoothed by a 2-D, five by five bins box filter. The place field was defined as a cluster of 9 or more adjacent bins of mean frequency above 0.5 Hz sharing at least one side with another bin in which the firing rate was higher than 20% of the peak firing rate.

2.4.5. Units classification

To classify units into interneurons or place cells, for each unit we calculated the spatial information, spatial coherence and sparsity. Spike times were shuffled 300 times and for shuffle, the spatial information, spatial coherence and sparsity were calculated. A unit was classified as a place cell when all criteria meet the following requirements: a spatial information value of the unit was greater than the 95^{th} percentile of the shuffled spatial information distribution; a coherence value was greater than the 95^{th} percentile of the shuffled coherence distribution and a sparsity value was smaller the 5^{th} percentile of the sparsity distribution. Otherwise, the unit was classified as interneuron.

2.4.6. Autocorrelation histograms

Autocorrelation histogram is a standard method to control the quality of the clustering and single-unit isolation. An autocorrelogram ρ_f (t) is defined for a discrete time series f(t) with a lag $\boldsymbol{l}$ as follow:

$$\boldsymbol{\rho_f(l) = \sum_{i=-\infty}^{n} f(n) f(n-l)}$$

1

The autocorrelation histogram was calculated with a time lag of -10 ms to 10 ms and 50 ms (figure 9.c and 9.d) for control of the cell isolation. Spikes within the refractory period (2 ms) were excluded. The -1000 to 1000 ms autocorrelation (Figure 9.e) was used to identify oscillatory patterns, mainly in the theta band frequency (4 -12 Hz).

2.4.7. Theta index

To estimate if a neuron spikes in theta frequency, a sin wave with a decaying amplitude was fitted to the 1000 ms autocorrelogram of the neuron.

The sine wave equation is defined as

$$y = \left[A\left(\sin\left(\frac{\pi}{2} - \omega t\right)\right) + b\right].e^{\frac{-|t|}{\tau_1}} + ce^{\frac{-t^2}{\tau_2}}$$

Where t is the time, A, b, τ_1, τ_2 and ω are the fit parameters. The least squares algorithm was used to fit the parameters to the autocorrelogram. The theta index is calculated by the ration A:b between the maximum amplitude of the waveform and the maximum, excluding the first peak (Royer et al., 2010).

2.4.8. Spatial Information

Proposed by Skaggs (Skaggs et al., 1993), the spatial information content of a cell in bits/spike is a measure of how much a spike can predict a feature, in this case, the location. The spatial information can be calculated using the equation:

$$I = \sum_i \left(\frac{\lambda_i}{\lambda}\right) . log_2 \left(\frac{\lambda_i}{\lambda}\right) . p_i$$

2

Where p_i is the probability of the animal being at the bin i, λ_i is the mean firing rate of the cell in the bin i, λ is the mean firing rate for the whole trial, and I is the information content. The change in the spatial information of a place field between two recordings was calculated as the difference between both recordings.

2.4.9. Bursting units

Burst was defined as a group of two or more spikes having an inter-spike interval smaller than 5 ms. A propensity to burst, also called burst index, was defined as the number of bursts divided by the number of spikes. This definition is often used

to quantify the overall bursting property of a neuron, units were classified as a bursting cells, if they had a burst index larger than 10% (Ramcharan et al., 2005, Anderson and O'Mara, 2003).

2.4.10. Grand Rate

The grand rate was defined as the average firing frequency of a cell within its place field, is also called the infield rate. It is calculated by the sum of all spikes inside the place field divided by the time spent inside the place field area.

2.4.11. Phase-Locking Value

The phase-locking value is a statistics method first developed to measure synchrony in brain signals (Lachaux et al., 1999). It measures the phase difference across trials, if the phase difference variability is small, the resulting measure is close to 1. Here the method was used as described in (Mamad et al., 2015). To calculate PLV, the hippocampal LFP signal was filtered using a band-pass filter and divided into 4s epochs. A Hilbert transformation was used to compute the instantaneous phase of the epochs. The transformed epochs were summed and normalized. To calculate the shuffled PLV, the epochs were shuffled 2.000 times. The result was the comparison between the shuffled and non-shuffled signal.

2.4.12. Passes score

Passes were defined as the number of times that the animal crossed from SW to NE or from NE to SW in both directions. The animals could cross from SW to NE through NW or SE. Passes score between the two sides of the arena was expressed by calculating a difference/sum score of the passes. The score for a pair (SW, NE) of each condition was obtained by calculating the unsigned difference (SW - NE) and dividing by their sum (SW + NE). The results ranged from -1 to 1. A score of 0 indicating that the animals equally passed on both sides; an extreme value of -1 indicates that the animals only passed on the NE side, whereas a passes score of 1 indicates that the only passed on the SW side.

2.4.13. Firing rate analysis

The firing rate change between the two sessions was calculated by dividing the signed difference between the mean firing rates by the sum of the mean rates.

$$R_s = \frac{r_{base} - r_{stim}}{r_{base} + r_{stim}}$$

3

Where r_{base} is the mean frequency of the baseline session, r_{stim} is the mean frequency of the stimulation session and R_s the diff/sum score. The resulting value varies from -1 to 1 where 0 represents no difference between sessions and 1 or -1 indicates that one of the rates were zero.

2.4.14. Field size analysis

The difference between field sizes was calculated analogue to the firing rate score.

$$F_s = \frac{f_{base} - f_{stim}}{f_{base} + f_{stim}}$$

4

Where F_s is the field score and f_{base} and f_{stim} are the field size for each respective session.

2.4.15. Running speed and spike frequency correlation

To identify if the firing frequency of cells was correlated with the animal's speed, the animal's raw speed data values were smoothed by a moving average windows of 5 samples (100 ms). The session was divided into time bins containing different speeds, from 1 m/s to 35 m/s. The spikes recorded were classified in relation to the speed bins. The number of spikes was normalized by the time that the rat spent in that speed, resulting in a firing rate. The points were fitted in linear regression, and a Pearson's correlation coefficient assessed the quality of the regression and only $p<0.001$ where considered.

2.4.16. Real-time place preference

Real-time place preference (Stamatakis and Stuber, 2012b) was performed using the linear squared maze described in session (3.2.2). The maze was situated in the

middle of the recording room where many visual cues were visible. Rats were allowed to run freely during recordings. Presentation of sugar pellets (TestDiet, Formula 5TUL) was alternated between the two different corners, i.e., the rat only received food in the corner when he completed half maze (from SE to NW). For one week the rats were trained to run in both sides of the maze equally by controlling the number of sugar pellets and directing the animal when necessary. The baselines recordings started when the rats began navigating approximately equally in both sides of the arena without intervention for at least three recordings. The baselines consisted of three recordings of 12 min followed by three stimulation recordings. The laser activation was programmed using a "Basic" script which was running on the recording equipment. The program read location information via the camera and delivery laser stimulation only when the animal was localized on the designated side of the maze. Every time the rat entered the designated reward area, the laser was turned on, delivering the stimulation protocol (5 ms pulse duration, 12 pulses per train at 50 Hz, 500 ms inter-train interval). As soon as the rat entered the reward area, the laser was turned on, and the stimulation protocol was set to be repeating for as long as the animal stayed in the reward area.

2.4.17. Classification of Photo-Responsive Cells

Cells that responded to light were identified by comparing the firing rate before and during stimulation. The spikes times of each cell were divided into epochs of maximum length around each stimulation time without superposition to form a raster plot. Cells were classified as into 2 groups: 'inhibited' group when the firing

rate during the stimulation reduced by at least 33% and 'disinhibited' group when the firing rate increased at the same proportion. A Wilcoxon signed-rank test was applied in a random subpopulation (n=15) of already classified cells to confirm that rate changes were statistically significant ($p<0.05$). The group of non-effected cells was all the remaining cells that were not classified based on the criteria above (Schoenenberger et al., 2016).

2.4.18. Centre of mass

Centre of mass (COM) derives from the physical concept, it is the unique point resulting from the average of all position vectors weighted by the mass. In neuroscience, the mass is substituted by the spiking frequency and is commonly used to describe the centroid of a place field (Mamad et al., 2017).

The coordinates of the centre of mass are calculated as follow:

$$x_{COM} = \frac{\sum_i \sum_j i \cdot f_{i,j}}{\sum_i \sum_j f_{i,j}} \cdot l_{bin} - \frac{l_{bin}}{2};\ \ y_{COM} = \frac{\sum_i \sum_j j \cdot f_{i,j}}{\sum_i \sum_j f_{i,j}} \cdot l_{bin} - \frac{l_{bin}}{2};$$

5

Where l_{bin} is the length of the edge of the bin, f_i is the frequency inside bin i.

To calculate the shift of a place cell between two consecutive recordings in the open field, we defined the ΔCOM, which is calculated as the distance between two coordinates as followed:

$$\Delta COM = \sqrt[2]{(x_{COMa} - x_{COMb})^2 + (y_{COMa} - y_{COMb})^2}$$

6

Where (x_{COMa}, y_{COMa}) are the coordinates of the COM of the place field A and (x_{COMb}, y_{COMb}) are the coordinates of COM of the place field B of the same cell in two consecutive sessions.

2.4.19. Symmetric COM distance

The ΔCOM defined above was used for open-field arena analysis; however, the simple calculation of the Euclidean distance used in the open arena cannot be used in arenas with complexes topologies. The method used, described in Mamad et al (2017) uses the symmetric property of the arena to calculate the centre of mass with reference to the symmetric axis of the arena. The distance between the symmetric axis and the centre of mass is calculated as:

$$dist_{COM/sym} = \frac{\left| det \begin{bmatrix} D_x - 0_x & D_y - 0_y \\ COM_x - 0_x & COM_y - 0_y \end{bmatrix} \right|}{\sqrt{(D_x - 0_x)^2 + (D_y - 0_y)^2}}$$

7

Where $0_{x,y}$ is the x, y coordinates of the NE corner of the arena, considered as the origin of the symmetric axis, $D_{x,y}$ the x, y coordinates of the SW corner of the arena and $COM_{x,y}$ are the coordinates x, y of the centre of mass.

The distance from the origin to the projection of the centre of mass to the symmetric axis can be calculated as the vector:

$$\overline{OP} = \sqrt{\left(COM_x^2 + COM_y^2\right) - dist_{COM/sym}{}^2}$$

8

The COM distance was normalized by the arena width as below:

$$dist_{norm} = \begin{cases} \dfrac{dist_{COM}}{\overline{OP} \cdot C}, \overline{OP} < \dfrac{\overline{OM}}{2} \\ \dfrac{dist_{COM}}{(\overline{OM} - \overline{OP}) \cdot C}, \overline{OP} > \dfrac{\overline{OM}}{2} \end{cases}$$

9

Where the $\overline{OM}$ is the diagonal, from the origin O (NW) to M (SE), C is a correction factor introduced to compensate outliers in the motion tracking.

2.4.20. COM angle

The COM angle was defined as a form of presenting the COM of a cell in relation to the axis of symmetry (north-west to the south-east corner), an angle of 45° represents total symmetry of the firing distribution. The symmetry angle was calculated as:

$$\theta_{COM} = \begin{cases} 45° \cdot (1 - dist_{norm}) \,,\; COM_x < COM_y \\ 45° \cdot (1 + dist_{norm}) \,,\; COM_x > COM_y \end{cases}$$

10

Where $dist_{norm}$ is the COM distance calculated in equation 9.

2.4.21. Spatial Population Vector

The spatial population vector was used to evaluate the influence of the laser stimulation on the firing behaviour of the whole population of recorded place cells. The population vector of place fields' distribution consists of the COM angle of each place cell, it is calculated as

$$SPV_{weighted} = \frac{F \cdot D}{\|F\|}$$

11

Where D is the vector of place fields' distributions, F is the vector of the firing rate distributions. The SPV average is calculated as the norm of the population vector divided by the number of place cells N.

$$SPV_{Avg} = \frac{\|D\|}{N}$$

2.5. Post-mortem verification

2.5.1. Transcardial perfusion and tissue fixation

After completion of electrophysiological recordings, brains were removed for histological verification of the expression of the virus and the localization of the electrodes and optic fibre. Animals were first anesthetized with isoflurane and injected with pentobarbital sodium (150 mg/kg) (Euthanal, UK). To remove intravascular blood, the animal was anesthetized deeply and perfused transcardially with ice-cold phosphate buffered saline (~200 ml per rat) followed by paraformaldehyde (4% (w/v)) at 4°C (~250 ml per rat). The entire brain was removed from the cranium and post-fixed in PFA (4% (w/v) at 4°C). For cryoprotection, brains were transferred to a sucrose solution (30% (w/v) sucrose in phosphate buffer) for at least 72h. Before freezing, brains were coated in an optimum cutting temperature (OCT) medium (TissueTek, VWR International). A cylinder of aluminium foil (moulded around a tube) was used to hold the brain

and coat it in OCT, and these brain cylinders (with OCT) were frozen dry ice and stored at -20°C for later sectioning.

2.5.2. Tissue preparation

Before post-mortem verification of the position of the electrodes, brains were sliced using a cryostat (Leica CM1900). Brains frozen in OCT were transferred to the cryostat (-20°C) where they were fixed with OCT on a cork disc, which was inserted in the cryostat. Brain tissue was coronally sectioned at 40µm thickness. For verification of the electrodes and viral expression, sessions were mounted onto microscope slides. Once all slices were collected, they were stored in slide boxes and kept at -20°C until the immunohistochemistry assay or imaging.

2.5.3. Verification of the virus expression and electrodes position

Sections were examined with an Olympus BX51 fluorescence microscope in 488 nm for the viral expression of YFP. No quantification of the expression was made, animals with no green fluorescence were excluded from the analysis. Moreover, the position of the tetrodes was identified using the rat brain atlas (Paxinos & Watson, 2007).

2.6. Statistical analysis

Statistical analysis of all data was performed using GraphPad Prism version 7.02 for Windows (GraphPad Software, San Diego California, USA). Statistical significance was estimated by using a 2-tailed independent samples t-test for non-paired or Student t-test for paired data. Repeated measures were evaluated with a 2-way analysis of variance (ANOVA) paired with a post hoc test. Correlations between datasets were determined using Pearson's correlation coefficient. The probability level interpreted as significant was fixed at $p < 0.05$. All data points are plotted ± SEM.

3. Chapter

The Effect of Nonselective Optogenetic Stimulation of The Medial Septum on Hippocampus Interneurons

3.1. Introduction

It is widely accepted that the hippocampus is crucial for learning, memory and spatial processing (Burgess et al., 2002, Burgess, 2002). These cognitive functions depend on synchronized coordination of a significant number of neurons, which is achieved by network oscillations (Fuentemilla et al., 2010, Lisman, 2010, Bocchio et al., 2017). The main hippocampal oscillation present in the LFP is the theta band (4-12 Hz in rodents), which can be detected during movement and REM sleep (Buzsaki, 2002). It is well documented that the MS is crucial to cognitive processing by contributing to theta generation for the hippocampus (Buzsaki, 2002, Berens and Horner, 2017). Theta bursting MS cells have been described to fire in phase with hippocampal theta oscillation (Alonso et al., 1987, Stewart and Fox, 1989b, Brazhnik and Fox, 1999). Likewise, electrolytic lesion of the medial septum permanently abolished hippocampal theta oscillation (Green and Arduini, 1954, Leung, 1987).

The hippocampal interneurons are inhibitory GABAergic neurons, which represent ~10-15% of the neuronal population in rats. They form a heterogeneous population concerning morphology, anatomy, and connectivity. They also differ in receptors and synaptic targets specificity from surrounding neurons (Pelkey et al., 2017). Interneurons are found scattered throughout all layers of hippocampus CA area, forming highly complex networks with the pyramidal cells and with other interneurons (Freund and Buzsaki, 1996, Klausberger and Somogyi, 2008, Bezaire and Soltesz, 2013, Pelkey et al., 2017). They can synchronize local and distal

networks and are suggested to be a critical component of hippocampal oscillations (Whittington et al., 1995, Bartos et al., 2007) since many different types of interneurons have their firing phase-locked to hippocampal theta frequency (Klausberger and Somogyi, 2008).

The MS is composed of GABAergic, cholinergic and glutamatergic neurons which project to the hippocampus via fimbria-fornix pathway (Freund and Antal, 1988, Frotscher and Leranth, 1985, Colom et al., 2005). These fibres terminate almost exclusively in hippocampal interneurons (Leranth and Frotscher, 1987, Toth et al., 1997). GABAergic MS neurons have been described to control hippocampal oscillations, for example, MS parvalbumin-positive (PV+) neurons exhibit theta-related firing patterns phase-locked with the hippocampus. Additionally, a subpopulation of MS GABAergic PV+ neurons which project to the hippocampus expresses HCN channels. These neurons have been described to function as local oscillators at theta frequency (Gogolak et al., 1968, Gaztelu and Buno, 1982). These GABAergic HCN positive neurons are likely to induce local theta synchronization in the MS and provide theta rhythmic drive to the hippocampus since they produce theta rhythmic activity independently of hippocampal connections (Borhegyi et al., 2004, Varga et al., 2008, Petsche et al., 1962). A recent study showed that optogenetic stimulation of MS (PV+) neurons could supersede the endogenous theta oscillator but had no effect on theta amplitude (Zutshi et al., 2018). Optogenetic stimulation of the MS has been shown to be an efficient way to entrain hippocampal oscillation, mainly at theta frequency (Laxpati et al., 2014, Blumberg et al., 2016, Mamad et al., 2015).

To understand how septal stimulation can affect hippocampal interneurons and consequently oscillations, we injected an AAV to express channelrhodopsin (ChR2) under control of the human synapsin promoter (Hsyn) into the MS. The Hsyn promoter is expressed exclusively in neurons and has a long-term transgene expression in the rat brain in vivo when transfected by an adenoviral vector (Kugler et al., 2003). Additionally, stimulation of the MS neurons expressing ChR2 mediated by Hsyn has been demonstrated to effectively entrain hippocampal oscillations (Blumberg et al., 2016). Although the use of MS stimulation has a strong effect on hippocampal theta oscillation, how the septal neurons are affected by nonselective optogenetic stimulation is still not known.

The first aim of this chapter is to understand how nonselective optogenetic stimulation of the MS affects theta and non-theta modulated neurons. For this purpose, we investigated both electrophysiological and firing parameters of the MS neurons during nonselective optogenetic stimulation. We hypothesized that nonselective optogenetic stimulation should excite theta-bursting septal neurons, which has been described to be in phase to the hippocampal theta oscillations (Freund and Antal, 1988, Toth et al., 1997).

Our second aim was to investigate how hippocampal CA1 interneurons are affected by MS nonselective stimulation. We hypothesized that theta oscillating hippocampal interneurons, which receives mostly GABAergic projections from MS should be inhibited by MS stimulation. The results of this chapter will contribute to the understanding of the septo-hippocampal interactions in behaving animals.

3.2. Methods

All animal work has been carried out in the Health Products Regulatory Authority (HPRA) authorised establishment, Trinity College Dublin (establishment authorisation number: AE19136) ensuring compliance with the requirements of Directive 2010/63/EU and S.I. No. 543 of 2012. This work has also been approved by the TCD Animal Research Ethics Committee (AREC) which is a Level 2 ethics committee responsible for reviewing the proposed use of animals in teaching and research in line with the Research Ethics Policies in operation in TCD.

3.2.1. Animals

In this study, a total of 12 male Lister Hooded adult rats (350 - 450 g) were injected with a recombinant AAV to express channelrhodopsin-YFP under control of Hsyn promoter into the MS. From these animals, three were used for the MS recordings; these animals had both optic fibre and electrodes implanted into MS. For the hippocampal recordings, nine animals had had optic fibre implanted into MS and electrodes into CA1.

The animals which had electrodes implanted into hippocampus CA1 were also used in Chapter 5 and Chapter 6.

3.2.2. Surgery

The surgical procedure was detailed in section (2.1.3.), in brief, rats were anesthetized with isoflurane and transferred to the stereotaxic frame, and the scalp was shaved and drilled. Rats were injected with AAV5.hSyn.hChR2(H134R)-eYFP.WPRE.hGH (Adgene #26973P). A total of 2 µL (0.1 µL/s) using a Hamilton syringe. The MS coordinated used: AP +0.8; ML 1.4; DV 5.5-6.5; and a mediolateral angle of 10 degrees for both optic fibre and electrodes. The CA1 coordinates -3.8 AP; -2.5 ML; 1.4 DV were used for both rats implanted with only electrodes and rats implanted with electrodes and optic fibre. The assembly was permanently attached to the skull with dental cement. Implanted animals were housed individually with ad libitum access to water, and in a food-controlled state to keep animals at 85-90% of their weight for the surgery day. Animals were left to recover for at least seven days after surgery. The housing conditions were described in section (2.1.)

3.2.3. Protocol

Animals were recorded on the (60 x 60 cm) arena as described in section (2.2.1.). In brief, animals were connected to the recording equipment (Axona Ltd., UK) and placed on the arena and food pellets were thrown in every 20 seconds to pseudo-random locations within the open field. During photostimulation sessions, the laser was applied every 6 seconds (473 nm, 50 Hz, 12 pulses, 5 ms pulse duration) and animals were recorded for 12 minutes. A camera positioned on the ceiling

recorded the rat's position. On average, the microdrive was lowered 50 μm after a stimulation section to detect new units. The recording of raw data was stored for later off-line analysis.

3.2.4. Data analysis

As described in detail in section (2.4.1.), the waveforms were clustered by the k-means algorithm, using graphical software (Tint, Axona Limited). Autocorrelation histograms were used as well as visual inspection to check the quality of the single unit's isolation. The local field potential (LFP) was sampled at 250 Hz and filtered using a band-pass filter (0.5 - 12 Hz). The short-time Fourier Transforming was performed by using a Hanning window of 2 seconds with an overlap of 1 second and plotted as color-coded using MATLAB's Signal Processing Toolbox (MATLAB, Natick, MA). Theta index (section 2.4.6) was calculated for each unit as well as the autocorrelation histograms. Units that responded to light were identified by comparing the firing rate before and after each stimulation (100 ms before and 100 ms after). The spikes time of each cell were divided into epochs of maximum length around each stimulation time without superposition to form a raster plot.

3.2.5. Unit classification

In this study, we focused only on septal cells and hippocampal interneurons. The place cells were analysed in chapter 6. Units which presented less than 200 spikes

during a recording were excluded from further analysis due to the under-sampling. The remaining units were classified based on firing and bursting properties (Tsanov et al., 2011, Ramcharan et al., 2005). The definition of the classification criteria is defined as follow: Bursting units - these units presented burst pattern of firing (Anderson and O'Mara, 2003). A burst was defined as a group of two or more spike having an inter-spike interval < 5 ms. The 'propensity to burst' was defined as an index of the proportion of bursting units (Ramcharan et al., 2005, Anderson and O'Mara, 2003).

Theta modulated units - were defined as units which presented an oscillatory pattern on the ISIs. A sine wave was fitted to the autocorrelation, and the theta index was calculated. This method has been used to quantify theta modulation. (Royer et al., 2010). In this thesis, it was used for classification. Every unit with theta index bigger than 0.1 was classified as theta modulated.

The remaining units were classified as regular-spiking units. These units had a spread ISIs distribution with no apparent peak.

3.2.6. Post-mortem verification

After the completion of electrophysiological recordings, the brains were removed for histological verification of the expression of the virus and the localization of the electrodes and optic fibres as described in section (2.5). Fluorophore images were collected using an Olympus BX51 fluorescence microscope in 488 nm for the viral expression of YFP.

3.2.7. Statistical analysis

Before analysis, all data were tested for normality using SPSS (Version 24.0. Armonk, NY: IBM Corp) Shapiro-Wilk's test. Where appropriated, differences between groups were analysed parametrically using one-way analysis of variance (ANOVA) or t-tests for independent samples. Most of the data were not normally distributed, in those cases, groups were tested using the Kruskal-Wallis test and Dunn's multiple comparisons test using GraphPad Prism (Version 7.02). For visualization and simplicity, data were plotted using the mean and standard error of the mean instead of median and inter-quartile for non-parametric data.

3.3. Results

3.3.1. Theta modulated medial septal units

We collected a total of 145 units in the MS from three rats during 21 sessions. Animals were recorded in the open field while searching for sugar pellets. Each session was 12 minutes length, and blue light (473 nm) was applied into the medial septum every 6 seconds. We use 12 pulses of 5 ms duration as it was efficient to affect the cells. The challenge of this study was to develop the surgical techniques necessary to implant microdrive and optic fibre which had to be stable for over five weeks, as the virus takes around four weeks to express fully. The tracks of the electrodes were reconstructed by visual inspection of the brain slices (Figure 10). The viral expression was observed by green fluorescence in the MS region.

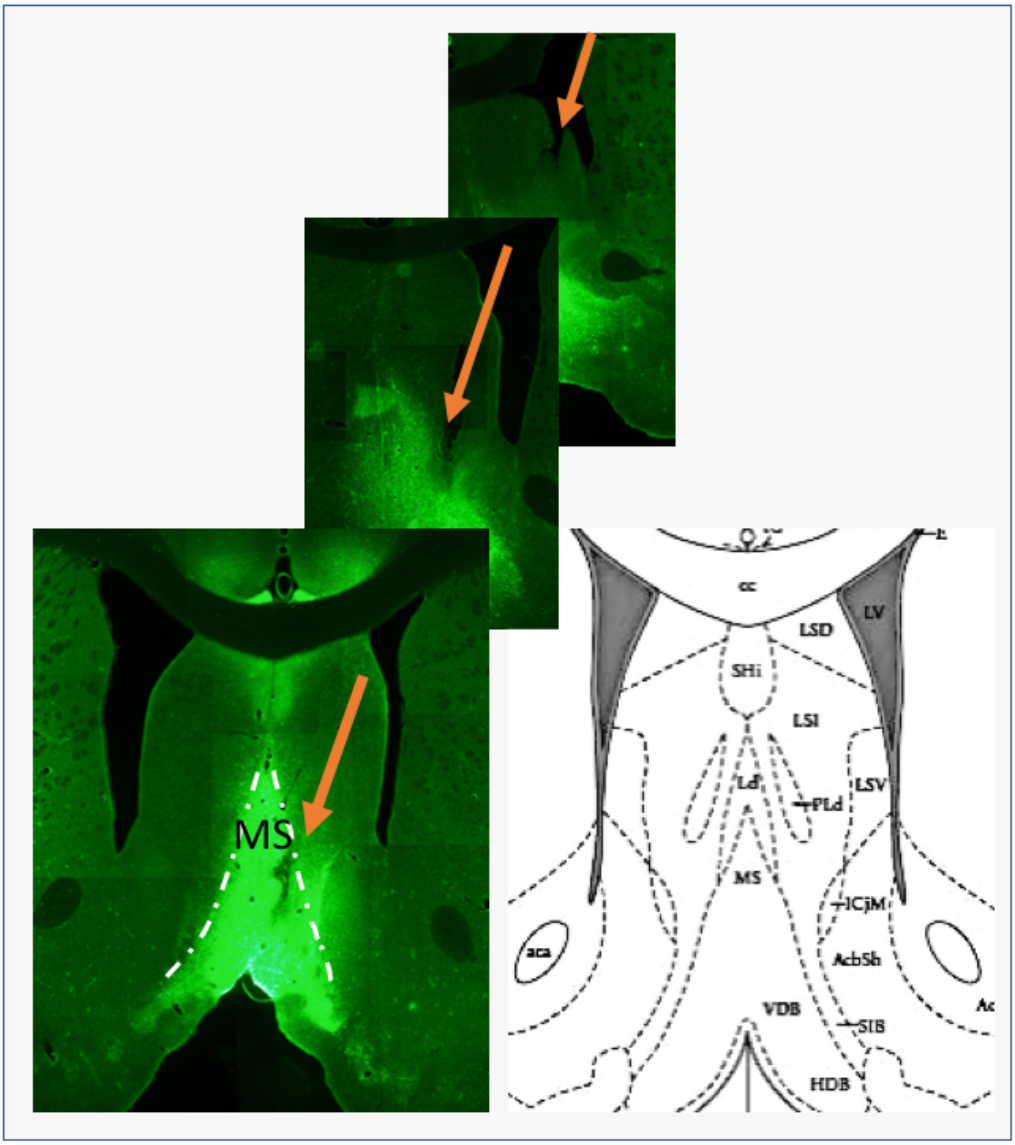

Figure 10. Track of the electrodes.

Representative histological specimen showing a reconstruction of an electrode track. The viral expression was limited to the MS and ventral diagonal band of Broca, abbreviated as VDB. Schematic image adapted from 'The Rat Brain in Stereotaxic Coordinates', 5th edition (Paxinos and Charles, 2007).

3.3.2. Medial septum unit classification

We recorded 145 well-isolated units which were anatomically confirmed by post-mortem histological verification to be within the MS. These cells were classified

based on bursting activity and theta modulation. We measured the propensity to burst (Anderson and O'Mara, 2003) and found that 25 units had had a propensity to burst > 0.1. These units were grouped as bursting units (25/145, 17.2%). To quantify the theta modulation of a unit, we fitted a sinusoidal function to the autocorrelograms, the frequency of the sinusoidal fitted curve was (7.90 ± 0.45 Hz), which is within the theta band (4-12 Hz). Being that, these units were sub classified as theta-bursting units. From the remainder non-bursting units, 56 were also theta modulated (56/145, 38.7%), these units were grouped as theta modulated non-bursting units (Table 3). Units which did not present burst firing or theta modulation were defined as regular spiking units. Overall, the majority of the units, including bursting and non-bursting units were theta modulated (55.8%).

Table 4. Electrophysiological characterization of the medial septum in freely behaving rats

Cell types	***Theta burst units***	***Theta non-burst units***	***Regular firing units***
Number of cells	25 (17.2%)	56(38.7%)	64(44.1%)
Average frequency	21.2 ± 12.8 Hz	11.08 ± 9.54 Hz	2.8 ± 2.23 Hz
Mean spike width	160.97 ± 42.17	167.91 ± 69.74	180.92 ± 48.96
Burst propensity	0.154 ± 0.06	0.04 ± 0.03	0.02 ± 0.01
Theta index	0.51 ± 0.50	0.39 ± 0.38	0.11 ± 1.90

We formally compared the spike width and firing frequency from the three classes and between groups. A Kruskal-Wallis H test between groups revealed significantly difference $X^2(2)=8.485$, $p=0.014$. Dunn's post hoc test showed that regular spiking had a significantly bigger spike width than theta bursting units ($p<0.05$) (figure 11.A). A Kruskal-Wallis H test showed that there was a statistically significant difference in frequency between the different groups, $X^2(2)=78.06$, $p<0.0001$ (figure 11.A). A Dunn's post hoc test revealed significant differences between all groups. The theta bursting units had the highest mean firing rate (21.2 ± 12.8 Hz), followed by the theta non-bursting units (11.08 ± 9.54 Hz) (figure 11.B). The regular firing units showed the smallest mean firing rate (2.8 ± 2.23 Hz).

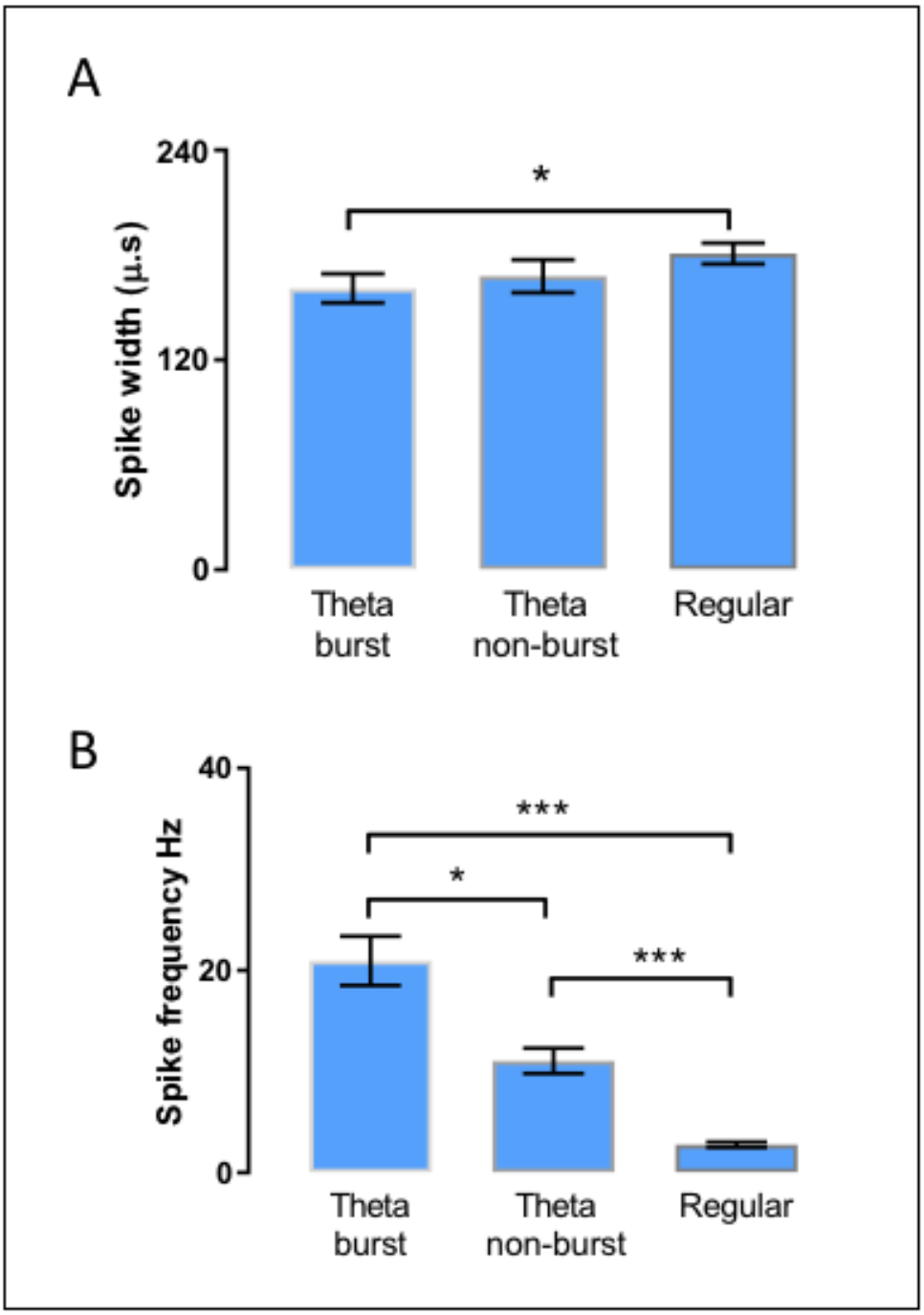

Figure 11. Electrophysiological differences between groups

(A) Comparing the width of the spikes between groups of MS cells. A Kruskal-Wallis/Dunn's test detected a significant difference between the theta burst units and regular units ($p < 0.05$). **(B)** Comparison of mean frequency between groups. A Kruskal-Wallis/Dunn's test detected a significant difference between theta burst and theta non-burst ($p<0.05$). Theta burst and regular ($p<0.001$), and theta non-burst and regular groups ($p<0.001$).

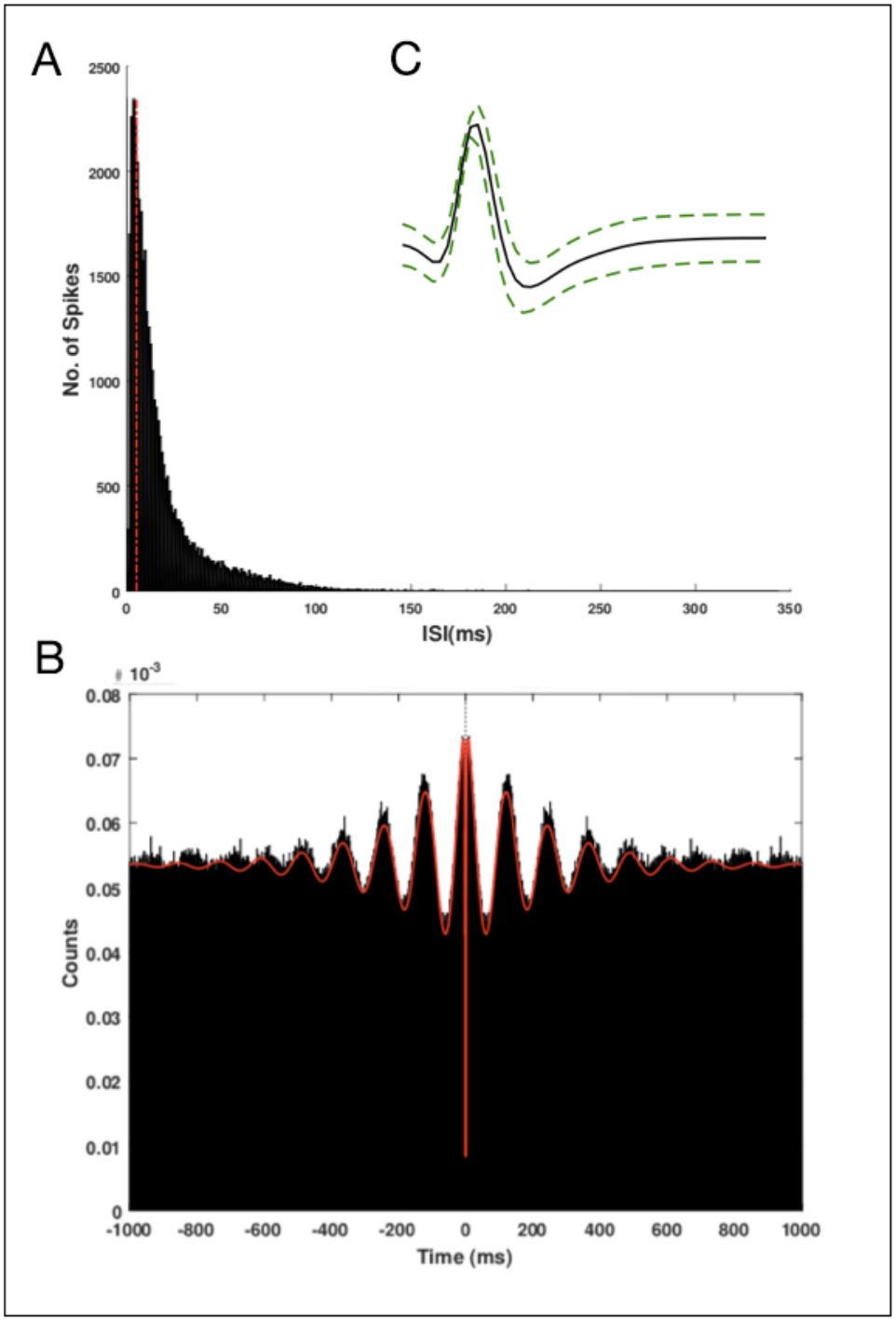

Figure 12. Theta Burst unit ISI histogram and autocorrelogram.

(A) A typical ISI of a theta burst unit recorded within the MS with a mean frequency of 53.1 Hz. **(B)** The autocorrelogram of the same unit showing the fitted decaying sinusoidal for theta index calculation, theta index of 0.90. **(C)** A spike waveform average from the same unit, showing width of 136.24 ± 21.9 µs.

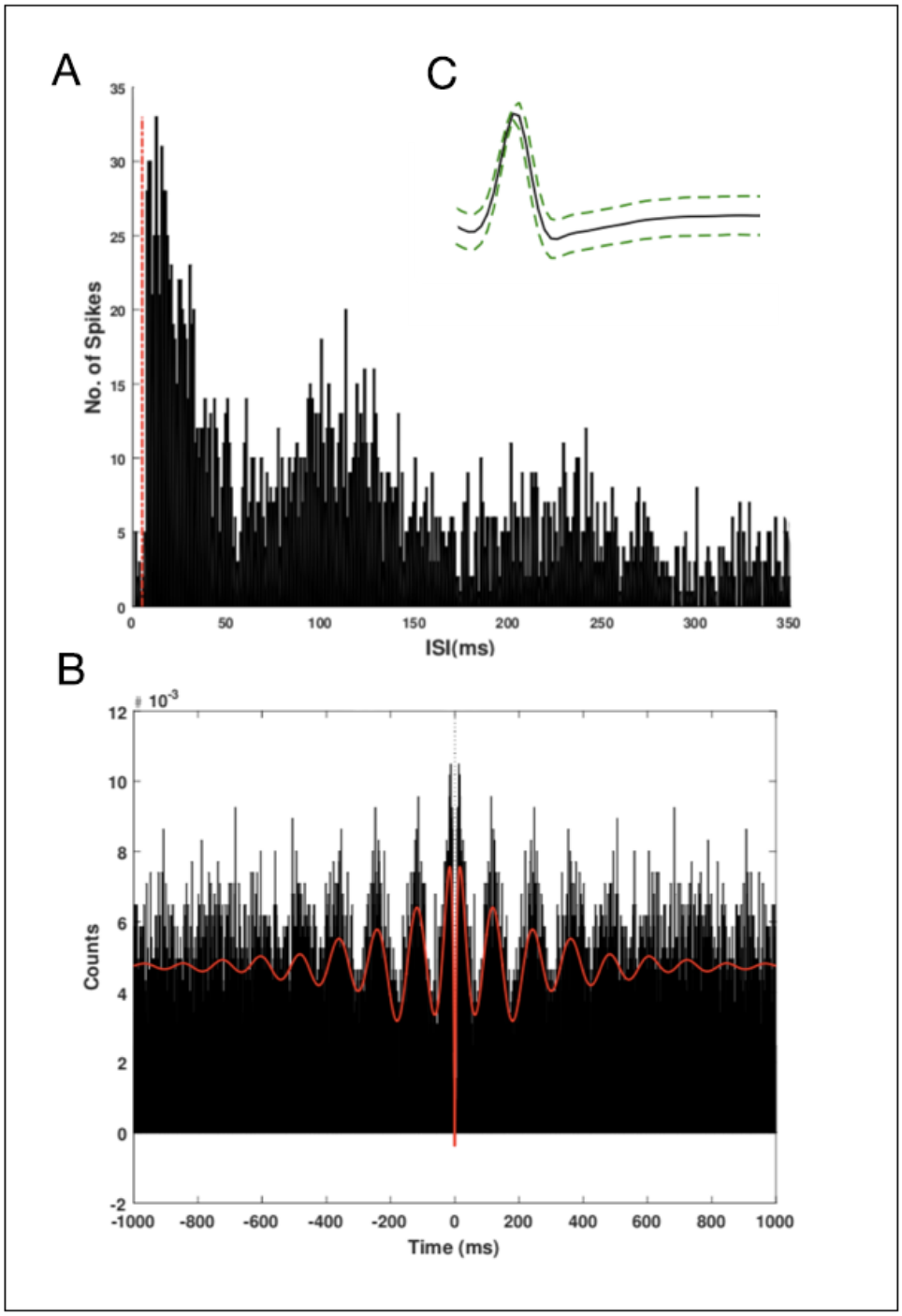

Figure 13. Theta Non-Burst unit ISI histogram and autocorrelogram.

(A) ISI of a theta non-burst unit recorded within the MS with a mean frequency of 4.51 Hz. **(B)** The autocorrelogram of the same unit showing the fitted decaying sinusoidal for theta index calculation, theta index of 0.53. **(C)** A spike waveform average from the same unit, showing spike width of 152.24 ± 20.6 μs.

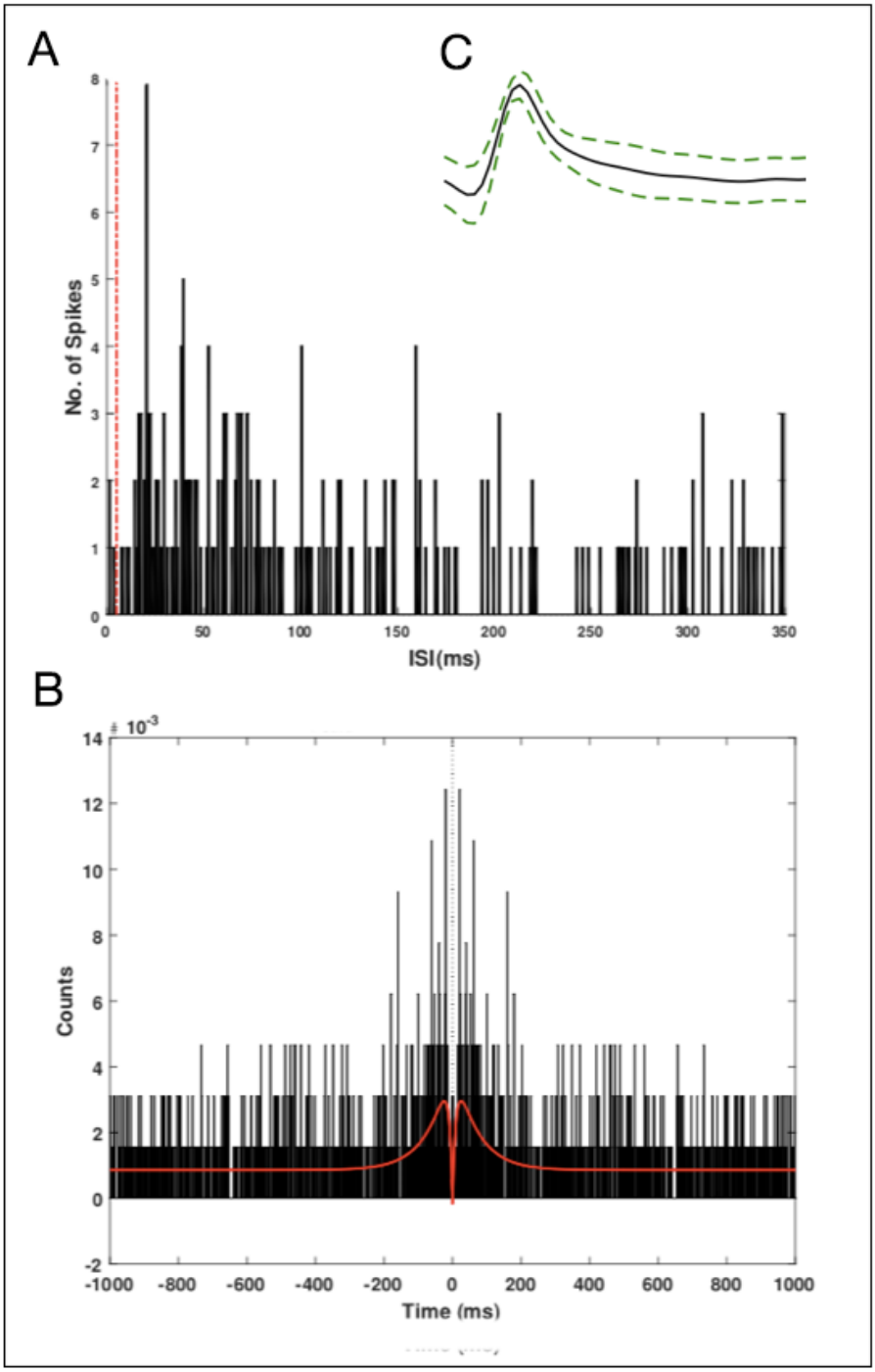

Figure 14. Regular spiking unit ISI histogram and autocorrelogram.

(A) ISI of a regular spiking unit recorded within the MS with a mean frequency of 0.89 Hz. **(B)** The autocorrelogram of the same unit showing the fitted decaying sinusoidal for theta index calculation, theta index of 0.02. **(C)** A spike waveform average from the same unit, showing spike width of 229.55 ± 95.6 μs.

3.3.3. MS units with firing correlated with running speed

We next investigated the relationship of these neurons with animal's speed for each group of cells. A Pearson correlation was used to assess the linear relationship between speed and firing frequency for each unit. We considered correlated units which showed Pearson correlation $p<0.001$. The majority of theta burst cells had the firing frequency modulated by speed (19/25, 76%). Only (3/25, 12%) units had the firing rate positively correlated with speed, and (16/25, 64%) units were negatively correlated (figure 15)

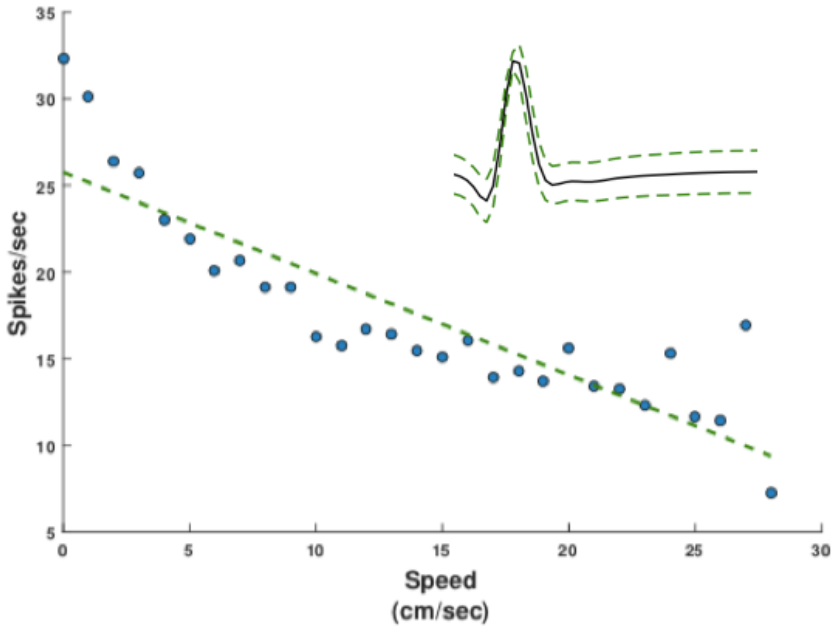

Figure 15. Theta burst unit with firing rate negatively correlated with speed.

An example of a theta burst unit which decreased in firing rate with the increase in the animal's speed, Pearson correlation r = -0.84.

The proportion of units with firing correlated with speed was smaller for theta non-burst units, (31/56, 55%) of these cells showed a Pearson correlation > |0.5|. From these cells, (11/56, 20%) were positively correlated and (20/56, 35%) negatively (figure 16). Lastly, in the regular firing group, the correlation with speed was proportionally much smaller, only (15/64, 24%) of the cells were positively

Correlated (6/64, 10%) or negatively correlated (9/64, 14%) (Figure 17).

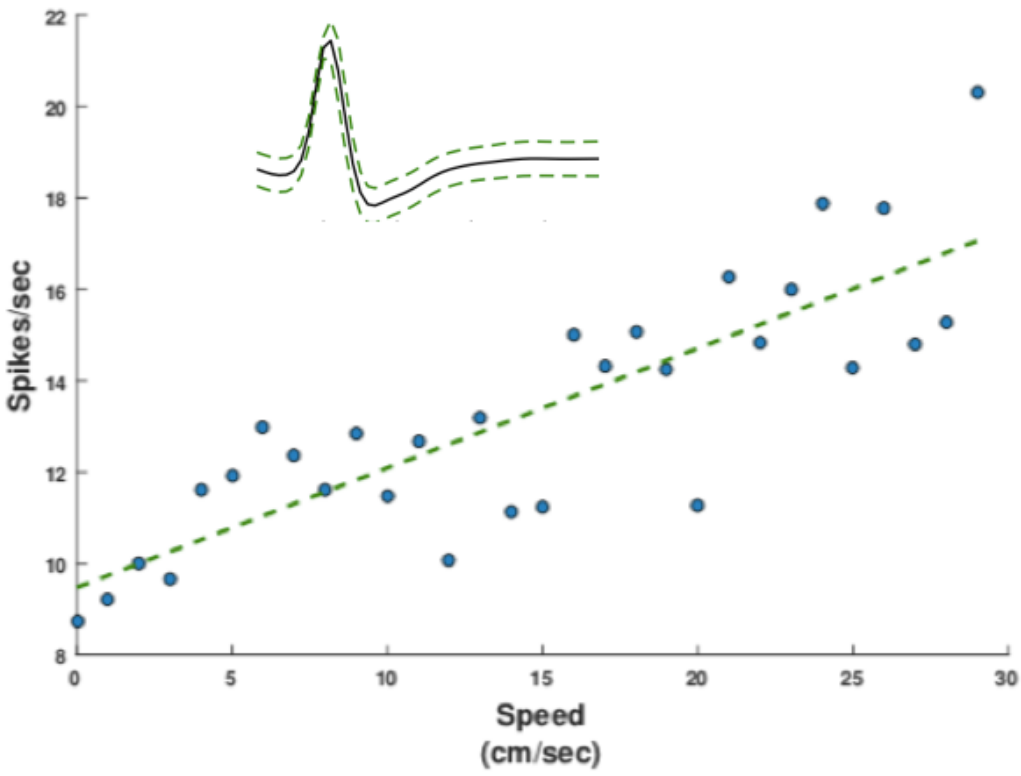

Figure 16. Theta non-burst unit with firing rate positively correlated with speed.

An example of a theta non-burst unit which increased in firing rate with the increase in the animal's speed, Pearson correlation r = 0.80.

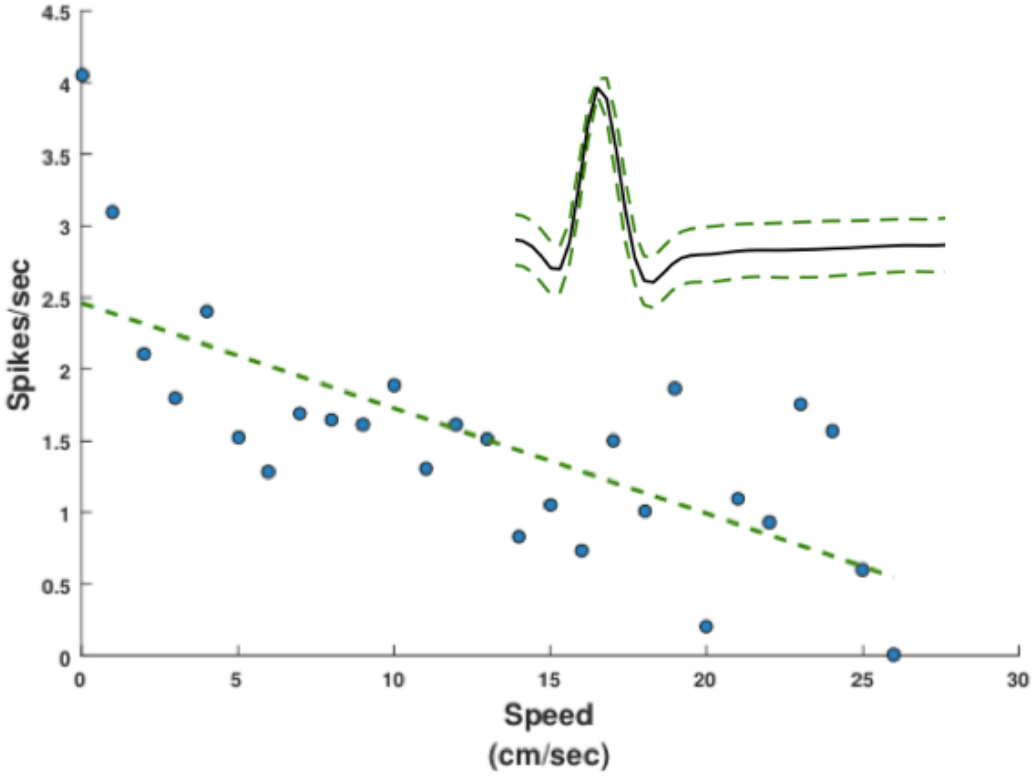

Figure 17. Regular spiking unit with firing rate negatively correlated with speed.

An example of a regular spiking unit which decreased in firing rate with the increase in the animal's speed, Pearson correlation r = -0.71.

Taking this together, we found that (65/145, 45%) units had the firing rate correlated with speed. The majority of the cells were negatively correlated (45/145, 31%) and only (20/145, 14%) positively correlated. The table summarises the proportion for each group (table 4).

Table 5. MS units which had firing rate correlated to the animal's speed

Cell types *Number of cells*	*Theta burst units* *25*	*Theta non-burst Units* *31*	*Regular firing units* *15*
Positively correlated	6/25, **24%**	6/31, **20%**	6/15, **40%**
Negatively correlated	19/25, **76%**	25/31, **80%**	9/15, **60%**

3.3.4. Nonselective optogenetic stimulation of the MS

To assess the effect of the laser stimulation on the MS cells, the rats were recorded for 12 minutes receiving light stimulation every six seconds. Only (24/145, 16.6%) of the cells were not affected by stimulation. We analysed the pre and post-stimulus time histograms of the affected cells. Based on the pattern of the histogram, we classified the effect of the light on the cells as excited or inhibited (figure 18).

Table 6. Effect of non-selective optogenetic stimulation of MS units

Cell types	*Theta burst units* *25*	*Theta non-burst units* *31*	*Regular firing units* *15*
Excited	5/25, **20%**	14/31, **45.2%**	7/15, **46.7%**
Inhibited	19/25, **76%**	12/31 **38.7%**	5/15, **33.3%**
No effect	1/25, **4%**	5/31, **16.1%**	3/15, **20%**

Most of the theta burst units (19/25, 76%) were indirectly inhibited by network effect as the ChR2 is a light-gate cation channel and it only depolarises cells. In contrast, the theta non-burst units were mostly excited (14/31, 45.2%). A similar pattern was observed for the regular spiking units, which had (7/15, 47.7%) of the cells excited (table 3). Some excited cells had a post-stimulus inhibitory period (figure 18.C), the opposite effect was observed in some cells (figure 18.D). To classify the cells, we compared 100 ms before and during stimulation.

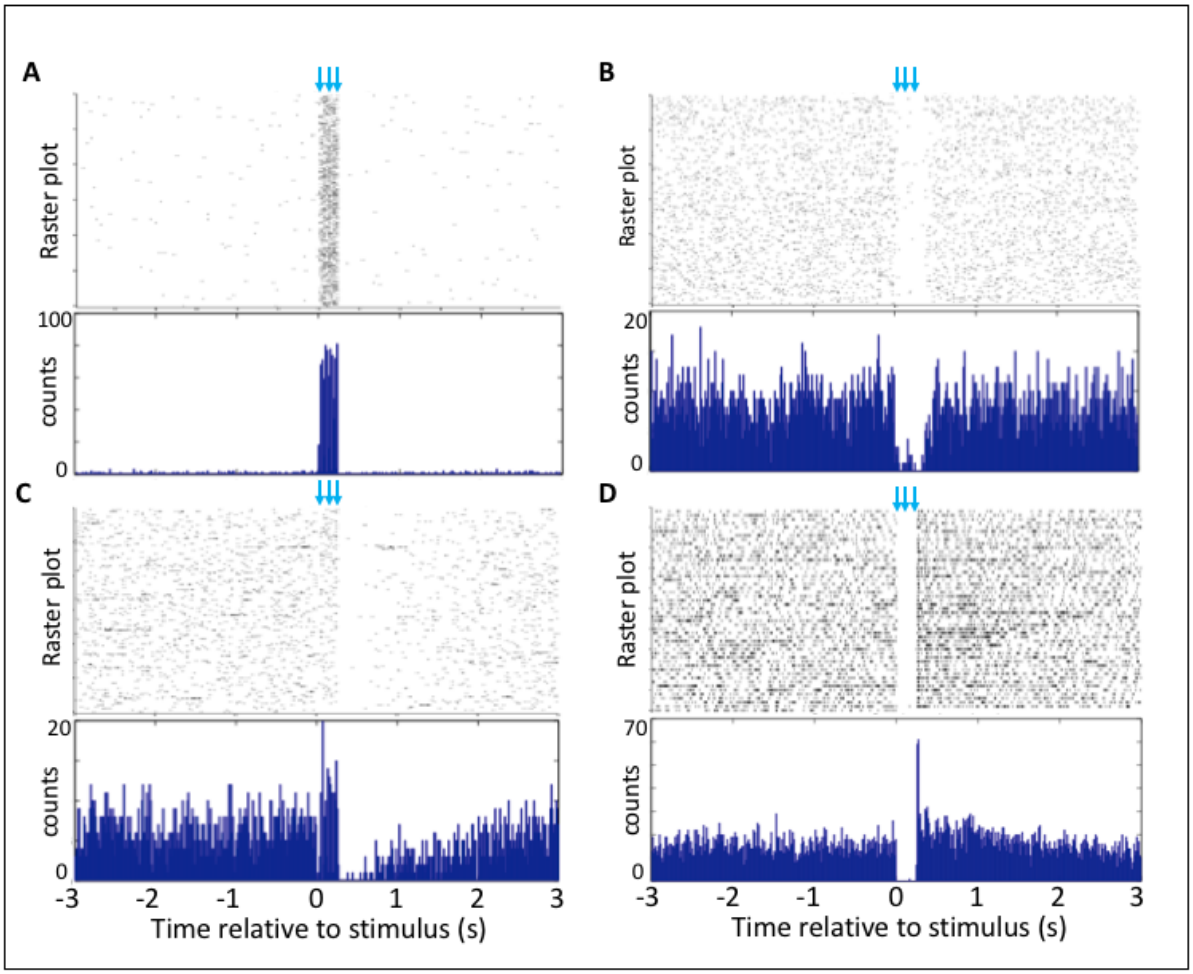

Figure 18. Effect of light stimulation.

(A) Example of an excited unit. **(B)** An example of an inhibited unit. **(C)** Example of an excited theta bursting unit which presented a post-stimulus transient inhibited phase. **(D)**

Example of an inhibited theta bursting during laser stimulation, which presented a post-stimulus transient peak on the histogram.

3.3.5. Classification of hippocampal CA1 interneurons

We recorded 67 well-isolated CA1 interneurons affected by MS stimulation from nine rats. Using the same criteria used to classify MS units, we found that all burst units were also theta modulated. The theta burst units consisted of (19/67, 28%) of the total units. The units which were theta modulated and had a propensity to burst lower than 0.1, were grouped as theta non-bursting units. These units composed (25/67, 37%) of the total units. The remaining units were classified as regular spiking units which consist of (23/67, 34%) of the total (table 4).

Table 7. Characterization of the CA1 interneurons affected by MS stimulation

Cell types	***Theta burst units***	***Theta non-burst units***	***Regular firing units***
Number of cells	19	25	23
Average frequency	25.2 ± 17.7 Hz	12.1 ± 8.3 Hz	3.7 ± 3.6 Hz
Mean spike width	198.6 ± 41.06	163.6 ± 34.0	192.2 ± 49.2
Burst propensity	0.17 ± 0.1	0.07 ± 1.03	0.03 ± 0.02
Theta index	0.8 ± 0.1	0.7 ± 0.1	0.3 ± 0.1

We use a Kruskal-Wallis test with a Dunn's post hoc to compare the waveform width between groups (figure 19). There was a significant difference between theta bursting units and theta non-burst units $X^2(2)=8.05$, $p=0.018$. Dunn's post hoc test detected a difference between theta burst and regular spiking units ($p<0.05$). Concerning average frequency, there were significant differences between groups $X^2(2)=23.57$, $p<0.001$. Dunn's port hoc detected a difference between theta burst and regular ($p<0.001$) and between theta non-burst and regular groups ($p<0.01$).

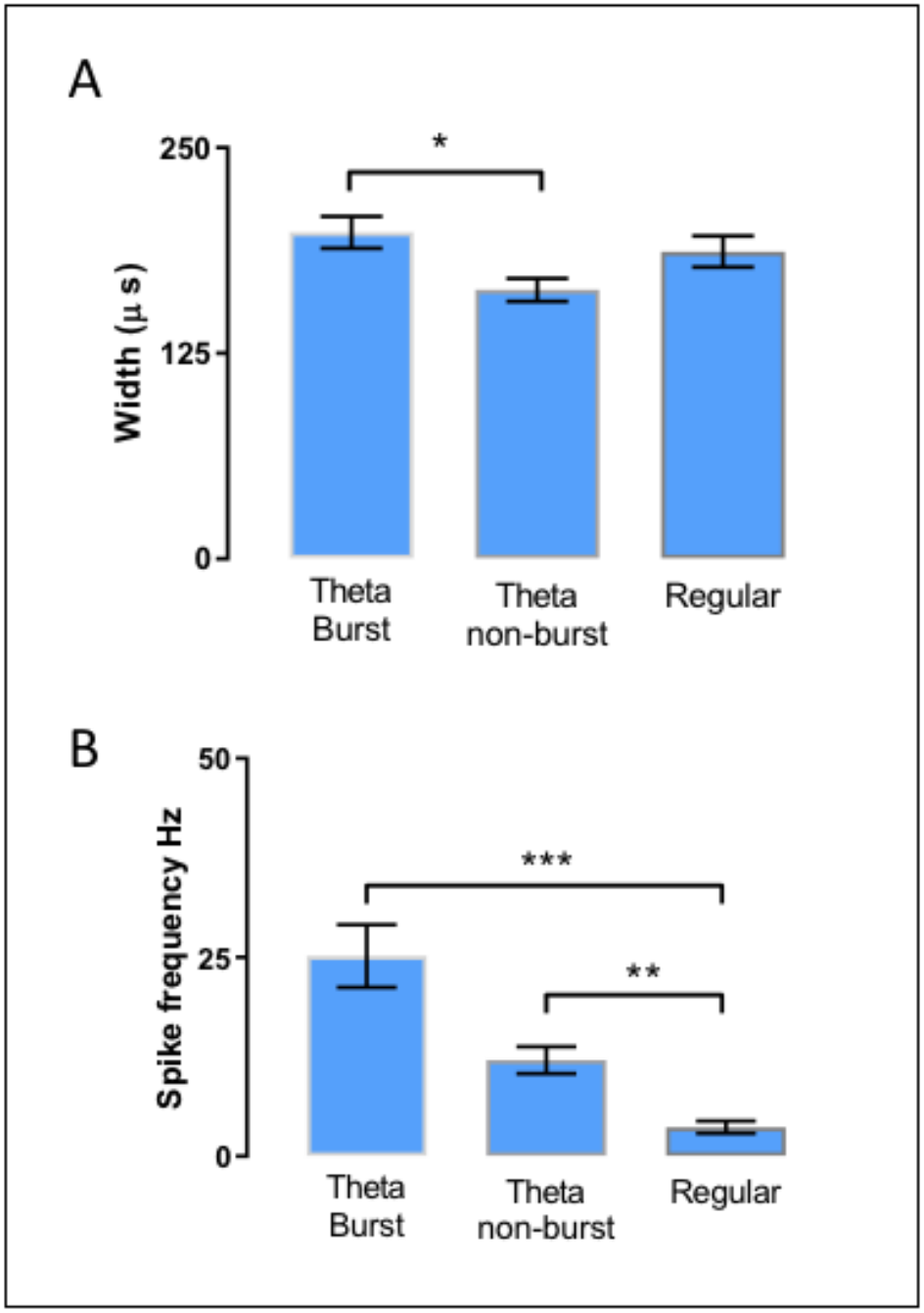

Figure 19. Electrophysiological differences between groups.

(A) Comparing the width of the spikes between groups of CA1 interneurons. A Kruskall-Wallis/Dunn's test detected a significant difference between the theta burst units and theta non-burst units ($p < 0.05$). **(B)** Comparison of mean frequency between groups. A Kruskal-Wallis/Dunn's test detected a significant difference between theta burst and regular units ($p<0.001$), and theta non-burst and regular ($p<0.01$).

3.3.6. CA1 interneurons with firing frequency correlated with speed

We also investigated the correlation between firing frequency and speed for all interneurons. We used the same analysis used for MS neurons. We considered units which showed Pearson correlation greater than |0.5|. Most of the units had the firing frequency linearly correlated with speed (39/67, 58.2%). In the theta burst group, (14/19, 73%) of the units were modulated by speed. The positively correlated were the majority (12/19, 63%) while only two units were negatively correlated (2/19, 10%) (Figure 20).

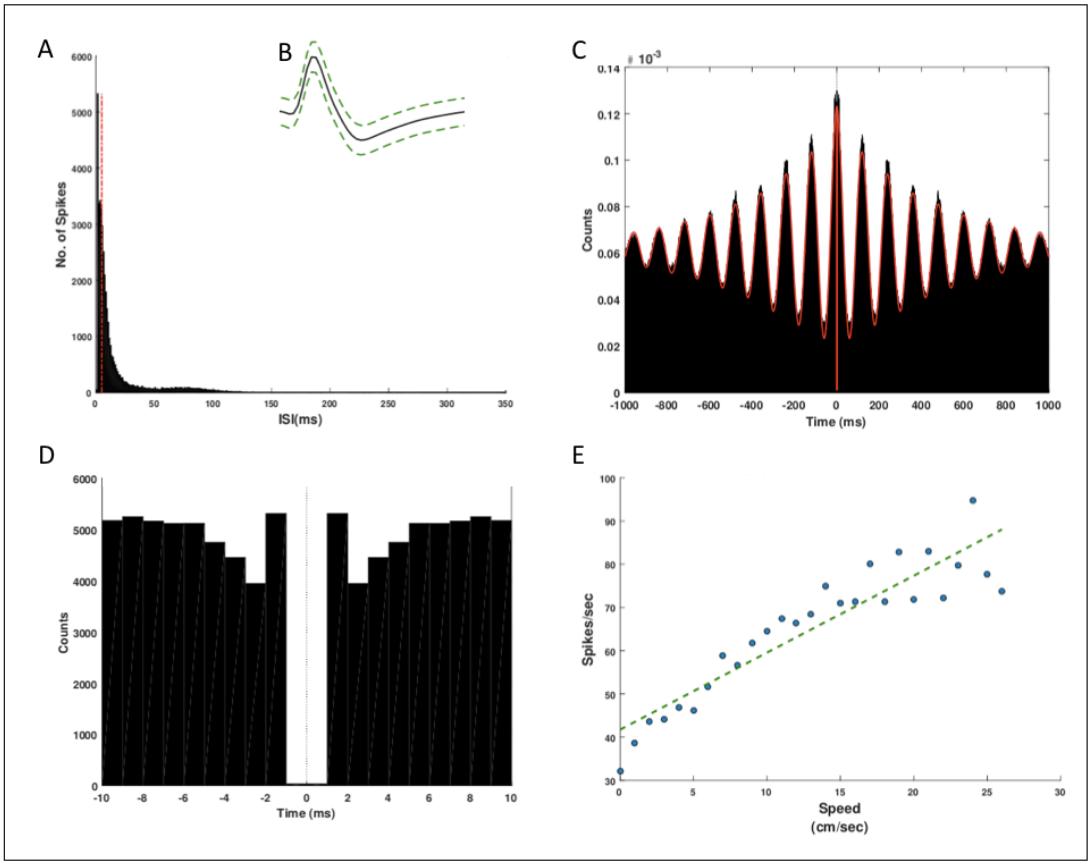

Figure 20. Theta burst unit with firing rate positively correlated with speed. **(A)** ISI of a theta bursting interneuron with a mean frequency of 56.96 Hz. **(B)** A spike waveform average from the same unit, showing spike width of 204.23 ± 21.83 µs. **(C)** The

autocorrelogram showing the fitted decaying sinusoidal used for theta index calculation, theta index of 0.8. **(D)** Autocorrelation (±10) used to verify unit isolation. **(E)** Firing rate positively correlated with speed (Pearson r = 0.92).

Most of the units of the theta non-bursting group had the firing rate correlated with speed (15/25, 60%), where (11/25, 44%) were positively correlated and (4/25, 16%) negatively (figure 21).

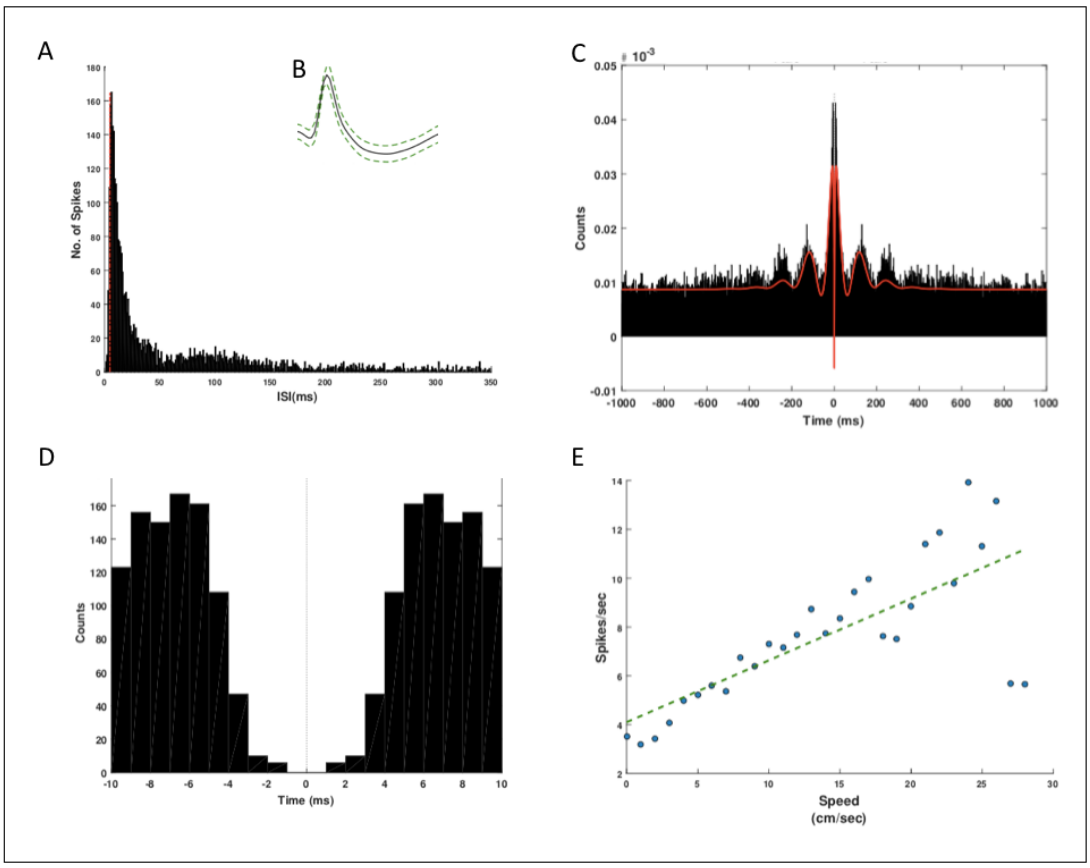

Figure 21. Theta non-burst unit with firing rate positively correlated with speed.

(A) ISI of a theta non-bursting interneuron with a mean frequency of 5.94 Hz. **(B)** A spike waveform average from the same unit, showing spike width of 171.15 ± 27.50 µs. **(C)** The autocorrelogram showing the fitted decaying sinusoidal used for theta index calculation, theta index of 0.86. **(D)** Autocorrelation (±10) used to verify unit isolation. **(E)** Firing rate positively correlated with speed (Pearson r = 0.74).

Lastly, the regular firing group had (9/23, 40%) of speed correlated cells. The majority were positively correlated (7/23, 32%), only two units were negatively correlated (2/23, 8%) (Figure 22).

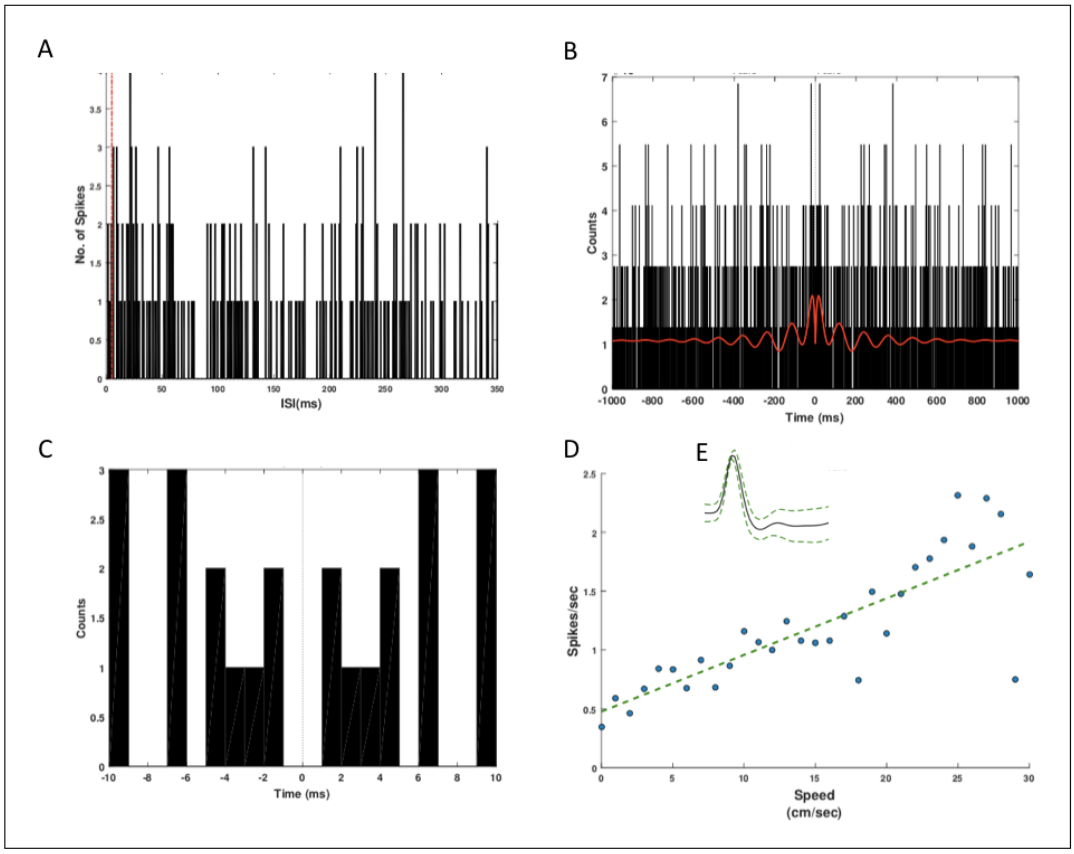

Figure 22. Regular unit with firing rate positively correlated with speed. **(A)** ISI of a theta non-bursting interneuron with a mean frequency of 1.01 Hz. **(B)** A spike waveform average from the same unit, showing spike width of 172.23 ± 29.25 µs. **(C)** The autocorrelogram without theta modulation, the theta index for this unit was 0.13. **(D)** Autocorrelation (±10) used to verify unit isolation. **(E)** Firing rate positively correlated with speed (Pearson r = 0.80).

Table 8. CA1 interneurons which had firing rate correlate with speed

Cell types	*Theta burst units* *19*	*Theta non-burst Units* *25*	*Regular firing units* *23*
Positively correlated	12/19, **63%**	11/25, **44%**	7/23, **32%**
Negatively correlated	2/19, **10%**	4/24, **16%**	2/23, **8%**

3.3.7. The effect of nonselective MS optogenetic stimulation on CA1 interneurons

Only affected hippocampal interneurons were analysed, in this experiment. We found that the majority of the units (52/67, 77.6%) were disinhibited during MS stimulation. The theta bursting neurons had (12/19, 63%) of the units disinhibited, and (7/19, 37%) inhibited. In the theta non-bursting group, (20/25, 80%) were disinhibited, and only (5/20, 20%) inhibited. Lastly, for the regular spiking units, the majority were disinhibited (20/23, 87%), and only (3/23, 13%) of the units were inhibited (Table 8).

Table 9. Effect of nonselective optogenetic stimulation of MS on CA1 interneurons

Cell types	*Theta burst units*	*Theta non-burst units*	*Regular firing units*
Inhibited	7/19, 37%	5/20, 20%	3/23, 13%
Disinhibited	12/19, 63%	20/25, 80%	20/23, 87%

3.3.8. Medial septal stimulation induced strong theta activity on hippocampal LFP

Lastly, we examined how MS optogenetic stimulation could affect the hippocampal LFP in theta frequency. A paired-samples t-test was conducted to compare the averaged evoked power in the theta band (4-12 Hz) before and after a stimulus. There was a significant difference in the evoked power before (M = 0.59, SD = 0.19) and after (M = 1.34, SD = 0.52) laser stimulation; $t(8) = -6.271$, $p < 0.001$ (figure 23).

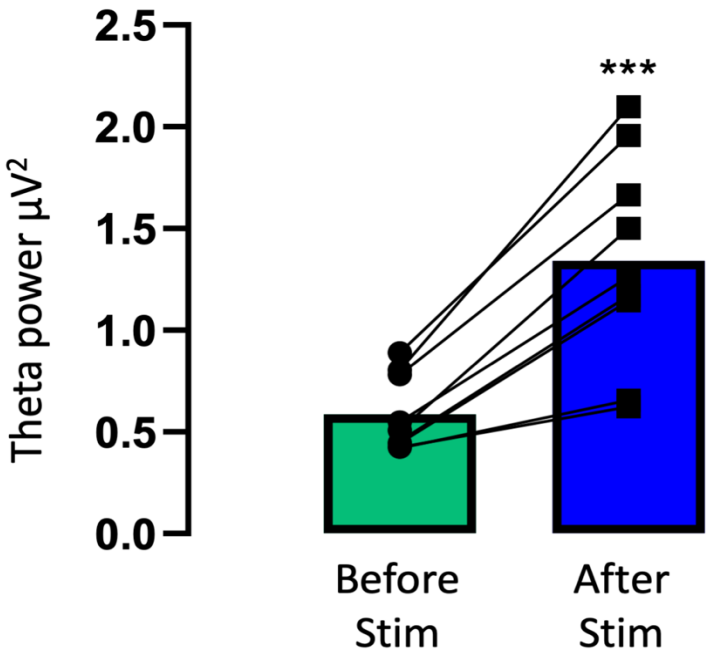

Figure 23. Evoked theta power before and after a stimulus. To confirm that MS stimulation affects the CA1 LFP, we calculated the difference of the evoked power between 4-12Hz (theta band). A paired t-test showed that the evoked power was significative higher after the laser stimulation $p < 0.001$).

The laser stimulation effect on the LFP can be clearly visualized by the power spectrogram as exemplified (figure 24).

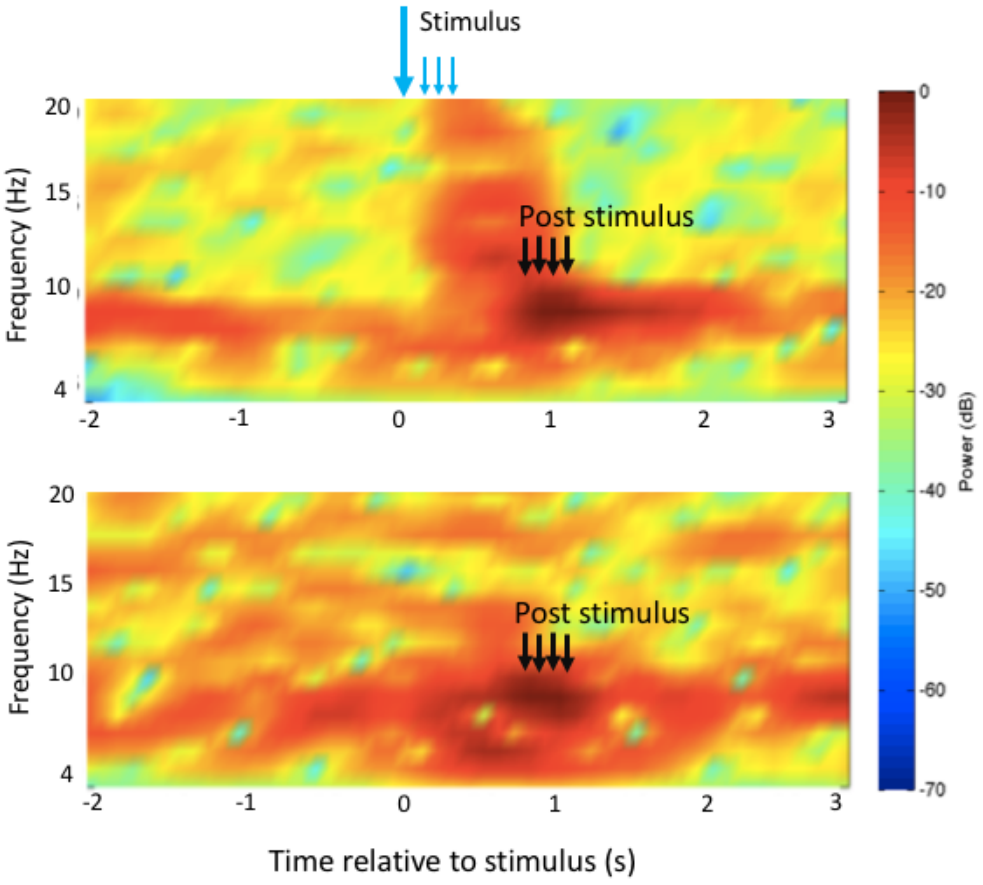

Figure 24. Power spectrogram of CA1 LFP. Example of two color-coded power spectrograms of hippocampal 4-20Hz oscillations before and after MS stimulation. The blue arrow indicates the time of the stimulus. The black arrows indicate the peak of the power around 8 Hz.

We observed that theta bursting units that were strongly affected by the MS stimulation. Some cells showed an oscillatory pattern after the stimulus that was easily observed on inhibited units (figure 25).

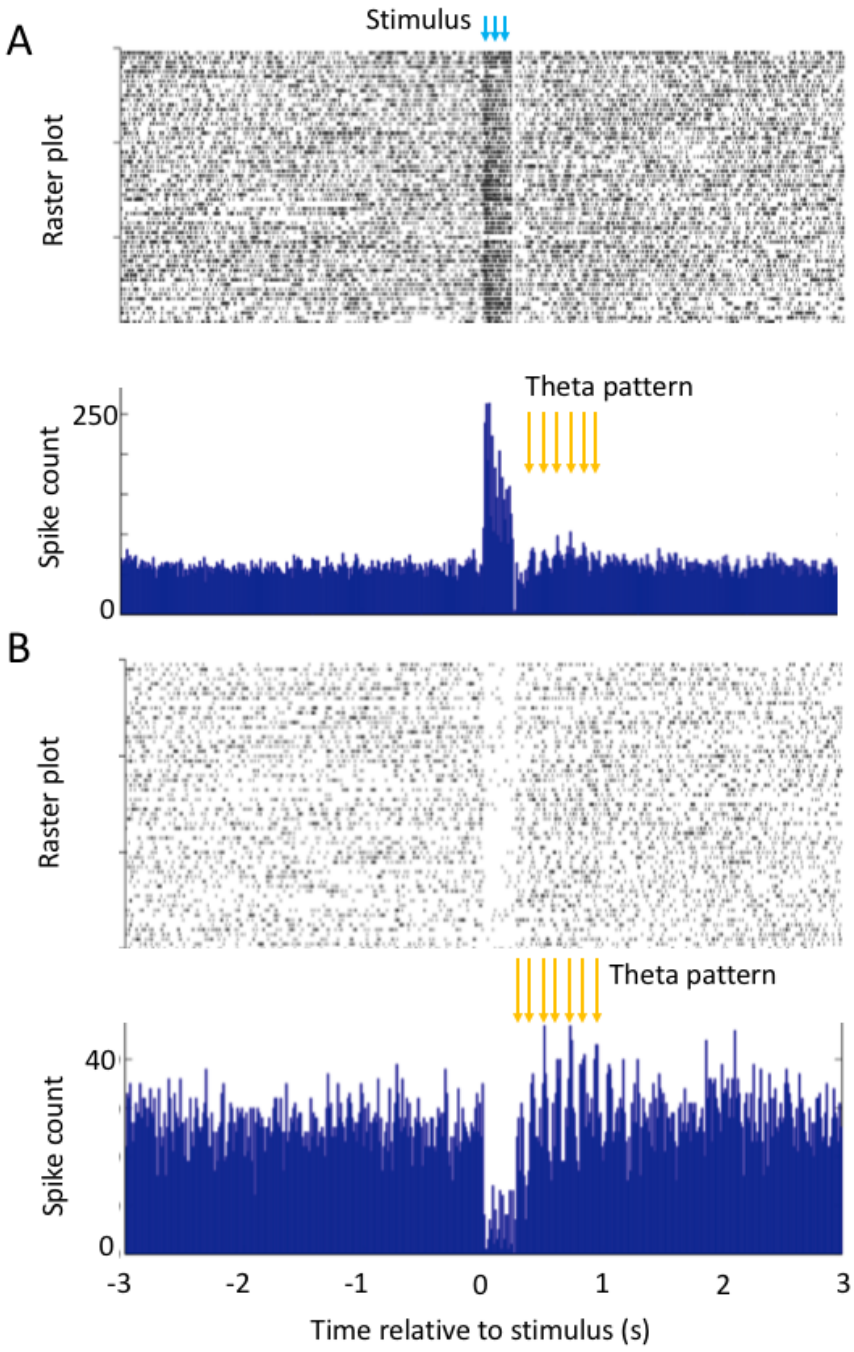

Figure 25. Theta bursting units affected by MS stimulation.

(A) Example of a strongly excited unit. The laser stimulation represented by the blue arrows started at time 0 seconds. The raster plot and histogram show increase in firing frequency during MS stimulation. It is possible to observe small peaks on the histogram after stimulation. **(B)** Example of an inhibited theta bursting unit represented by its raster plot and histogram. The peaks after stimulus indicate that this unit is theta modulated and the phase was reset by MS stimulation.

3.4. Discussion

This chapter aimed to explore how nonselective optogenetic MS stimulation mediated by the Hsyn could affect the septohippocampal circuit. We designed two experiments to address this question. In the first experiment, we expressed ChR2 on MS neurons under the control of Hsyn promoter, and optogenetically stimulated these neurons while recording extracellular activity locally within the septum. In the second experiment, we repeated the expression of ChR2 under the control of Hsyn in the MS and stimulated the MS while recording extracellular activity in the hippocampal CA1 area. Interestingly, our results showed that the majority of MS neurons recorded were inhibited by optogenetic stimulation. Additionally, we investigated the correlation between firing rate and speed showing that the majority of MS neurons had the firing rate negative correlated to animal's speed.

The extracellular recordings used in this study could detect waveforms that come from neurons relatively close to the tip of the electrodes. The primary advantage of this technique is the possibility to record several neurons during behaviour, as the animal can move freely, only attached by a lightweight cable. A downside of this technique is its limitation to electrophysiological recordings and the incapacity to identify the chemical profile of the recorded neurons. To have an idea of the neuronal subpopulations detected by the electrodes, we could compare the firing parameters of recorded neurons to data available in the literature. For this reason, units were classified based on their firing properties in an attempt to

distinguish between groups that have been already described (Stewart and Fox, 1989a, Brazhnik and Fox, 1999, Borhegyi et al., 2004, Henderson et al., 2001, Tsanov et al., 2011).

The theta-bursting group was first classified by its propensity to burst and later we observed that these neurons were also theta modulated. The theta-bursting group showed the highest firing rate and smallest average cell width. In fact, the firing rate and cell width were inversely proportional for all MS groups.

The core of this chapter was the classification of MS units and later understanding the effect of the laser stimulation on these groups. Bursting classification comes from in vitro studies by measuring the neuron response from an electronic current injection. However, theta index is usually used as a quantifier of theta modulation, here it was used as a classifier. As the theta index is calculated by a division of two factors, it always results in a value different from zero, for example, the minimal theta index calculated for a unit that had absolutely no theta modulation was 0.003. However, it is possible to visually identify that very low-value theta index resulted from cells that had no oscillation pattern in the autocorrelation. To overcome this issue, a minimal theta index was defined by visual inspection of the autocorrelation.

The MS bursting neurons have been described to be GABAergic GAD positive cells, including parvalbumin-positive neurons that present theta-bursting activity coupled to hippocampal theta oscillations (Borhegyi et al., 2004, Bassant et al., 2005, Simon et al., 2006, Joshi et al., 2017). Not only GABAergic, but MS glutamatergic neurons were also described to exhibit a highly heterogeneous set

of firing patterns including fast-firing, burst-spiking and slow-firing (Sotty et al., 2003). The second group was composed of non-bursting units that presented oscillation pattern at theta frequency. This group was intermediate in both firing frequency and waveform width. Theta modulated neurons are likely to be GABAergic or glutamatergic neurons (Jones et al., 1999, Sotty et al., 2003, Huh et al., 2010, Hangya et al., 2009). The regular-spiking group showed the smallest firing frequency and no theta modulation. Slow spiking MS neurons have been described to be cholinergic and innervate both pyramidal and interneurons in the hippocampus.

In this chapter, we also analysed the correlation between the speed of the animal and the firing frequency of MS neurons. Theta frequency has been described to be linearly proportional to the animal's speed, increasing the firing rate of theta-modulated neurons in the hippocampus (Ekstrom et al., 2001, McNaughton et al., 1983b). Interestingly, in this study, we found that the firing rate of the MS neurons was negatively correlated with the animal's speed. The theta-bursting units were the most affected by speed (76%), 64% of which were negatively correlated with speed. Considering that most of the MS connections to hippocampal interneurons are GABAergic to GABAergic (Freund and Antal, 1988), and hippocampal interneurons increase their firing rate relative to speed (Czurkó et al., 2011), our findings should be expected since inhibition of MS GABAergic neurons result in disinhibition of hippocampal interneurons.

Lastly, we evaluated the effect of optogenetic stimulation on MS neurons. Beforehand, it is essential to explain that the experiments were based on ChR2

which are nonspecific cation channels that depolarize the cell membrane when exposed to blue light, which can only depolarize neurons. Unexpectedly, we observed more inhibited than excited units within the MS when the light was applied. The Hsyn promoter is nonspecific and theoretically can be used as a promoter in all types of neurons when transported by adeno associated virus. One possible explanation to the inhibited neurons is that the virus expressed in a subpopulation of MS GABAergic cells and consequently inhibited the majority of the cells when the light was applied. However, there is not enough anatomical data about the MS interconnections. Patch clamp recordings showed that glutamatergic and GABAergic MS neurons make connections within the MS and cholinergic neurons receive both glutamatergic and GABAergic connections, forming recurrent networks (Leão et al., 2015). However, this data is not enough to determine the precise intra-septal connections and our suggestion of a subpopulation of GABAergic inhibiting other neurons cannot be proved.

One limitation of this study is that we did not quantify the expression of ChR2 controlled by Hsyn promoter in different cell types. The Hsyn promoter is nonspecific and theoretically can be used as a promoter in all types of neurons. However, little is known about the process of the internalization adeno associated virus by neurons. Viral transduction is determined empirically for each brain region and cell types (Hammond et al., 2017). So, we cannot determine what neurons expressed ChR2 without immunohistochemistry techniques. The quantification is feasible by combining viral expression of fluorophores to immunohistochemistry and could be proposed as future work. Another point to consider is that we included the light stimulation periods in the calculation of

speed to spike rate correlation. The inhibition or stimulation of units certainly induced more or fewer spikes during the recording, but the laser was applied every 6 seconds for a short duration, which would not have an effect on the overall speed correlation calculation.

It is important to discuss that classification of units in theta and bursting are dependent on firing rate because both methods used interspike interval in the calculations. For instance, bursts were defined as sequences of at least three spikes having less than 5 ms from one to another. The probability of a fast-spiking cell to being classified as bursting is higher compared to a slow spiking cell. In both figures 11B for MS units and 19B for CA1 interneurons, we could observe that bursting units were the groups with the highest firing rate. The bursting definition comes from in vitro patch clamp experiments, usually associating the propensity to burst to membrane properties (Connors et al., 1982). In this thesis, the bursting classification was an attempt to segregate medial septum PV positive cells, which have been described as fast spiking theta modulated bursting units (Varga et al., 2008) and hippocampal interneurons which are both bursting and theta modulated. These units were suggested to mediate theta modulation in the hippocampus.

In the second part of this chapter, we analysed the effect of MS stimulation in the hippocampal interneurons. This study aimed to investigate the effect of MS stimulation on hippocampal interneurons, for this reason, only affected cells were included in the analysis. We used the same classification in bursting and theta modulated units, and as observed in the MS, bursting units were also theta

modulated. Compared to MS units, hippocampal interneurons firing frequencies followed the same pattern, theta-bursting units showing the highest firing frequency, followed by theta modulated and regular spiking units. However, regarding waveform width, the non-bursting theta group was the smallest, and no difference was found between the theta-bursting and regular units. Interneurons have been demonstrated to be positively correlated to an animal's speed, and theta modulated interneurons showing stronger correlation (Czurkó et al., 2011). In accordance with previous results, we found that most of the hippocampal interneurons were positively correlated with speed and the correlation was stronger for theta modulated interneurons. However, we found that a significant subpopulation of interneurons was negatively correlated with speed. These results are in agreement with a study which characterized interneurons in the dorsal CA1 and found that a small proportion (8/93, 8.6%) were negatively correlated with speed. Very close to (6/67, 9%) described here (Góis and Tort, 2018).

Lastly, we evaluated the effect of nonselective MS stimulation on CA1 interneurons. In the theta bursting group, we had the opposite effect from the MS. In the MS most of the theta bursting units were inhibited, and in the CA1 the majority were disinhibited. As described before, the theta bursting MS units are most likely to be inhibitory GABAergic cells (Morris et al., 1999, Knapp et al., 2000, Borhegyi et al., 2004, Simon et al., 2006). The inhibitory effect on the majority of theta bursting MS neurons could explain the increase in firing frequency of the hippocampal theta bursting interneurons.

In the non-bursting theta group, most of the interneurons were also disinhibited, so we would expect an increase in theta power in the hippocampus. Indeed, the power spectrograms showed a peak in theta power after MS stimulation. MS GABAergic PV+ neurons were described to project to hippocampal PV+ neurons including basket cells, which can innervate many pyramidal neurons and are strong candidates to synchronize MS oscillations to hippocampal oscillations (Ognjanovski et al., 2017, Hu et al., 2014, Freund, 1989, Freund and Antal, 1988, Freund and Katona, 2007).

It has been shown that electrical theta bursting stimulation of the MS can reset hippocampal theta-bursting units (Mamad et al., 2015). We also observed that a subpopulation of theta-bursting units was strongly affected by MS stimulation. These units showed peaks on the histogram at theta frequency and the phase synchronization extended for more than one second after MS stimulation. Moreover, we observed an oscillatory pattern on the LFP of the event-related potential (ERP) filtered in both 0-45 Hz and in the theta band.

To summarize, in this study we expressed ChR2 in MS and recorded MS neurons and interneurons of freely moving rats. We found that most of MS neurons were inhibited, although ChR2 can only excite neurons. Moreover, we showed that hippocampal interneurons are mostly disinhibited during MS stimulation. We also showed a relationship between firing rate and speed, and unexpectedly most of the MS neurons were negatively correlated with speed.

Chapter 4

Optogenetic Stimulation of the Medial Septum Induces Real-Time Place Preference

4.1. Introduction

Deep brain stimulation (DBS), a surgical procedure involving the implant of a neural stimulator in target areas, recently re-emerged as a chosen technique for the treatment of refractory neurological and psychiatric disorders. The septal area has been known as a "pleasure centre" for over sixty years, and recently it was considered as a target of DBS for treatment of schizophrenia and epilepsy (Ma and Leung, 2014, Fisher, 2013).

The septal area is the primary modulator of hippocampal oscillations, and it provides the hippocampus with GABAergic, cholinergic and glutamatergic fibres which are intimately related to memory (Amaral and Kurz, 1985, Colom et al., 2005). Septal lesions have been linked with a reduction in performance on a variety of learning and memory tasks and decline of hippocampal acetylcholine levels (Herzog et al., 2000, Givens and Olton, 1990, Kesner et al., 1986, Mizumori et al., 1990, Morris et al., 1992). Moreover, cholinergic modulation of the hippocampus is depreciated in Alzheimer's disease or during healthy aging, in both rats and humans (Gill and Gallagher, 1998, Schmitz et al., 2018). Stimulation of the septum has been proposed to improve spatial working memory in rats after traumatic brain injury. Furthermore, DBS in the septal area enhances memory in rats with a cholinergic deficit and pilocarpine-induced status epilepticus (Lee et al., 2013, Jeong et al., 2014, Lee et al., 2017).

The septum is intimately related to areas associated with the mesocorticolimbic dopamine (DA) system, including the lateral hypothalamus (LH) (Risold and Swanson, 1996, Jakab and Leranth, 1993, Geisler and Zahm, 2005, Oades and

Halliday, 1987, Gaykema et al., 1990, Sweeney and Yang, 2016). Moreover, the septum was the first brain region to be observed to elicit intracranial self-stimulation in rats. Animals were described to compulsively press a lever in order to receive an electrical stimulation in this area (Olds and Milner, 1954). Within the septal area, the medial septum displayed higher self-stimulation rates and lower self-stimulation thresholds. i.e., rats could learn faster to press a lever in order to receive stimulation when the electrode was close to the midline compared to lateral regions (Cazala et al., 1988). Furthermore, pharmacological studies showed that the midline region of the septal complex promotes self-administration of $GABA_A$ receptor agonist muscimol (Gavello-Baudy et al., 2008), suggesting that medial septal GABAergic neurons could be involved in septal electrical self-stimulation.

Rewards have substantial importance in life as it can modulate goal-oriented behaviour for food, water or sex. Indeed, animals can perform better in tasks if a reward is expected (Wise, 2004). Furthermore, it is closely related to memory and attention (Watanabe and Sakagami, 2007, Engelmann et al., 2009, Pessoa, 2008, Pessoa and Engelmann, 2010, Doallo et al., 2013). Accumulated data suggest that the mesocorticolimbic dopamine (DA) system plays a role in reward and reinforcement processing, motivation, and goal-directed behaviour. These functions mediated by dopaminergic release in the VTA and nucleus accumbens (NAc) (Wise, 2004, Hollerman and Schultz, 1998, Schultz, 1998). The LH also play a role in reward, GABAergic LH projections to the VTA was suggested to induced positive reinforcement and place preference while increasing dopaminergic release in NAc (Nieh et al., 2016).

The septum projects to multiple hypothalamic areas including the LH which has been associated to reward (Stuber and Wise, 2016). Studies have demonstrated that LH modulates reward via projections to the mesolimbic dopamine system (Fouriezos et al., 1978, Nieh et al., 2015, Nieh et al., 2016), including GABAergic projections to the VTA (Barbano et al., 2016). Inhibition of GABAergic interneurons in the VTA, induces disinhibition of the DA neurons (Johnson and North, 1992, Szabo et al., 2002, Tan et al., 2012).

Whereas reward dependent behaviour can be acquired by electrical septal stimulation, how MS neurons mediate this behaviour it is not fully understood. Here we proposed an experiment to assess real-time place preference (Stamatakis and Stuber, 2012a) while optogenetically stimulating MS neurons.

The aims of this study were first to, mimic the well-described reward-related response from septal stimulation using optogenetics. We hypothesized that nonselective optogenetic MS stimulation would mimic the electrical MS stimulation. To test the behaviour effect, we use a place preference test adapted for an optogenetic real-time response. Second, we use a transgenic rat model which allow for the specific expression of ChR2 in glutamate decarboxylase 1 (GAD1) positive neurons. These animals were used to test the hypothesis that the MS GABAergic neurons could be mediating the place preference behaviour. Lastly, we tested the effect of MS cholinergic stimulation. To specifically stimulate MS cholinergic neurons, we used a transgenic model which allowed the expression of ChR2 in choline acetyltransferase (ChAT) positive neurons.

4.2. Methods

All animal work has been carried out in the Health Products Regulatory Authority (HPRA) authorised establishment, Trinity College Dublin (establishment authorisation number: AE19136) ensuring compliance with the requirements of Directive 2010/63/EU and S.I. No. 543 of 2012. This work has also been approved by the TCD Animal Research Ethics Committee (AREC) which is a Level 2 ethics committee responsible for reviewing the proposed use of animals in teaching and research in line with the Research Ethics Policies in operation in TCD.

4.2.1. Animals

A total of 18 animals were used in this study: six male (250-350 g) Lister-Hooded rats (Harlan, UK), four male (250-350 g) Long Evans rats Chat-Cre, strain LE-Tg(ChAT-Cre)5.1Deis (Rat Resource & Research Centre, RRRC#: 658), which express Cre-recombinase enzyme under control of choline acetyltransferase (ChAT) expressed in cholinergic neurons, and lastly, six male GAD1-Cre rats, strain LE-Tg(Gad1-iCre)3Ottc (Rat Resource & Research Centre, RRRC#: 751). These rats express Cre-recombinase enzyme under control of the glutamate decarboxylase 1 (GAD1) promoter, one of two genes encoding the GAD enzyme that converts glutamate to GABA.

Before any experimental procedures, the rats could acclimate to their housing for at least five days, during this time they were handled and habituated to the

laboratory environment and experimenter. They had ad libitum access to food and water in a temperature-controlled (18-22 °C) laminar airflow unit, maintained on a 12 hour of light (8 a.m. - 8 p.m.) and 12-hour dark cycle. After surgery, animals recovered for ten days having ad libitum access to food and water. During recording sessions, rats received 10-25g of food as standard each day and 15-20 mg of food pellets (TestDiet, Formula 5TUL, USA) during each trial. The recording sessions were conducted during the light phase (10 a.m. - 18 p.m.) and, in between session the rats were kept in the conditions described above.

4.2.2. Stereotaxic surgeries and viral injections

The surgery was described in detail in section (2.1.2). Briefly, rats were anesthetized with isoflurane, and once the animal was deeply anesthetized, the scalp was shaved, and rats were placed in the stereotactic apparatus. After skull drilling, animals were injected with a recombinant AAV. Non-transgenic animals were injected with AAV5.hSyn.hChR2(H134R)-eYFP.WPRE.hGH (Adgene #26973P). A total of 2 µL (0.1 µL.s-1). The transgenic animals, both LE-Tg(ChAT-Cre)5.1Deis and LE-Tg(Gad1-iCre)3Ottc were injected with 2 µL (0.1 µL.s-1) of AAV5.EF1a-DIO.hChR2-(E123T/T159C).EYFP.WPRE.hGH (Adgene #35509) using a Hamilton syringe. The MS coordinated used: AP +0.8; ML 1.4; DV 5.5-6.5; and a mediolateral angle of 10 degrees. After virus injection, an optic fibre (200 µm core diameter, Thorlabs Inc.) was chronically implanted at the same coordinates. To target the LH, a second optic fibre was implanted at the following coordinates: -2.4 AP; +2.6 ML; 8.8 DV; and mediolateral angle of 25 degrees. For neural recordings, the

tetrodes were inserted into the hippocampus CA1 area at the following coordinates: -3.8 AP; -2.5 ML; 1.4 DV. The assembly was permanently attached to the skull with dental cement. Implanted animals were housed individually with ad libitum access to water, and in food controlled stated to keep animals 85-90% their weight at surgery day. Animals were left to recover for at least seven days after surgery.

4.2.3. Viral constructions

All the viral constructions were serotyped with AAV5 coat proteins which demonstrated to be strongly expressed in the MS. Vector Core packaged both viral constructions at the University of North Carolina. Viral titers ranged from 1.5 to 1.8 x 10^{12} particles per ML. Transgenic animals were injected with AAV5.EF1a-DIO.hChR2-(E123T/T159C).EYFP.WPRE.hGH (Adgene #35509), and non-transgenic rats with AAV5.hSyn.hChR2(H134R)-eYFP.WPRE.hGH (Adgene #26973P).

4.2.4. Phase-Locking Value

As described in section (2.4.9) we used phase-locking value (Lachaux et al., 1999) to assess the effect of MS stimulation on hippocampal CA1 LFP. In short, the hippocampal LFP signal was filtered using a band-pass filter and divided into six seconds epochs. A Hilbert transformation was used to compute the instantaneous phase of the epochs. The transformed epochs were summed and normalized. The

phase-locking value ranges between 0 and 1; values close to 0 means that sum of a random signal. Values close to 1 meaning that the stimulus-induced a change in the phase-locking value (Tsanov et al., 2014).

4.2.5. Open field

Before and after the behaviour test, we recorded hippocampal CA1 LFP and single units during MS stimulation to ensure that the virus was expressed. The rats were recorded for 12 min on the (60 x 60 cm) arena (see section 2.2.1), and photostimulation (473 nm, 50 Hz, 12 pulses, 5 ms pulse duration) was applied every 6 seconds. During the recordings, food pellets (TestDiet, Formula 5TUL) were thrown in every 20 seconds to pseudo-random locations within the open field ("random foraging" task). In this way the laser stimulation tends to be randomly distributed on all extension of the arena, avoiding the association of the laser with the position.

4.2.6. Real-time place preference

Real-time place preference (Stamatakis and Stuber, 2012b) was performed using a linear squared maze, detailed described in section (2.4.14). In short, it was a squared (85cm x 85 cm and 10 cm wide) made of plywood painted black. The maze was situated in the middle of the recording room where many visual cues were visible. Rats were allowed to run freely during recordings. Sugar pellets (TestDiet,

Formula 5TUL) were alternated presented in two different corners, i.e., the rat only received food in the corner when he completed half maze (from SE to NW). During approximately one week the rats were trained to run equally in both sides of the maze by controlling the number of sugar pellets and directing the animal when necessary. Once rats were navigating approximately equally in both sides of the arena without any intervention for at least three recordings, the protocol started. The recording protocol consisted of 12 min baseline followed by 12 minutes of laser stimulation. The laser activation was programmed using a "Basic" script which runs on the recording equipment. The program read the camera information and delivers the laser stimulation only when the animal was localized on the designated side of the maze, i.e., when the animal was localized on the NW-SW or SW-NE arms (figure 10). Every time the rat entered in the designated reward area, the laser turned on, delivering the stimulation protocol (5 ms pulse duration, 12 pulses per train at 50 Hz, 500 ms inter-train interval). The stimulation protocol was set to be repeated for as long as the animal stayed in the reward area.

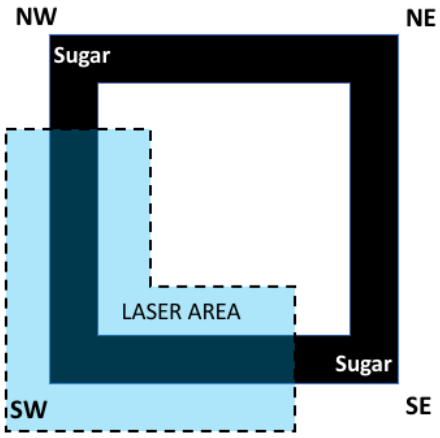

Figure 26 Schematic of the linear square arena.

Rats could navigate freely to collect sugar pellets on the opposite corners (SE and NW). During the 12 min stimulation, the rats receive stimulation only at one side of the area marked by the blue colour.

4.2.7. Passes score

Passes score between the two sides of the arena were expressed by calculating a difference/sum score. The score for a pair (SW, NE) of each condition was obtained by calculating the signed difference (SW - NE) and dividing by their sum (SW + NE). The results ranged from -1 to 1. A score of 0 meaning that the animal equally passed on both sides; the extreme value -1 meaning that the rat only passed on the NE side; lastly the result 1 meaning that the animals only passed on the SW side.

4.2.8. Spike sorting

The spiking sorting used in this chapter has been described in section (2.4.1). In short, the candidate waveforms were clustered by the k-means algorithm using tint graphical software (Tint, Axona Limited). Waveforms were separate based on spike amplitude, duration, maximum and minimum spike voltages and duration of the peaks.

4.2.9. Post-mortem verification

After completion of electrophysiological recordings, brains were removed for histological verification of the expression of the virus and the localization of the electrodes and optic fibres as described in section (2.5). In short, animals were first anesthetized with isoflurane and injected with pentobarbital sodium (Euthanal, UK) and perfused transcardially with ice-cold phosphate-buffered saline followed by paraformaldehyde. The brain was removed from and transferred to a sucrose solution. Brains were frozen and sectioned at 40μm thickness. Fluorophore images were collected using an Olympus BX51 fluorescence microscope. Unfortunately, we lost the frozen brains from the ChAT: Cre transgenic animals due to a freezer problem over the weekend.

4.2.10. Statistical analysis

Statistical analysis of all data was performed using GraphPad Prism version 7.02 for Windows, (GraphPad Software, La Jolla California). All data are represented and expressed as the mean ± standard error of the mean (SEM). The analysis was carried out using both one-way ANOVA (Analysis of Variance) when one factor was compared among three groups, independent t-test and dependent t-test were used to compare distributions. When data did not follow a normal distribution, the adequate non-parametric test was used. The difference was considered significant when $P < 0.05$.

4.3. Results

Place cells and interneurons were recorded from the non-transgenic animals and described in chapter 4 and chapter 6. We also recorded interneurons and place cells from ChAT-Cre and GAD1-Cre transgenic animals. However, units recorded from ChAT-Cre animals were not affected by optogenetic stimulation. In contrast, we recorded place cells and interneurons from GAD1-Cre rats. The 35 place cells were recorded in only one animal and 24 interneurons from 2 animals. All place cells recorded during MS stimulation were disinhibited, and 62% of the interneurons also disinhibited. Due to the low number of animals we decided to not include this study.

4.3.1. Viral expression in the MS of non-transgenic rats

To test the behavioural effects of MS non-specific optogenetic stimulation, rats (n=6) received injections of AAV-Hsyn-ChR2-YFP vectors, an optic fibre implant over the MS and recording tetrodes in the pyramidal layer of dorsal hippocampal CA1. First, these animals were placed on an open field for a relatively simple behavioural task, for 12 minutes they were free to move while sugar pellets were thrown on the arena. The MS was stimulated every six seconds (473 nm, 50 Hz, 12 pulses, 5 ms pulse duration) while the hippocampal LFP was recorded. Phase-locking value (PLV) (Lachaux et al., 1999, Mamad et al., 2015) was used to evaluate the degree of the hippocampal LFP synchronization during non-specific optogenetic MS stimulation (M = 0.60 ± 0.15, n = 6) (figure 27A). A post-mortem

verification of the viral expression and optic fibre position confirmed a strong viral expression precisely limited to the MS (figure 27B).

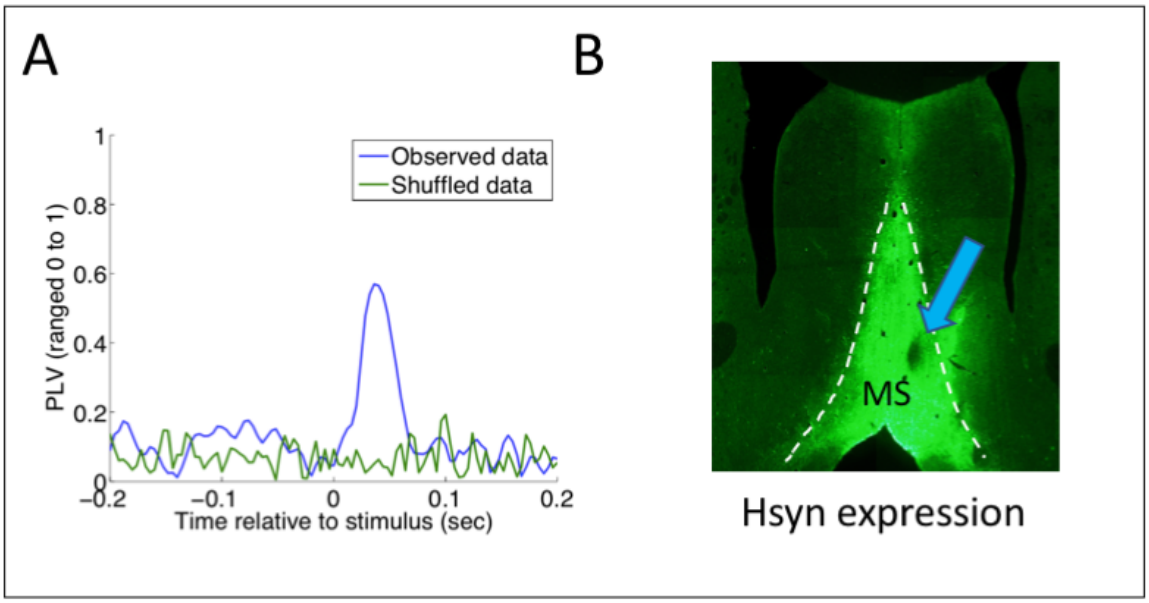

Figure 27. Viral expression in MS.

(A) Example of a phase-locking value (PLV) evaluated on hippocampal LFP for theta band. The PLV is a statistic to investigate the synchronization of neural activity (Lachaux et al., 1999). The blue trace is the calculated PLV on the hippocampal LFP epochs while the green trace is the calculated PLV on the shuffled LFP epochs. Time 0 indicate the time of optogenetic MS stimulation. **(B)** Strong viral expression of the AAV-Hsyn-ChR2-YFP in the MS, the blue arrow shows where the tip of the optic fibre was localized.

4.3.2. Initial place preference test

Before testing for the effect of the light stimulation on place preference, rats were placed on the linear squared maze to be tested without stimulation to access the baseline place preference. For 12 minutes, rats were allowed to move freely on the

maze were food was presented on southeast (SE) and northwest (NW) corners (figure 28A). An independent-samples t-test was conducted to compare the time in seconds spent on NE and SW sides of the maze without laser stimulation (baseline). There was not a significant difference in the scores for place preference from the NE (M = 91.19, SD = 11.71) and SW (M = 94.14, SD = 12.74) sides t(10) = -0.417, p = 0.685. The lack of significant differences in time spent by rats on both sides before stimulation confirmed that both sides were equally attractive for the animals (figure 28B).

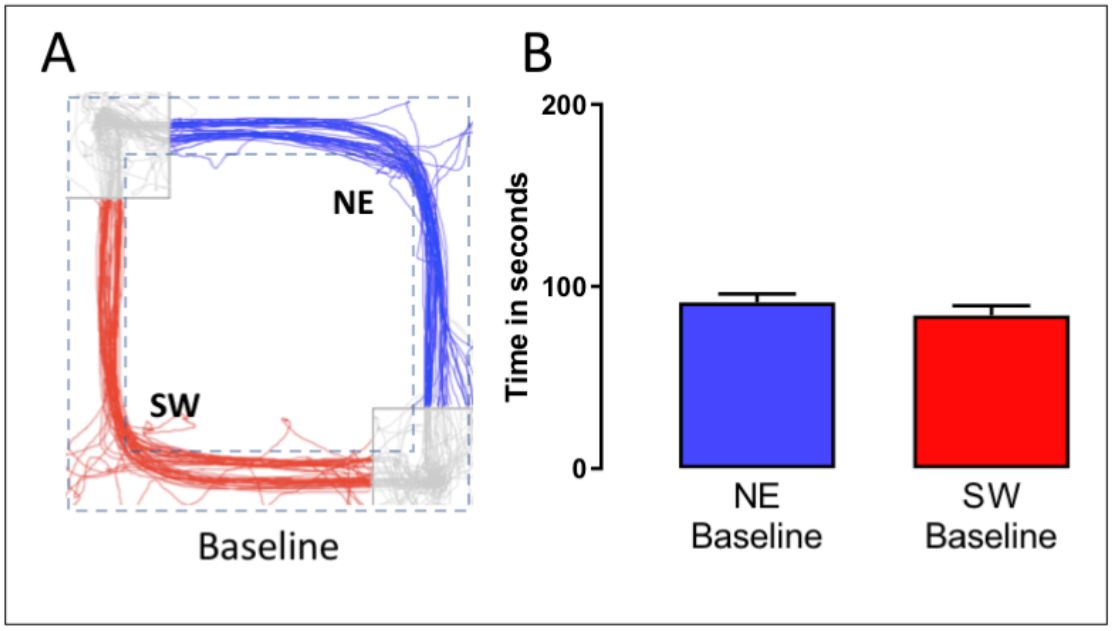

Figure 28. Rats had no place preference during baseline recordings.

Animals were tested for 12 minutes on the linear squared maze to assess the baseline preference for one of the sides. There were no significant differences in time spent on each side during the initial preference test ($p > 0.05$). Bars are plotted with the Mean ± SEM.

4.3.3. Stimulation of non-specific MS neurons induce real-time place preference

To assess the effect of the MS laser stimulation on the real-time place preference, rats were recorded in the same conditions present during the baseline, except for the laser, which was turned on automatically every time the rat entered the SW side of the maze (figure 3.A). A stimulation protocol (5 ms pulse duration, 12 pulses per train at 50 Hz, 500 ms inter-train interval) was repeated until the rat left the SW side. A paired-samples t-test was conducted to compare the time in seconds spent on SW side in the baseline and SW side during stimulation. Statistical analyses demonstrated that there was a significant difference in the time in seconds spent on $SW_{Baseline}$ (M = 94.13, SD = 12.73) and $SW_{Stimulation}$ (M = 220.23, SD = 86.49); t(5) = -3.793, p = 0.013. Showing a strong effect on the preference behaviour during MS stimulation (figure 29B).

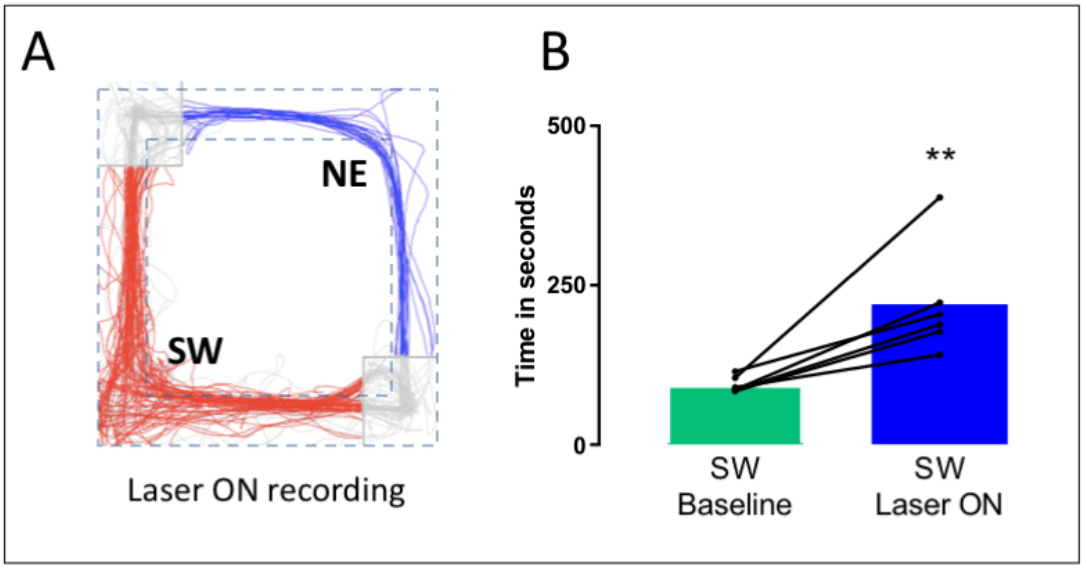

Figure 29. Effect of non-specific MS stimulation on real-time place preference.

(**A**) Example of stimulation recording. The rat was allowed to move freely for 12 minutes, sugar pellets were presented on opposite corners (SE and NW), during stimulation recording, the laser was turned ON while the rat was on the SW side. (**B**) A paired t-test compared the amount of time spent on SW side during baseline and SW side during stimulation. The test showed a significant increase in time spent on the SW side during septal stimulation, p = 0.013.

To confirm the place preference, we also evaluate how many times the animals crossed by each side of the arena. We calculated a score based on the signed difference divided by the sum. The score was used to quantify the number of passes between baseline and stimulation. It ranges from -1 to 1; where -1 means that the rat only passed on the NE side, zero means that the animals passed equally in both sides, and 1 meaning that animals only passed on the SW side (figure 30). A Wilcoxon matched pairs signed rank test showed a slightly significance (p = 0.031) when comparing the number of passes score between baseline and stimulation.

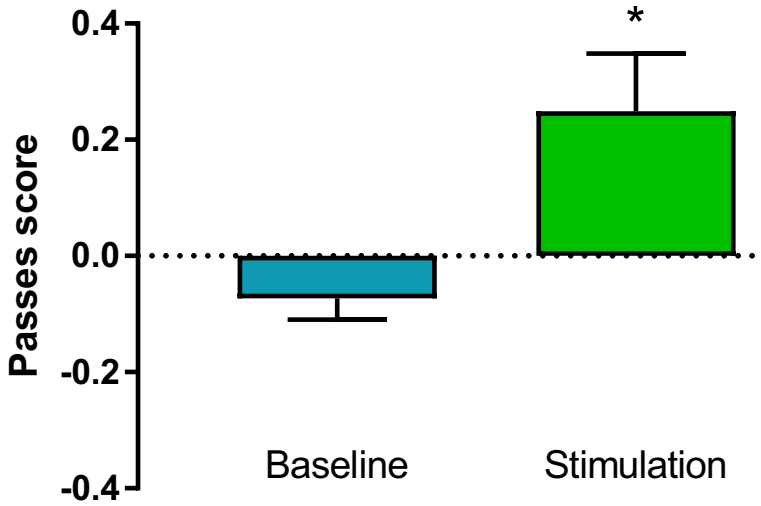

Figure 30. Non-specific MS stimulation induce place preference.

The number of passes was counted for each side during baseline and stimulation. The passes score ranges from -1 to 1. Where -1 would result from all passes on the NE side; 0 meaning an equal number of passes from both sides, and 1 representing all passes on the SW side. Wilcoxon matched pairs signed rank test showed significant preference for the passes on SW during laser stimulation ($p = 0.031$)

4.3.4. Viral expression of Cre-dependent virus on Gad1-Cre rats

To examine if stimulation of MS GABAergic neurons affected the place preference behaviour, we injected Gad1-Cre (n=6) rats with a Cre-dependent AAV (AAV5 - EF1a - DIO - ChR2 - E123T/T159C) which mediates blue light–induced depolarization on GABAergic GAD1 neurons. The Gad1-Cre rats have been demonstrated to have a high co-expression of Cre and GAD1 mRNA in the midbrain (76% ± 11%) and LH (80% ± 6%) (Sharpe et al., 2017). An optic fibre

implant over the MS and recording tetrodes in the pyramidal layer of dorsal hippocampal CA. The PLV showed that stimulation of the MS GABAergic neurons induced a strong phase-locking value on the hippocampal LFP (figure 31A).

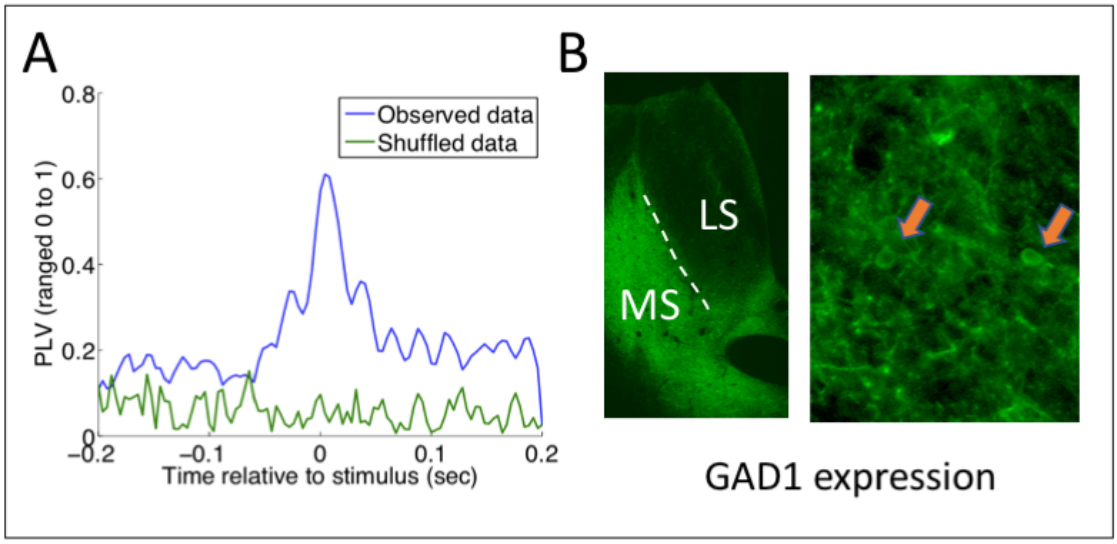

Figure 31. Viral expression in Gad1-Cre transgenic rats

(A) Example of a phase-locking value (PLV) evaluated on hippocampal LFP for theta band during MS stimulation. The blue trace is the calculated PLV on the hippocampal LFP epochs while the green trace is the calculated PLV on the shuffled LFP epochs. Time 0 indicates the MS stimulation. **(B)** Strong viral expression of the Cre-dependent AAV5-EF1a-DIO-ChR2 - E123T/T159C in the MS, the orange arrows indicate cell bodies.

4.3.5. Initial place preference test for Gad1 rats

Following the same protocol, we tested the place preference without laser stimulation to assess the baseline preference. Baselines were recorded for 12 minutes, and rats were allowed to move freely on the maze were food was presented on SE and NW corners. An independent-samples t-test was conducted to compare the time in seconds spent on NE and SW sides of the maze (figure 32).

No significant difference was observed in the time spent on NE (M = 98.12, SD = 10.21) and SW (M = 98.74, SD = 14.11) sides; t(10) = -0.088, p = 0.932. The number of passes on each side was also evaluated during the baseline. There was no significant difference in the scores for place preference comparing the NE (M = 67.67, SD = 6.89) and SW (M = 63.17, SD = 12.92) sides; t(10) = 0.753, p = 0.469 (figure 32B).

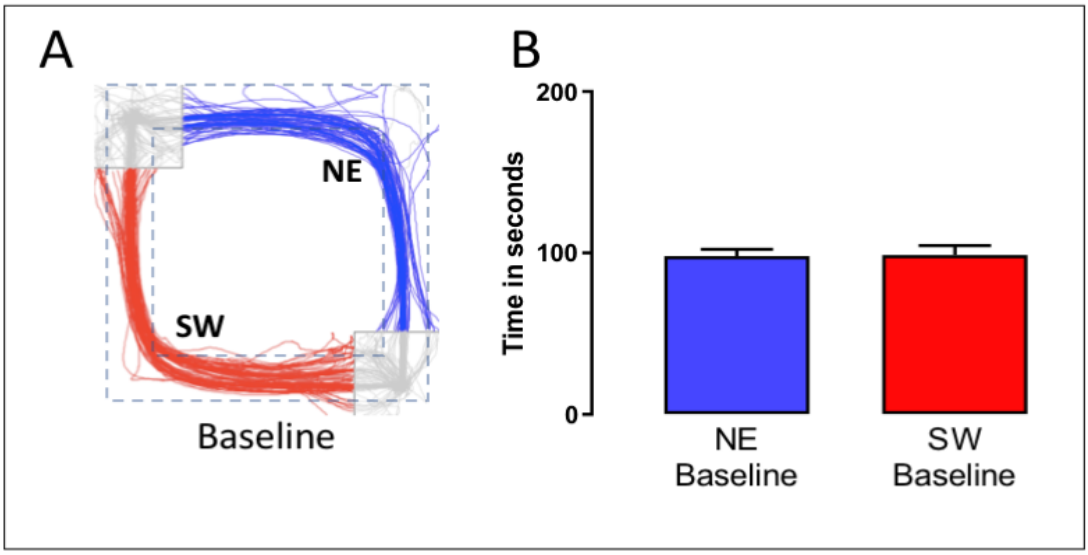

Figure 32. Transgenic GAD1 rats had no place preference during baseline recordings.

Transgenic GAD1-Cre rats were tested for 12 minutes on the linear squared maze to assess the baseline preference for one of the sides. There were no significant differences in time spent on each side during the initial preference test ($p > 0.05$). Bars are plotted with the Mean ± SEM.

4.3.6. Stimulation of GABAergic neurons induced real-time place preference

We next tested the GAD1 rats on the linear squared maze activating the laser every time the rats were on the SW side. The stimulation of MS GABAergic neurons induces a strong in real-time place preference. A paired-samples t-test was conducted to compare the time in seconds spent on SW side in the baseline and SW side in the stimulation. There was a significant difference in the time spent on $SW_{Baseline}$ (M = 98.12, SD = 10.21) and $SW_{Stimulation}$ (M = 127.49, SD = 17.32) sides; t(5) = -4.247, p = 0.008 (figure 33B).

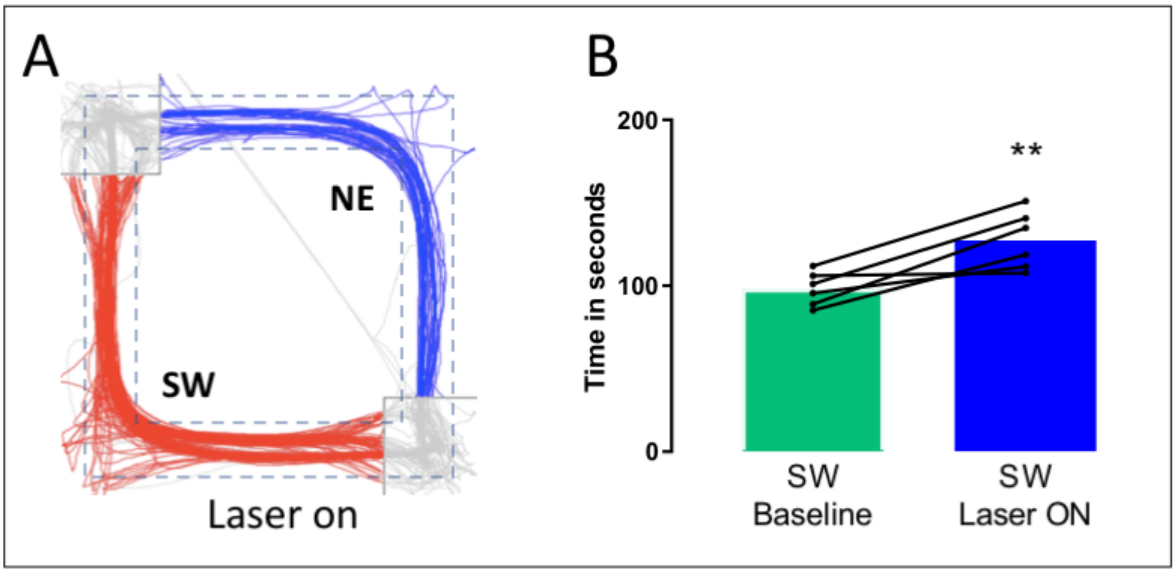

Figure 33. Effect of GABAergic MS stimulation on real-time place preference.

(**A**) Example of stimulation recording of a GAD1-Cre transgenic rat. The laser was ON on the red side (SW) (**B**) The amount of time spent on SW side during baseline and SW side during stimulation. A paired t-test showed a significant increase in time spent on the SW side during septal stimulation, p = 0.008.

We also calculated the signed diff/sum score for the passes computed during baseline and stimulation recordings. A paired-samples t-test was conducted to compare the passes score between the baseline and the stimulation of MS GABAergic neurons. A Wilcoxon matched pairs signed rank test showed a slight preference for the NE side during the baseline and significant preference for the SW side during laser stimulation on SW ($p = 0.015$) (figure 34).

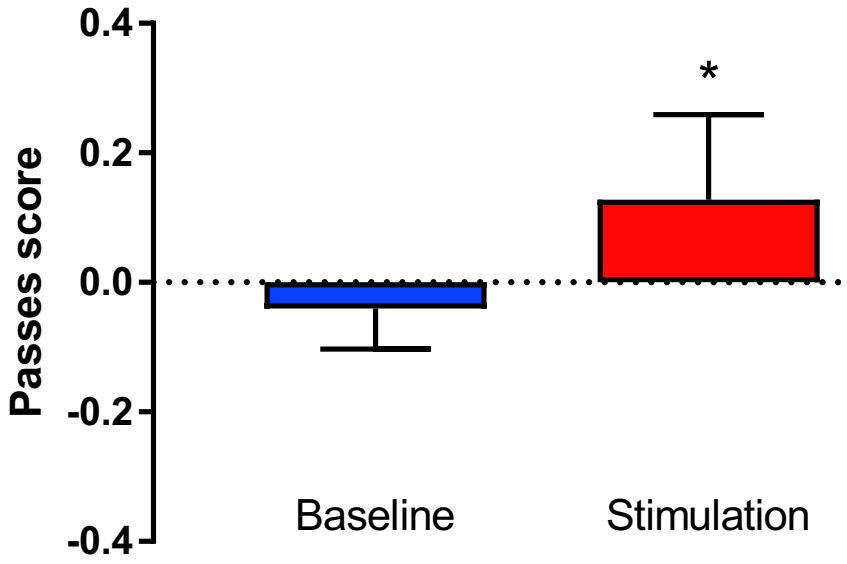

Figure 34. GABAergic stimulation induces place preference.

The number of passes was counted for each side during baseline and stimulation. The passes score ranges from -1 to 1. Where -1 would result from all passes on the NE side; 0 equal number of passes from both sides, and 1 representing all passes on the SW side. A Wilcoxon matched pairs signed rank test showed a slight preference for the NE side during the baseline and significant preference for the SW side during laser stimulation on SW ($p = 0.015$).

4.3.7. Stimulation of MS GABAergic fibres in the lateral hypothalamus

To further investigate a possible pathway by which MS GABAergic neurons could mediate place preference, we stimulated the MS projections to the LH area. The LH was also described on early self-stimulation studies to be a locus of reward (Hoebel, 1979, Huguet et al., 2009). Moreover, the LH GABAergic neurons send and receive dense projections from VTA (Nieh et al., 2015). The LH area is localized deep ventrally in the brain, which increases the difficulty to reach by stereotaxic implantations. A small error on the implantation angle can result in a big error on the tip of the optic fibre. Moreover, rats implanted in the LH were more susceptible implantation problems due to the complexity of the surgery. For this reason, only tree rats were used to investigate the effect of LH stimulation. The same protocol was used to test for real-time place preference, and a Wilcoxon signed rank test was used to compare the time in seconds spent on $SW_{Baseline}$ and $SW_{Stimulation}$ during LH stimulation (figure 35). There was no significant difference in the medians of time spent on $SW_{Baseline}$ and $SW_{Stimulation}$. Moreover, a Wilcoxon matched pairs signed rank test showed no significant preference for the SW side during laser stimulation on SW ($p = 0.25$)

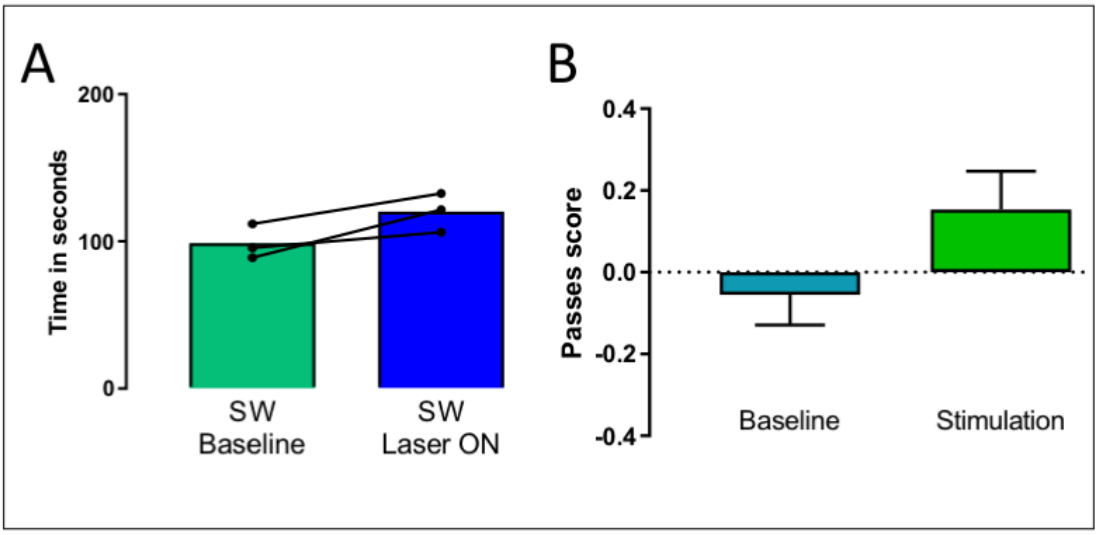

Figure 35. Stimulation of GABAergic fibres to LH.

(A) There was no significant difference in the amount of time spent on SW side during baseline and SW side during stimulation MS GABAergic fibres in LH. **(B)** The passes score from baseline and stimulation recordings were compared. A Wilcoxon matched pairs signed rank test showed no significant preference for the SW side during laser stimulation on SW ($p = 0.25$).

4.3.8. No place preference was observed during stimulation of MS cholinergic neurons

In our last experiment, we selectively targeted cholinergic neurons using a transgenic rat line which expressed the Cre-recombinase enzyme in choline acetyltransferase expressing neurons (ChAT). In the MS, the (ChAT)::Cre rat line has been shown to target cholinergic neurons specifically. Around 90% of the neurons which expressed yellow fluorescent protein (YFP) also expressed ChAT, and around 50% of the ChAT neurons expressed YFP (Mamad et al., 2015, Witten et al., 2011). We injected (ChAT)::Cre transgenic rats (n=4) with a Cre-dependent AAV (AAV5 - EF1a - DIO - ChR2 - E123T/T159C) which mediates blue light–induced

depolarization of the cholinergic neurons. We first tested for place preference for without laser stimulation. An independent-samples t-test showed no difference in the time spent on NE (M = 107.95, SD = 9.92) and SW (M = 99.70, SD = 6.43) sides; t(6) = 0.698, p = 0.615 of ChAT-Cre rats during the initial place preference (figure 36A). We also measured the real-time place preference by applying light on MS on the SW side of the linear squared maze. There was not a significant difference in the time spent on $SW_{Baseline}$ (M = 107.96, SD = 9.92) and $SW_{Stimulation}$ (M = 114.30, SD = 6.22) sides; t(6) = 0.698, p = 0.541 (figure 36B). The PLV was calculated for MS stimulation, the measured value was not different from the shuffled data (figure 36C). Finally, we measured the number of passes from each side. A Wilcoxon matched pairs signed rank test showed no difference between baseline and stimulation scores (p= >0.05) (figure 36D).

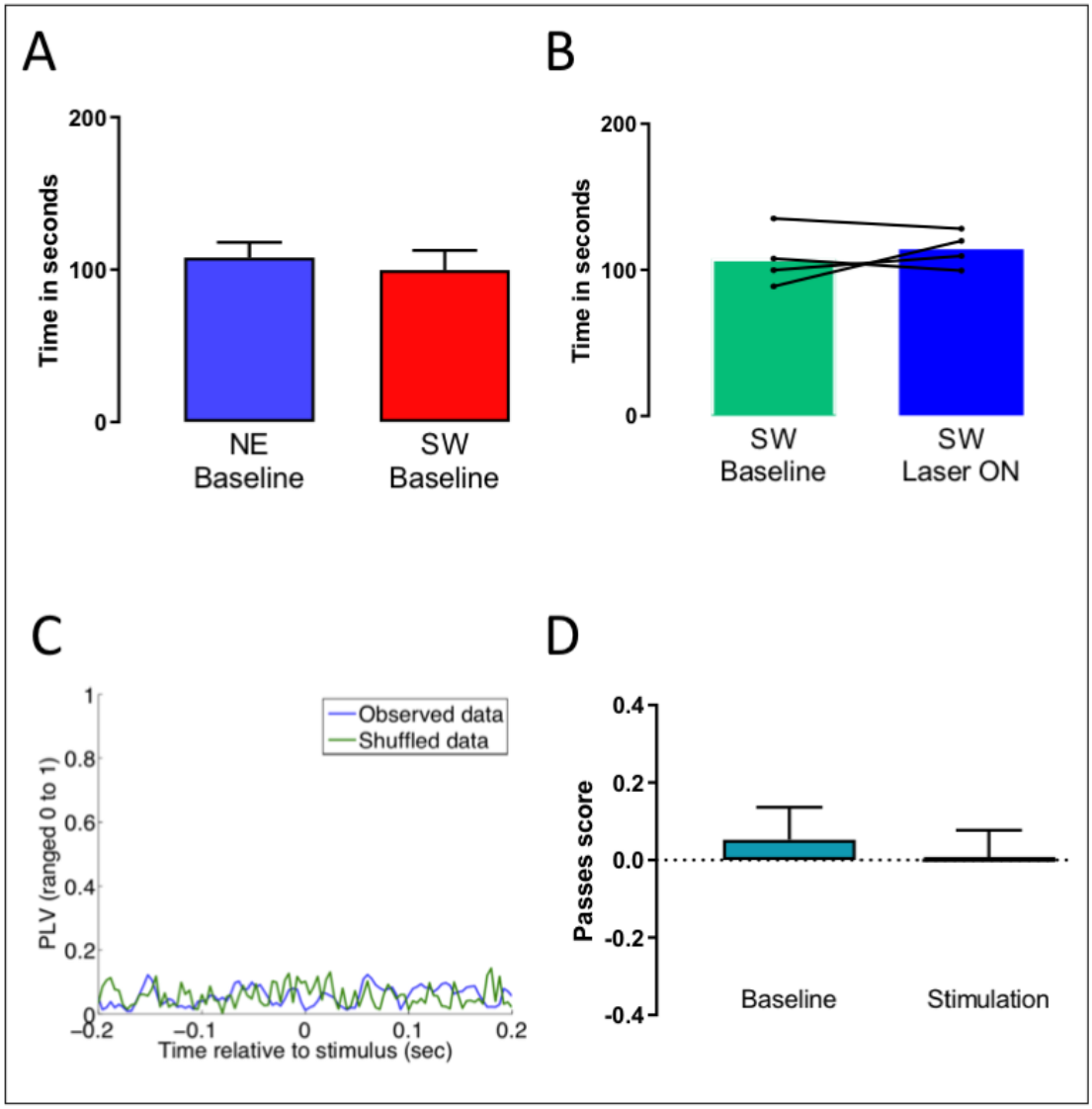

Figure 36. Stimulation of MS cholinergic neurons

(A) There were no significant differences in time spent on each side during the initial preference test ($p > 0.05$) for ChAT-Cre rats (n=4). **(B)** There was no significant difference in the amount of time spent on SW side during baseline and SW side during stimulation of the SW side of the maze. **(C)** Example of PLV evaluated on hippocampal LFP for theta band during MS cholinergic stimulation. MS stimulation did not have effect on PLV. **(D)** The passes score from baseline, and stimulation recordings were compared. A Wilcoxon matched pairs signed rank test showed no difference between baseline and stimulation scores ($p = >0.05$).

4.3.9. Phase-locking value comparison

Lastly, we compared the PLV between GABAergic, cholinergic and nonselective MS stimulation. One-way between subject ANOVA was conducted to compare the PVL between groups. There was a significant difference of PLV ($p<0.0001$) for the three groups [$F(2, 13) = 24.23$, $p < 0.0001$]. Post hoc comparisons using the Tukey HSD test indicated that the mean score for the nonspecific MS stimulation did not significantly differ from the GABAergic MS stimulation. Moreover, both non-specific and GABAergic were significantly different from the cholinergic group ($p<0.0001$) (figure 37). These results suggest that both non-specific and GABAergic MS stimulation resulted in strong LFP synchronization.

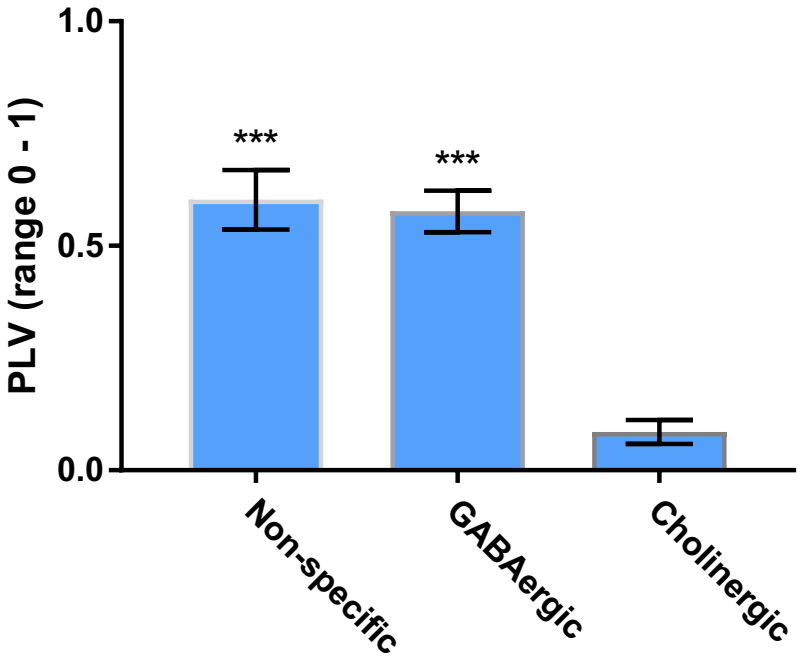

Figure 37. The phase-locking value between groups.

The comparison between PLV on the hippocampal LFP from the three different rat strains during MS stimulation. There was a significant effect of MS stimulation on PLV ($p<0.0001$) for the three strains [$F(2, 13) = 24.23$, $p < 0.0001$]. Moreover, a post hoc test indicated that there was not a significant difference between nonspecific MS stimulation and GABAergic stimulation. Both groups were different from cholinergic ($p<0.0001$).

4.4. Discussion

In this chapter, we aimed to explore the classically described involvement of the MS in reward processing (Olds, 1958a, Cazala et al., 1988, Carlezon and Chartoff, 2007). The major advances of this chapter are; first, we demonstrated that nonselective MS stimulation induced a strong reward-seeking behavioural effect on rats. Second, we showed that stimulation of MS GABAergic neurons was sufficient to elicit reward-related behaviour, suggesting that MS GABAergic neurons could be mediating the reward circuit.

4.4.1. Real-time place preference pathways

As described before, Hsyn is a gene found in all types of neurons and commonly used as a nonspecific promoter to express channelrhodopsin in neurons (Kugler et al., 2003). Before any behaviour test, we assessed the viral expression by measuring the phase locking value (PLV) on hippocampus LFP. The PLV is a statistic that measures responses to a repeated stimulus and compares latencies where the phase varied little across trials. The result is close to one if the stimulus causes changes on the signal or zero otherwise (Lachaux et al., 1999). In this thesis, the PLV was used to compare phase variations to the laser stimulation, using as a control, the same LFP shuffled 2000 times as in (Tsanov et al., 2014). During both nonselective MS stimulation, we observed PLV value close to one, meaning that MS stimulation effectively entrained hippocampal oscillations. In agreement with our results, the nonselective MS stimulation based on Hsyn promoter has been

applied to successfully modulate hippocampal oscillations (Laxpati et al., 2014, Blumberg et al., 2016).

MS GABAergic neurons are known to exhibit rhythmic bursting phase-locked to hippocampal theta oscillations (King et al., 1998, Borhegyi et al., 2004, Joshi et al., 2017), and optogenetic stimulation of MS GABAergic neurons has also been shown to control the hippocampal LFP frequency (Zutshi et al., 2018). These results suggest that nonselective stimulation could be affecting MS GABAergic neurons. To support this hypothesis, in our results we observed positive PLV in GABAergic Gad-Cre animals, very similar to the result observed on non-selective stimulation.

We found that stimulation of MS cholinergic neurons had no effect on PLV. Similar experiments using transgenic animals have shown that optogenetic stimulation of the MS cholinergic neurons had a weak effect on hippocampal LFP during active exploration (Vandecasteele et al., 2014, Mamad et al., 2015). Although, MS cholinergic neurons are the primary septal projections to the hippocampus (Dutar et al., 1995) and lesion or pharmacological blockade of MS cholinergic neurons can attenuate the hippocampal theta (Yoder and Pang, 2005, Newman et al., 2013). They are slow-firing neurons and do not contribute to theta frequency (Simon et al., 2006).

4.4.2. Real-time place preference pathways

Next, we tested if stimulation of the MS expressing ChR2 could induce place preference. The MS is composed of GABAergic, cholinergic and glutamatergic

neurons. The behaviour must be mediated by one of these populations or more than one of these subpopulations at the same time. The reward-behaviour task used in this study was relatively simple. We hypothesized that rats would spend more time or return more frequently to the side that light stimulation was applied. We had designed the task based on the first self-stimulation study which described that rats would return to the same portions of the environment where they received electrical stimulation (Olds, 1958a). Similar to Olds experiment, the optogenetically stimulated animals developed a strong preference for the region of the arena where the laser was on.

4.4.3. Glutamatergic neurons

MS glutamatergic fibres have been described to project to the ventral tegmental area (VTA) (Geisler and Wise, 2008, Fuhrmann et al., 2015), which is known to process the reward prediction error by increasing or decreasing the firing of dopaminergic neurons (Schultz et al., 1997, Tobler et al., 2005, Ungless et al., 2004). Indeed, direct stimulation of VTA dopaminergic neurons can induce conditioned place preference and positive reinforcement (Adamantidis et al., 2011, Tsai et al., 2009). Another target area to MS glutamatergic fibres is the lateral hypothalamus (LH), which also sends projections back to the MS while mediates motivational and reward behaviours (Harris et al., 2005, Stuber and Wise, 2016, Swanson and Cowan, 1977, Berk and Finkelstein, 1982). Similar to the MS, the LH is classically known by electrical self-stimulation, in even in higher rates than the MS (Cazala et al., 1988).

The LH is densely connected to the VTA and stimulation of LH - VTA GABAergic pathway causes disinhibition of dopaminergic neurons and consequently place preference behaviour (Barbano et al., 2016). The LH is also known for its role in energy balance and food intake, and recently, a study showed that optogenetic or chemogenetic stimulation of the MS glutamatergic neurons decreased food intake. Curiously, the stimulation of the MS glutamatergic projections into the LH did not alter feeding (Sweeney et al., 2017). Data from an in vitro study showed that glutamatergic and GABAergic neurons are reciprocally connected within the MS (Leão et al., 2015). Considering the pathways that glutamatergic MS neurons could contribute to reward behaviour, they need to be considered as a potential mediator of reward behaviour.

4.4.4. GABAergic neurons

To assess the effect of MS GABAergic stimulation, we used a transgenic rat model genetically modified to express Cre recombinase under the control of the GAD1 promoter. GAD1 and GAD2, also known as Gad 67 and Gad 65, are the two isoforms of glutamate decarboxylase enzymes responsible to produce gamma-aminobutyric acid from L-glutamic acid (Erlander et al., 1991). Characterization of the GAD1-Cre rat strain showed that Cre and GAD1 were highly co-expressed in the midbrain. Furthermore, it was also demonstrated a high colocalization of GA1-Cre in the lateral hypothalamus (Sharpe et al., 2017). Our results revealed that stimulation of MS GABAergic neurons induces a strong place preference.

To support this result, it has been already shown that mice learn to self-administer the $GABA_A$ receptor agonist muscimol into the MS. Moreover, systemic injections of dopaminergic receptor antagonist or local injection of dopaminergic antagonist in the VTA blocked the self-administration of muscimol, indicating that MS GABAergic neurons could be indirectly disinhibiting VTA dopaminergic neurons (Gavello-Baudy et al., 2008). One possible pathway is via the hippocampus.

The hippocampal formation is the primary target of MS GABAergic neurons and indirectly connects to the VTA through a polysynaptic pathway involving the subiculum, nucleus accumbens, and ventral pallidum (Nazari-Serenjeh et al., 2011). Besides, it has been shown that the activation of MS neurons increases the firing rate of VTA dopaminergic neurons via ventral subiculum in anesthetized rats (Bortz and Grace, 2018). Another possible pathway exists indirectly through the lateral hypothalamus. Anatomical data showed that MS and LH are interconnected (Hahn and Swanson, 2012). Furthermore, as described before, LH GABAergic neurons can disinhibit VTA dopaminergic neurons inducing place preference (Barbano et al., 2016).

During post-mortem verification of GABAergic GAD1-Cre rats, we could observe fluorescence on the lateral hypothalamic area. We also used data from the Allen Mouse Brain Connectivity Atlas to confirm the existence of MS GABAergic projections to the LH (Oh et al., 2014). To test the MS-LH GABAergic pathway, we attached an optic fibre to stimulate MS fibres into the LH region. Our result could not measure the difference in place preference during stimulation. In fact, electrophysiological experiments in the LH are technically challenging as the LH

is localized in the bottom of the brain. Due to the difficult to assess this region, the number of animals was low. However, we could observe a slight preference for the laser stimulation region.

4.4.5. MS cholinergic neurons

Lastly, we assessed the effect of the MS cholinergic stimulation on the place preference by using a transgenic rat model that express Cre recombinase under the control of choline acetyltransferase ChAT. This model has been confirmed to be very specific to cholinergic neurons in MS (Witten et al., 2011, Mamad et al., 2015). The major intention of this experiment was to understand the contribution of MS cholinergic neurons to the reward-related behaviour. Our data showed no place preference during MS stimulation, indicating that MS cholinergic neurons are not directly related to reward-behaviour. We also did not observe PLV during MS cholinergic stimulation.

One possible factor omitting the effect is that acetylcholine has been described to be highly expressed during active behaviour and could be already saturated. It has been shown, that stimulation of MS cholinergic neurons using the same type of virus and rats only entrained hippocampal oscillations during resting periods (Mamad et al., 2015). Although we could observe place preference, cholinergic animals could be considered a negative control for the experiment.

In experiments involving lasers, is common to have a light leakage that could catch the attention of the animal. To avoid this, we used two black shrinkable sleeves to

cover the junction between the optic cable and the cannula. The negative results in place preference from the cholinergic animals confirm that the place preference was not caused by the light leaking.

We should also consider two strong limitations for the experiment using cholinergic transgenic animals: first, viral expression was not verified post-mortem due to a freezer failure over the weekend, so there is a possibility that the lack of effect was caused by the lack of viral expression. Second, we use the same laser stimulation protocol for all animals; cholinergic neurons are much slower than GABAergic, and perhaps the stimulation frequency should be tuned in an input response manner for the optimal protocol.

5. Chapter

Manipulating Hippocampal Spatial Representation by nonselective Optogenetic Stimulation of The Medial Septum in Freely Moving Rats

5.1. Introduction

The ability to understand and interact with the environment is a fundamental capacity of all animals and notably present in humans. Mammals are capable of efficient navigation in complex environments to fulfil all essential needs for life and memory plays a vital role in this process. The capacity to learn and retrieve information gave these animals a crucial advantage in the evolutionary process. Among others, episodic memories are defined as the human faculty to remember and describe events in the context which they occurred. The hippocampus is crucial for the processing of episodic memories, which is commonly referred to as 'where', 'what and 'where memory (E Tulving and Madigan, 1970, Tulving, 2002). The discovery of place cells almost five decades ago revolutionized the way that we understand the brain, revealing that single neurons can encode the spatial information in the dorsal hippocampus (O'Keefe and Dostrovsky, 1971).

Place cells have the distinct attribute of becoming active only in a specific location of the environment, which was named place field (O'Keefe, 1976). The place field can be formed during the first minutes during the initial exploration of a new environment (Hill, 1978, Wilson and McNaughton, 1993, Frank et al., 2004, Geiller et al., 2017). Once a place field is formed, it can remain stable for weeks if the animal is exposed to the same environment conditions (Muller and Kubie, 1987, Frank et al., 2004). Besides, the set of place cells collectively represents the environment, providing a substrate of the 'cognitive map' proposed by O'Keefe (O'Keefe and Nadel, 1978).

Since the discovery of place cells, a vast amount of studies have focused on understanding how manipulation of the environment could change the representation maps (O'Keefe and Conway, 1978, Muller et al., 1987, Gothard et al., 1996a, Save et al., 2000, Knierim et al., 1998). For example, exposing the animals to a new environment or significantly changing the environment which they are habituated can induce a dramatic reorganization of the set of the place fields; this process is called global remapping (Muller and Kubie, 1987, Bostock et al., 1991). While global remapping is likely to occur when the animal is exposed to new environments, changes in the surroundings can induce partial alterations in the set of place cells, which was named partial remapping (Bostock et al., 1991, Leutgeb et al., 2005a). Concerning firing frequency, changes in the firing rate of a place cell, but not its position was described as rate remapping (Anderson and Jeffery, 2003).

Global remapping generates a unique set of place cells for each new environment, which is in accord with the idea of memory formation, providing a distinct combination for every context (Skaggs and McNaughton, 1998, Colgin et al., 2010, Knierim et al., 1998, Fuhs et al., 2005). However, the notion that hippocampus is involved in the encoding of episodic memories requires the encoding of diverse types of information in addition to the spatial data. A growing amount of evidence indicates that place cells can encode non-spatial information. For example, the firing rate of place cells can be modulated by frequency tones (Aronov et al., 2017). Additionally, place cells can fire in a different location if the animal goes in distinct directions in the same environment, indicating that different context has different encodings (McNaughton et al., 1983a, Ferbinteanu and Shapiro, 2003).

Further evidence that place cells can encode non-spatial information is the recent finding of a dedicated subpopulation of place cells that encode reward location (Gauthier and Tank, 2018), these results are in accordance with several experiments showing that the simple presence of a goal, can alter the map representation (Gothard et al., 1996a, Hollup et al., 2001, Hok et al., 2007, Dupret et al., 2010, McKenzie et al., 2013, Danielson et al., 2016, Sarel et al., 2017). Additionally, optogenetic stimulation of the VTA, an area related to reward processing, has been shown to change the field assembly towards the local field where the stimulation was applied (Mamad et al., 2017).

In this chapter, we hypothesized that MS stimulation could exert a modulatory effect on the hippocampal spatial representation by the indirect impact on the interneurons, which were described to be affected by nonselective MS stimulation in chapter 4. We also investigated how MS stimulation could affect the basic properties of the place fields during simple behavioural tasks. Additionally, we hypothesized that nonselective MS stimulation, which induced reward-related behaviour, described in chapter 5, should induce place field remapping by changing the contextual information through the introduction of the laser stimulation.

5.2. Methods

All animal work has been carried out in the Health Products Regulatory Authority (HPRA) authorised establishment, Trinity College Dublin (establishment authorisation number: AE19136) ensuring compliance with the requirements of Directive 2010/63/EU and S.I. No. 543 of 2012. This work has also been approved by the TCD Animal Research Ethics Committee (AREC) which is a Level 2 ethics committee responsible for reviewing the proposed use of animals in teaching and research in line with the Research Ethics Policies in operation in TCD.

5.2.1. Animals

Male adult rats (Lister Hooded, 350-450 gr) were used in this study. All the animals were the same as used in chapter 4 and chapter 5. The surgery details described in section (2.1.2). In short, the animals were injected with 2µL of AAV5.hSyn.hChR2(H134R)-eYFP.WPRE.hGH (Adgene #26973P) into the MS. The stereotaxic coordinates used were AP +0.8; ML 1.4; DV 5.5-6.5; and a mediolateral angle of 10 degrees. The electrodes were mounted on a microdrive and implanted on the dorsal hippocampus CA1 area using the coordinates: -3.8 AP; -2.5 ML; 1.4 DV. The assembly was permanently attached to the skull with dental cement. Implanted animals were housed individually with ad libitum assess to water, and in food controlled stated to keep animals 85-90% their weight at surgery day. Animals were left to recover for at least seven days after surgery. The housing conditions were described in section (2.1)

5.2.2. Experimental protocol

At least one day after the behavioural test (chapter 5), animals started to be recorded on the open field arena (60 cm x 60 cm) described in (2.2.1) in the morning and on a linear square maze arena (85cm x 85 cm and 10 cm wide) defined in (2.2.2) in the afternoon. Animals were recorded for 24 minutes in the morning and 24 minutes in the afternoon. The recordings were divided into 12 minutes of baseline, followed by 12 minutes of MS stimulation. During a session, animals were removed from the cage and transported to the recording area. The recording system cable and the optic fibre were plugged, and the animal was placed on the arena. On the first 12 minutes, the laser was off (baseline), without touching the animal, on the second 12 minutes the stimulation protocol was applied to the MS. We avoided touching the animals between baseline and stimulation to ensure the stability of the recordings. The stimulation protocol used in the morning was different from the protocol used in the afternoon.

In the morning, the animals were stimulated every six seconds (473 nm, 5 ms pulse duration, 12 pulses at 50 Hz), which is randomly distributed on the arena.

In the afternoon, the animals were recorded on a linear square maze arena. The animals were free to navigate between the SW and NE corners, where two food pellets (TestDiet, Formula 5TUL) were alternated placed on the corners. During the 12 minutes stimulation, the laser was switched on while the animal was on the north arm or the west arm of the maze, with continuous photo-stimulation trains (473 nm, 5 ms pulse duration, 12 pulses per train at 50 Hz, 500 ms inter-train

interval). During sessions, cells were recorded as well as rat's trajectory path by the LED tracking system.

5.3. Data analysis

The data analysis was described in detail in section (2.4), in short, waveforms were separate, and units isolated using the k-means algorithm in a graphical software (Tint, Axona Limited). Autocorrelation was plotted for inspection of the clustering quality using -10 to 10 ms time window and plotted as a histogram. Units with less than 50 spikes per session were removed from further analysis. The place fields were calculated by synchronizing the animal's position with the time stamp of each spike. The arena was divided into squared bins of $2cm^2$ and the time spent within the bin was normalized by the number of spikes in each bin. The rate map was smoothed by a 2-D, five by five bins box filter. The place field was defined as a cluster of 9 or more adjacent bins, i.e., sharing at least one side with another bin, of mean frequency above 0.5 Hz and firing rate higher than 20% of the peak firing rate.

5.3.1. Place fields properties

The spikes times of each cell were divided into epochs of maximum length around each stimulation time without superposition to form a raster plot. The cells were classified as inhibited, disinhibited or not affected, based on the signed difference

between the number of spikes 200 ms after laser stimulation minus the number of spikes 200 ms before laser stimulation, divided by the sum of these values. The result is a -1 to 1 index where -1 represents total inhibition, 0 represents no effect, and 1 represents total disinhibition. Cells were classified by inhibited or disinhibited if the firing rate increased or decreased by 33% during MS stimulation. The group of non-effected cells was all the remaining cells that were not classified based on the criteria above.

To understand how MS stimulation could affect place fields, we measured spatial information and firing rate inside the place field. The spatial information content of a cell in bits/spike is a measure of how much a spike can predict the location. The firing rate inside the place field was defined named grand rate is calculated by dividing the number of spikes by the time spent inside a place field.

5.3.2. Spatial population vector

The spatial population vector was used to evaluate the influence of the laser stimulation on the firing behaviour of the whole population of recorded place cells (Mamad et al. 2017). First, the centre of mass (COM) was calculated for each place field as an average of all positions vectors weighted by the firing rate (see session 2.4.16). The axis of symmetry was defined as the line between the SE and NW corners of the arena. For each place field, a vector was calculated from the origin defined as the coordinates of the SE corner to the COM of the place field, forming an angle with the symmetry axis, defined as COM angle (see 2.4.18). Two resulting

vectors were calculated, resulting in a weighted COM angle (weighted by the firing rate) and an averaged COM angle.

5.3.3. Statistical analysis

Statistical analysis of all data was performed using GraphPad Prism version 7.02 for Windows (GraphPad Software, San Diego California, USA). Statistical significance was estimated by using a 2-tailed independent samples t-test for non-paired or Student t-test for paired data. The probability level interpreted as significant was fixed at $p < 0.05$. All data points were plotted ± SEM.

5.4. Results

We expressed Channelrhodopsin (ChR2) under control of the Hsyn promoter in the MS area of 6 rats using an adeno-associated virus. We recorded 97 place cells from the dorsal hippocampus CA1 area during recordings on the open field and 143 place cells during recordings on the linear squared maze.

5.4.1. Effect of the MS stimulation on the hippocampal place cells

To explore the effect of nonselective MS stimulation on the pyramidal cells, we recorded the animals on the open field arena for 24 minutes, 12 minutes baseline (no stimulation) and 12 minutes applying light in the MS every 6 seconds. Using this protocol, we recorded 97 pyramidal neurons which were classified as place cells from hippocampus CA1.

From these 97 units, we observed that (36/97, 37.1%) were not affected by MS stimulation. From the affected units, (22/61, 36%) were disinhibited and (39/61, 64%) were inhibited. In total, 61 from 97 place cells were affected by MS stimulation (62.8 %) (Figure 39).

We observed that suppressed pyramidal cells responded with approximately 40 ms delay after the laser onset, and almost half (19/20) of the inhibited cells showed an increase of firing rate on the laser onset, followed by inhibition (figures 38A, B).

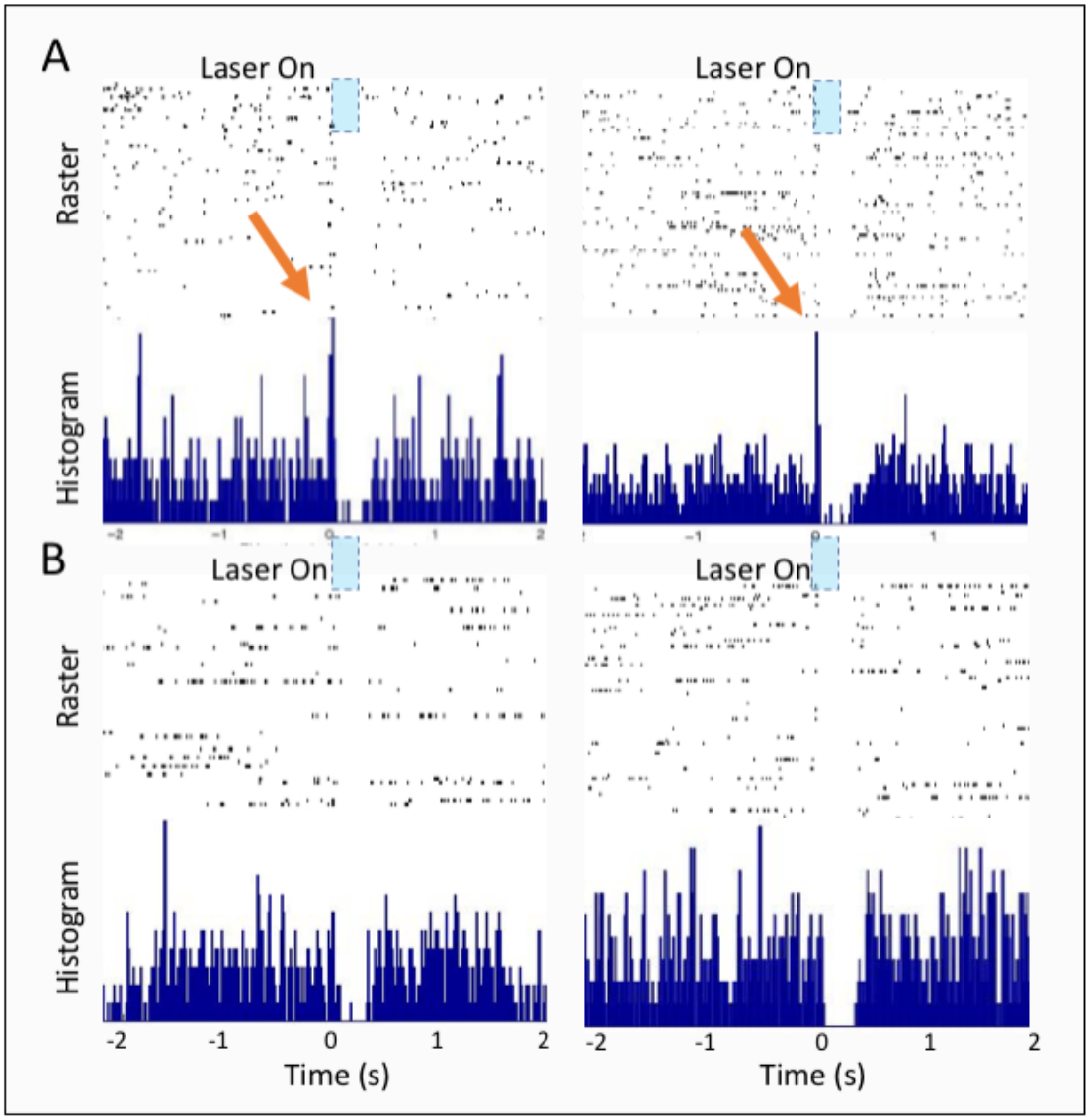

Figure 38. Inhibited place cells.

The figure displays examples of four inhibited units. Each unit is represented by the raster plot and histogram from -2s to 2s before and after MS stimulation (time 0). The inhibitory effect caused by MS stimulation started at around 40 ms after time 0. **(A)** From the 39 inhibited units, 49% showed a peak followed by inhibition, indicated by the orange arrow. **(B)** Examples of two place cells which had no peak on the histogram.

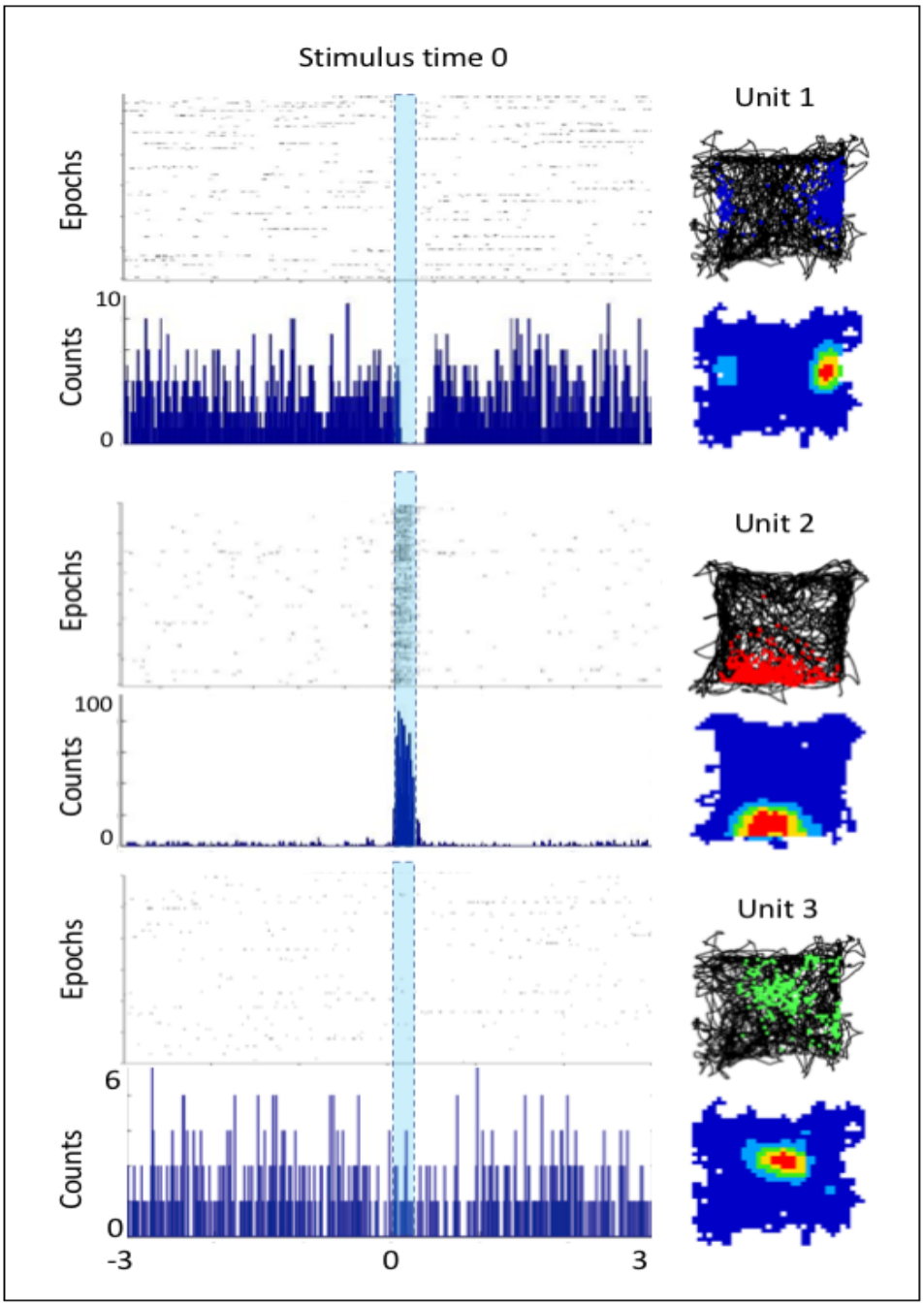

Figure 39. MS stimulation affects place cells firing.

Examples of inhibited (top), disinhibited (middle) and not affected units (bottom). The graphs show the raster plot and spike counts during the six seconds interval. The laser stimulation occurred on time 0 (middle of the figures), represented by the light blue. On the right of the map and firing map of each unit. We observed that 31.8% were inhibited, 27.3% disinhibited and 40.9% were not affected.

We classified these cells by comparing the average firing rate 200 ms before and after the stimulation. To calculate the increase or decrease of firing rate, the index used was the signed difference divided by the sum (see 2.4.12). A Kruskal-Wallis H test showed that there was a statistically significant difference in firing frequency index between the inhibited and disinhibited groups, $X^2(2) = 25.58$, $p<0.0001$. A Dunn's post hoc test revealed significant differences between not affected and inhibited ($p<0.05$) and also between not affected and disinhibited ($p<0.05$) (figure 40).

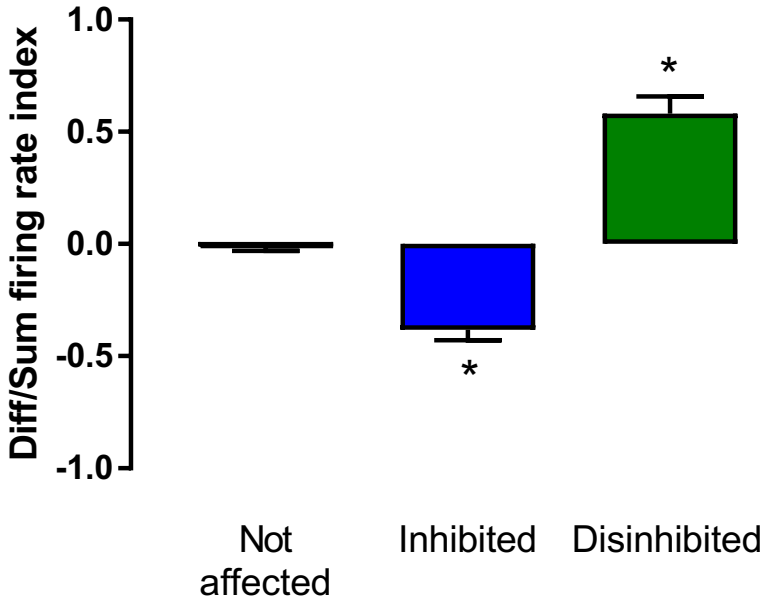

Figure 40. Firing rate index before and after MS stimulation.

We compared the firing rate index which varies from -1 to 1. The negative values indicate that the units were inhibited, and a positive number means that units were disinhibited. The 0 represents no change in firing rate before and after stimulation. A Kruskal-Wallis H test showed that there was a statistically significant difference in firing frequency index between the different groups, $X^2(2) = 25.58$, $p<0.0001$. A Dunn's post hoc test revealed

significant differences between not affected and inhibited ($p<0.05$) and between not affected and disinhibited ($p<0.05$).

5.4.2. Medial septum stimulation does not affect place fields properties

One of our objectives was to understand how MS stimulation could modify the place fields' properties of the affected units. We compared the spatial information, and place field size for the same units during baseline and stimulation. To compare the place field size, we only considered the biggest place field in case two or more place fields were detected from a place cell. The spatial information is a statistical measure that indicates how well a place field can predict the location of the animal on the arena (Skaggs et al., 1993). The place field size is also a measure of stability between recordings. A paired t-tests were used to compare the difference between place field sizes during baseline and during MS septal stimulation. We use paired t-test and found no significant difference in the spatial information for disinhibited units $t(15) = 0.661$, $p=0.518$, and there was not a significant difference for field size $t(15)=0,666$ $p=0.516$ (figure 41).

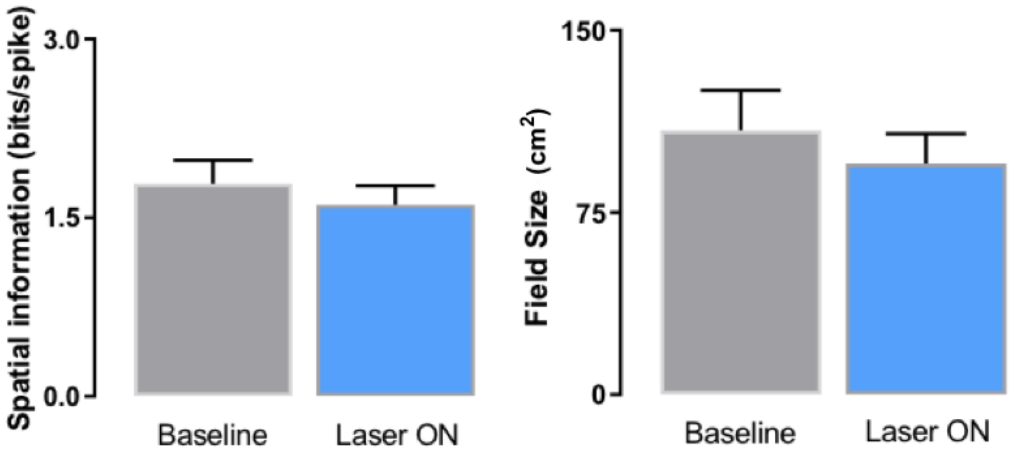

Figure 41. Disinhibited units' spatial information and field size.

We compared spatial information and field size of disinhibited place cells between baseline and stimulation. We found no significant difference in the spatial information ($t(15)= 0.661$, $p=0.518$) and field size ($t(15)=0{,}666$ $p=0.516$) for disinhibited units.

Next, we evaluated the same properties for the inhibited units. We found no significant difference in the spatial information for disinhibited units $t(36)= 1.235$, $p=0.225$, using an independent t-test. We observed that place field sizes had a slight decrease that was significant $t(36) = 2.165$, $p=0.037$ (figure 42).

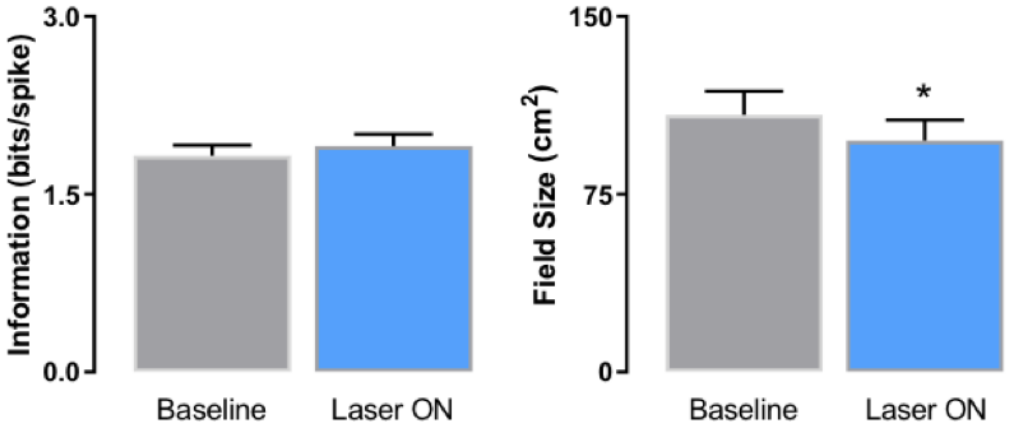

Figure 42. Inhibited units' spatial information and field size.

We use an independent t-test to compare the same place cells during baseline and stimulation. There was not a significant difference in the spatial information $t(36)= 1.235$, $p=0.225$ for baseline compared to MS stimulation sections. However, there was a significant decrease in field size during stimulation (laser ON) $t(36)=2.165$, $p=0.037$.

5.4.3. Medial septum stimulation induces place field remapping

Next, we investigate how MS stimulation could affect the stability of the place fields. To consider a remapping place field, we first calculated the absolute Cartesian difference of the coordinates of the bin of maximum frequency of each place field between baseline and MS stimulation from each group of cells. The remapping cells were defined as the cells which had the absolute distance at least three times the standard deviation of distances of the non-affected group ($M=3.535$, $SD=2.114$). Based on these criteria, 18% of the affected place cells remapped, including three units in which the place field only appeared during the stimulation.

During MS stimulation we have not perceived global remapping, only partial remapping.

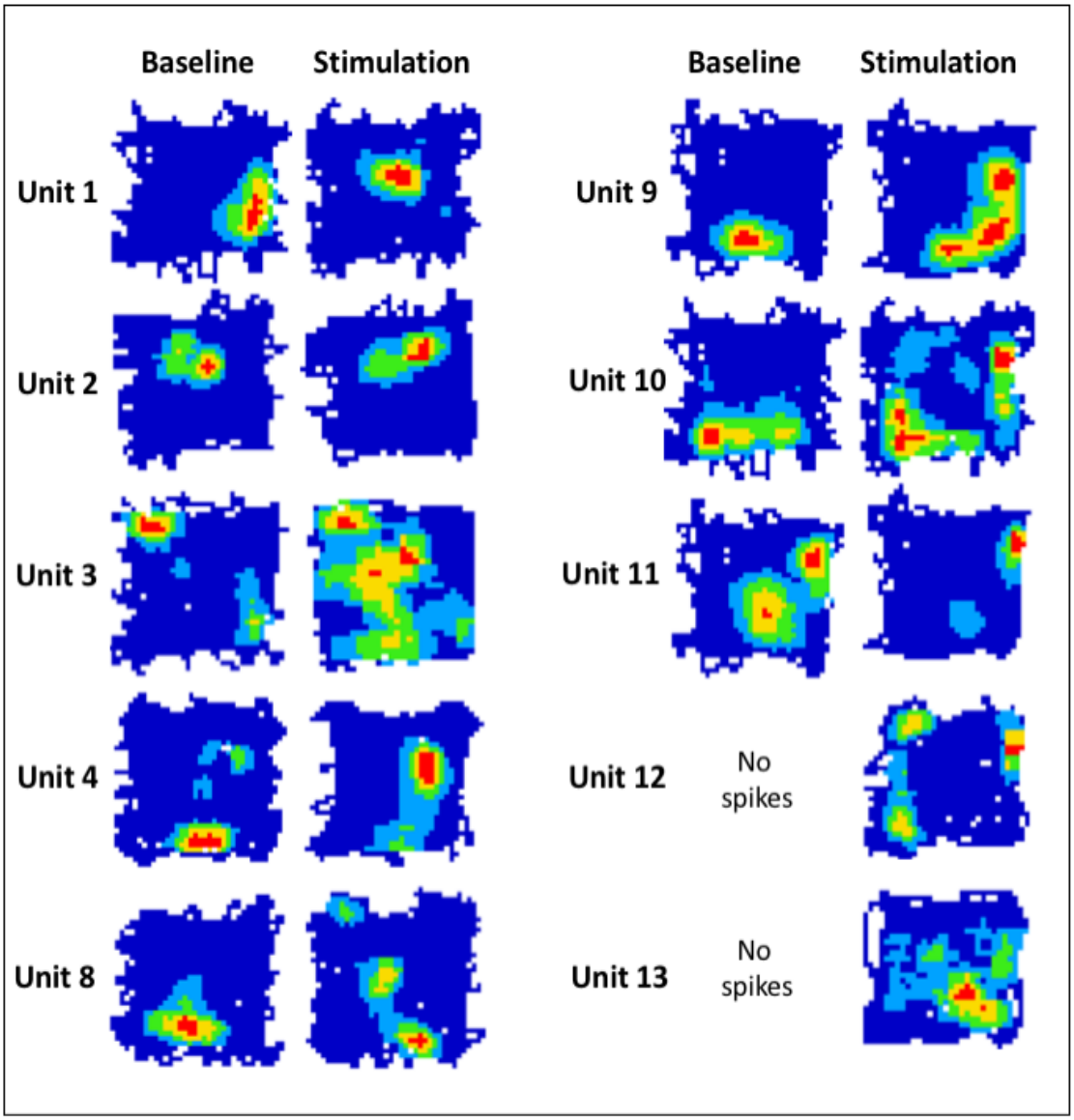

Figure 43. MS stimulation degrades the stability of the place fields.

The figure shows the firing rate of eight units which were considered remapping cells. These units correspond to 18% of the total affected place cells. We included two units that had the firing induced by the MS stimulation (unit 12 and 13).

5.4.4. Firing rate analysis

Next, we compared the averaged firing rate inside the place fields, defined as grand rate. The rate index was calculated by subtracting the averaged firing rate of each place field during stimulation recording from the averaged firing rate of the same unit during baseline and dividing by the sum of these two values. The resulting index has extreme values from -1 to 1. Negative values indicate that there was a decrease in firing rate, zero means no change and positive values an increase. A one-way ANOVA was used to compare the difference in grand rate index between not affected, inhibited and disinhibited units. There was a significant effect of MS stimulation on a grand rate index [$F(2,74)=29.32$, $p<0.001$]. Holm-Sidak's multiple comparisons tests showed a considerable difference between not affected and disinhibited units ($p<0.001$) (figure 44).

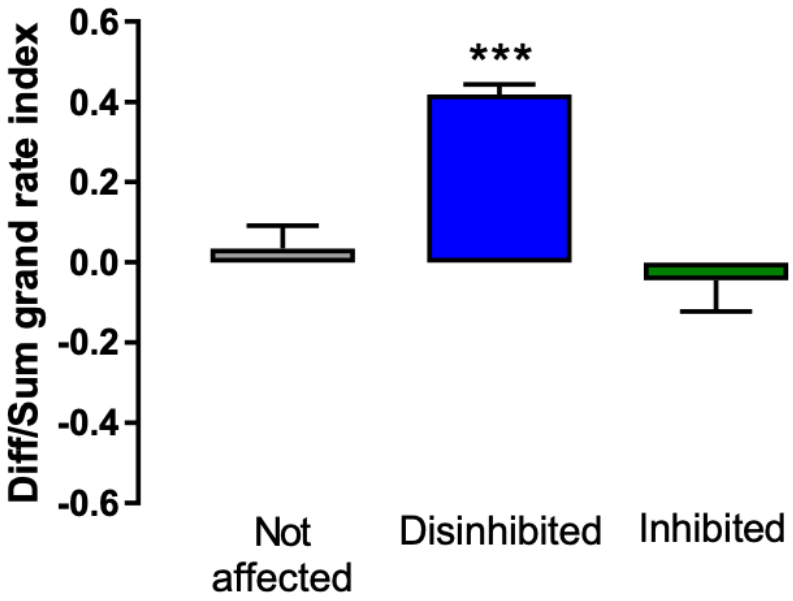

Figure 44. Grand rate index between groups.

For each place cell, we calculate the diff/sum grand rate index between baseline and MS stimulation. The measure is related to the variation of averaged firing rate inside the place fields. A one-way ANOVA between groups showed a significant increase in firing rate during MS stimulation ($p<0.001$).

5.4.5. MS stimulation did not affect place field properties during recordings on the linear squared maze

We also examined 143 place cells that were recorded on the linear squared maze. The idea was the same as before; animals were recorded for 12 minutes without laser stimulation followed by 12 minutes of light stimulation in the MS. During analysis, we could observe that place fields were not symmetric concerning the direction of the movement, and some place fields only appeared in one direction:

clockwise (CW) or counterclockwise (CCW). To understand if MS stimulation could affect these cells, we first separated the spikes from each cell in different directions and then compared the field size, mean firing rate and peak firing rate between baseline and MS stimulation. First, we examined the field sizes using independent t-test. No significant differences were found in place fields size on CCW direction (p=0.973). Furthermore, no significant no significant difference was found between the baseline and stimulation in the CW direction (p=0.706) (figure 45).

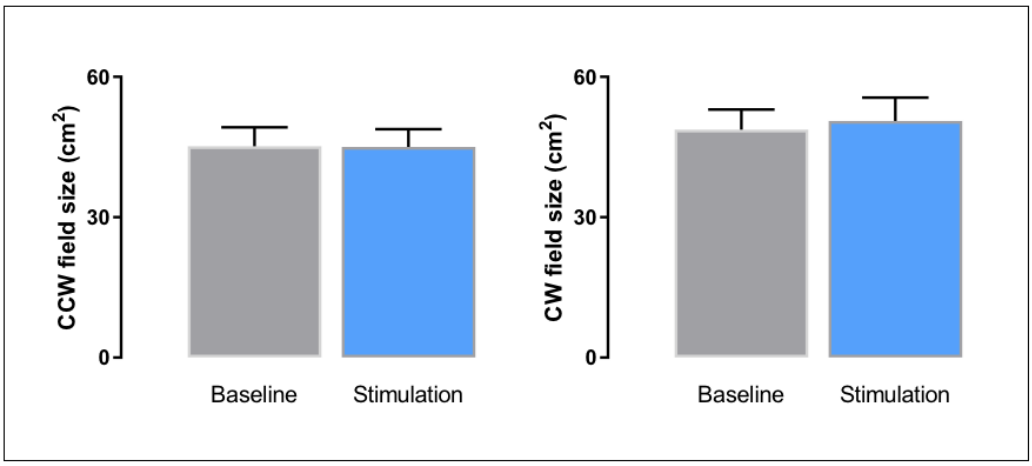

Figure 45. Place field size comparison between baseline and MS stimulation.

On the left, the field size comparison between baseline and MS stimulation of the spikes which occurred during the counterclockwise (CCW) movement direction. No significant differences were found in place fields size CCW (p=0.973). On the left, the comparison between field sizes recorded on a clockwise direction of the movement. A t-test showed no significant difference in CW (p=0.706).

We next examined the mean firing rate for the CCW direction and found no significant difference between baseline and stimulation CCW (p=0.847). We also

compared the baseline and stimulation for CW side we also found no significant difference (p=0.790) (figure 46).

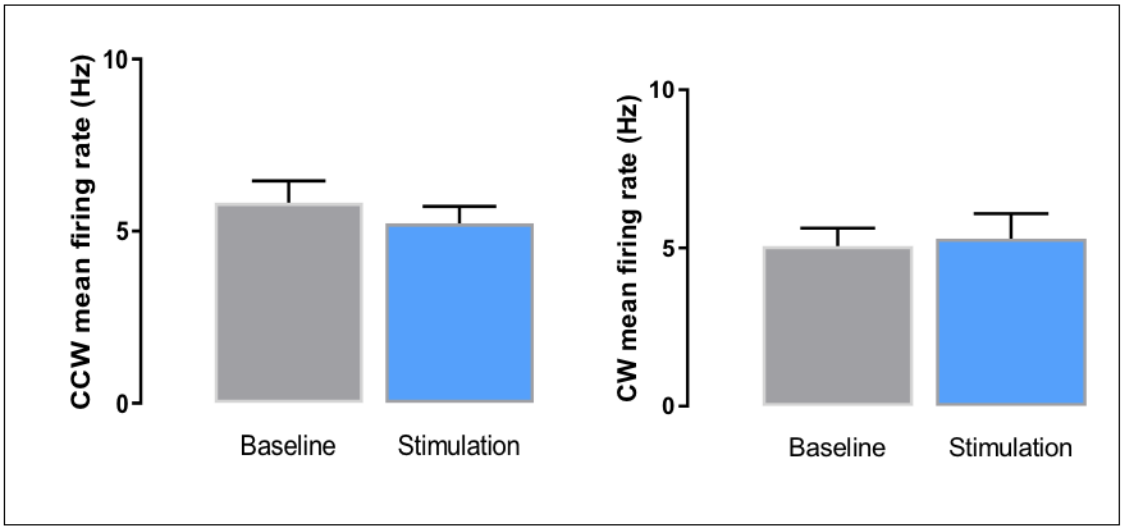

Figure 46. Mean firing rate between baseline and MS stimulation.

The mean firing rate was compared between baseline and stimulation on the linear squared maze for both CCW and CW. There were no significant differences in the mean firing rates for both CCW (p=0.973) and CW (p=0.706).

Lastly, we exanimated the peak firing rate of place cells between baseline and MS stimulation in both directions between baseline and stimulation. No difference was found for both CCW (p=0.550) and CW (p=0.789).

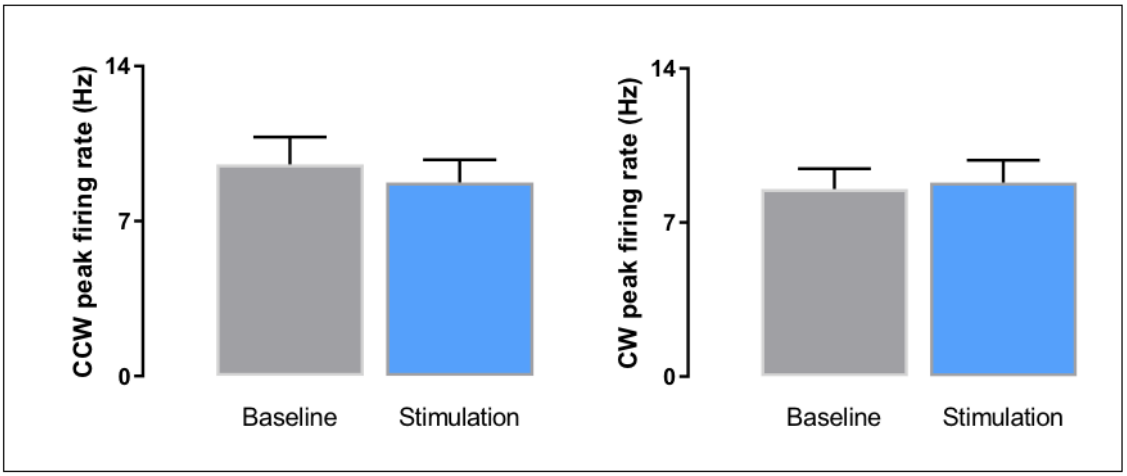

Figure 47. Peak firing rate between baseline and stimulation.

The peak firing rates were compared between baseline and stimulation on the linear squared maze for both CCW and CW. There were no significant differences in the mean firing rates for both CCW (p=0.550) and CW (p=0.789).

5.4.6. MS stimulation induce changing on the place fields assembly

Our last experiment was to evaluate whether the reward induced by the MS stimulation (see chapter 5) could affect the place field assembly. To test the hypothesis, we analysed the centre of mass (COM) angle of all place fields recorded from each animal that showed place preference during MS stimulation. To calculate de COM angle, we first calculated the 45 degrees diagonal of the arena by dividing the maze into two equal parts. For each place field, a COM angle was calculated using the 45° diagonal (SE to NW) as the reference. Place fields on the SW (side of the stimulation) shifted the angle towards 0 degree. In contrast, place fields on the NE side moved the angle towards 90 degrees. Once all the COM angles were calculated, two spatial population vector angles were calculated: a weighted

angle, which was weighted by their firing rate, and an averaged angle which all cells were weighted equally by the number of cells.

First, we used a paired t-test to compare the weighted angle between baseline and MS stimulation (Laser ON). Interesting, we found a significant shift in the spatial population vector angle towards the stimulation corner $t(5)=3.695$, $p=0.0141$ (figure 48).

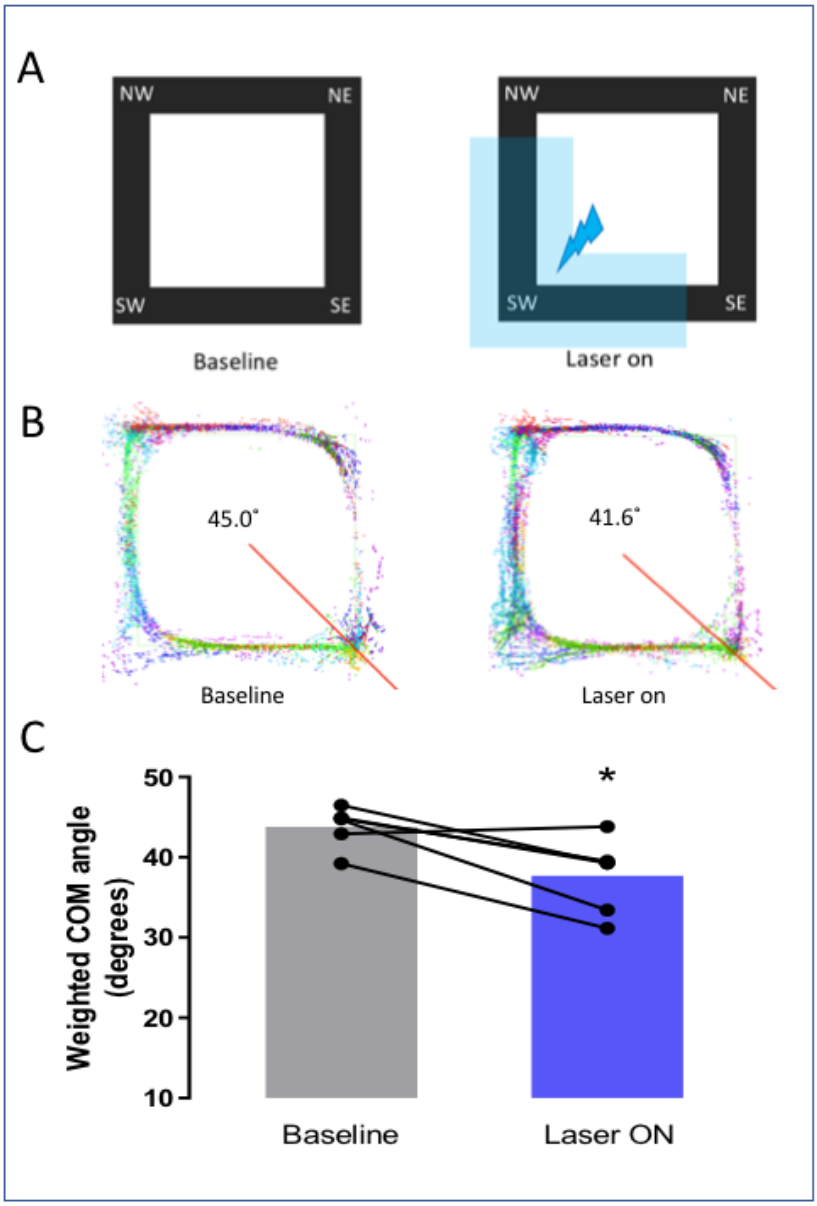

Figure 48. MS stimulation induced a change in the place field assembly measured by weighted COM angle

(A) Schematic of the baseline and stimulation protocol. The animals could navigate freely to collect sugar pellets on the SE and NW corners for 24 minutes. On the first 12 minutes the laser was off, and on the second 12 minutes, the MS was stimulated. **(B)** An example of the weighted COM angle calculation for the place cells of one animal. The coloured dots represent the spikes of each place cell. The COM angle resulted in the place cell distribution (precisely 45˚ for baseline recording and 41˚ degrees during MS stimulation). **(C)** A paired t-test showed a significant difference between weighted COM between baseline and MS stimulus for the six rats recorded $t(5)=3.695$, $p=0.0141$.

Lastly, we compared the averaged angle which is only related to the number of place cells on each side. Unexpectedly, we found a significant change of the averaged spatial population vector towards the stimulation side using a paired t-test $t(5)=2.937$, $p=0.0324$ (figure 49).

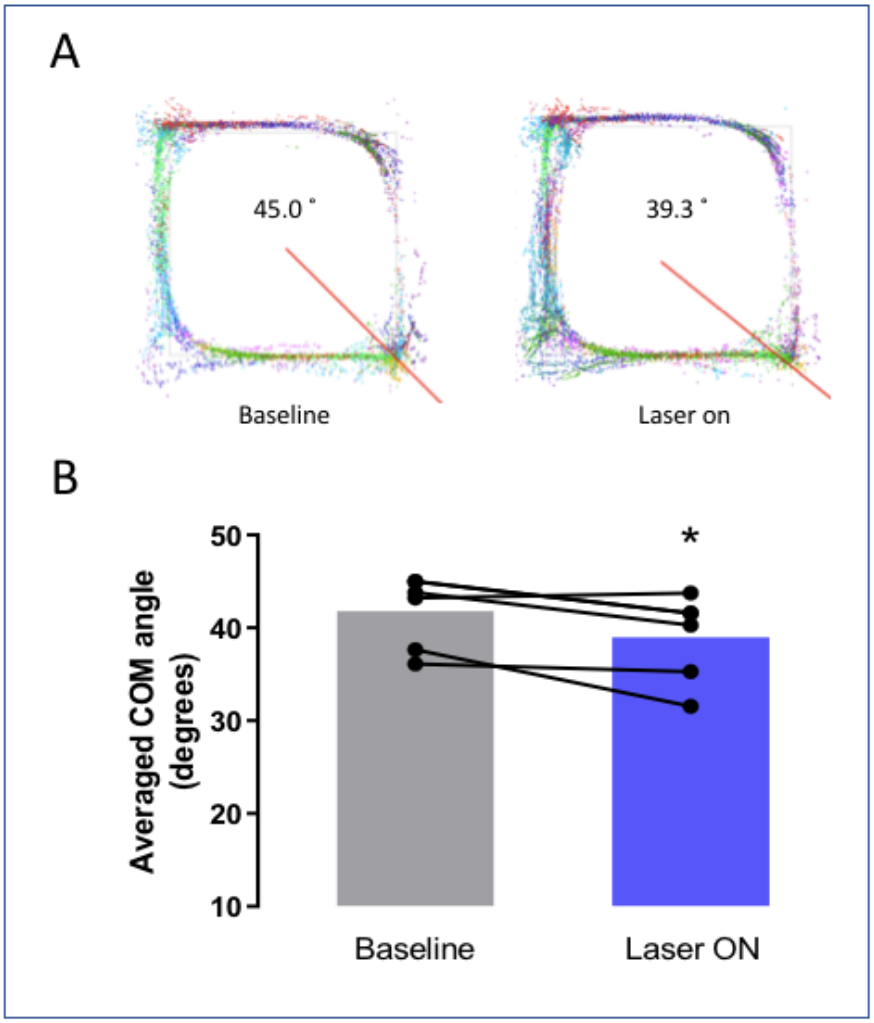

Figure 49. MS stimulation induced a change in the place field assembly distribution measured by the averaged COM angle

(A) An example of COM angle calculation for the place cells of one animal. The coloured dots represent the spikes of each place cell. The averaged COM angle resulted in the place cell distribution (precisely 45° for baseline recording and 41° degrees during MS stimulation). **(B)** A paired t-test showed a significant difference between averaged COM angled between baseline and MS stimulation for the six rats recorded $t(5)=2.937$, $p=0.0324$.

5.5. Discussion

In this chapter, we demonstrated that nonselective MS stimulation could induce transient firing rate increase or decrease in hippocampal place cells. Moreover, we demonstrated that MS stimulation induced partial remapping on place cells without affecting the overall spatial information and induced a slight decrease in field size in inhibited cells. Finally, we demonstrated that the place cells population COM angle were biased towards the stimulation side of the arena, which has been associated to the reward-related behaviour in chapter 5, indicating that the population of place cells can encode reward.

5.5.1. Nonselective MS stimulation can induce both inhibition and disinhibition of CA1 pyramidal neurons

CA1 pyramidal neurons are entirely covered by GABAergic synapses, from the thinnest dendritic shafts to the initial axon segments, some GABAergic neurons, including PV positive basket-cells and cholecystokinin (CCK) basket cells, exert control of oscillations and network excitability of pyramidal cells (Buzsaki and Wang, 2012, Miles et al., 1996, Freund and Katona, 2007, Miyoshi, 2018). From the septo-hippocampal circuit, CA1 interneurons receive in great majority projections from MS GABAergic neurons (Sun et al., 2014). Thus, stimulation of the MS should inhibit CA1 interneurons and consequently disinhibit pyramidal cells.

However, in this study we observed the opposite effect, most of the pyramidal cells were inhibited during MS stimulation. To understand the inhibitory effect on place cells, we must return to the results of chapter 4. We showed that MS stimulation induced an increase in firing rate in the majority of CA1 interneurons, which certainly includes PV+ basket cells. Therefore, we should expect an inhibitory effect on pyramidal cells.

We also observed a smaller, but still considerable amount of pyramidal cells that increased their firing during MS stimulation, which reflects the smaller proportion of excited interneurons from chapter 4 results. Moreover, CA1 pyramidal cells receive several excitatory inputs, including cholinergic and glutamatergic from MS (Sun et al., 2014), which could be contributing to the excitatory effect.

Curiously, half of the inhibited pyramidal cells presented a brief increase in firing rate followed by inhibition. We could attribute this phenomenon to the inhibitory feedback caused by a specific type of CA1 interneurons. These interneurons receive glutamatergic inputs from the pyramidal cell and project back to the dendrite of the same cell, so they cannot stop the cell from firing, but they can control the time which the cell will be active (Klausberger, 2009); (Müller and Remy, 2014, Jang et al., 2015).

The pyramidal cells receive glutamatergic from CA3 and entorhinal cortex (Ishizuka et al., 1990, Steward, 1976, Witter et al., 1988, Speed and Dobrunz, 2009) and dopaminergic from locus coeruleus and VTA connections (Kempadoo et al., 2016) that contribute to the excitatory signals. Moreover, both cholinergic and glutamatergic MS projections can excite CA1 interneurons, which in contrast, can

result in an inhibitory effect on pyramidal cells. For example, oriens-lacunosum moleculare interneurons receive cholinergic innervation from MS (Leao et al., 2012). These interneurons can induce a potent inhibition of dendritic tufts of distal pyramidal cells (Leao et al., 2012).

5.5.2. Analysis of place field properties in the open field

Once we found that MS stimulation had a differing effect on hippocampal place cells, we divided the units into groups of inhibited, disinhibited and not affected units. When animals are exposed for the first time to an environment, the CA1 place fields form rapidly (Wilson and McNaughton, 1993, Frank et al., 2004, Leutgeb et al., 2004). In subsequent exposures, as the animal gain experience in the environment, the place fields get smaller and the spatial information increases. This process is LTP dependent and essential for memory formation (McHugh et al., 1996, Jeantet and Cho, 2012, Kentros et al., 1998, Karlsson and Frank, 2008). We analysed spatial information and place field size to understand the contribution of the MS stimulation to this process. Our results showed a slight decrease in place field size for the inhibited group. However, no changes in spatial information were observed giving the impression that the inhibitory effect on pyramidal cells provoked the reduction in field.

5.5.3. MS stimulation induced place fields remapping

The hippocampus is involved in episodic memory and navigation. These processes are mediated by the capacity of place field formation, which encodes a map of the environment (Eichenbaum, 2017, Wilson and McNaughton, 1993, Frank et al., 2004, Cohen et al., 2017). The place fields form rapidly when animals explore the environment for the first time, and once it is formed, it will remain stable during consequent exposures to the same environment (Muller and Kubie, 1987, Dupret et al., 2010). We hypothesized that MS stimulation could disturb the place fields due to the close relation between place fields and theta oscillations. Interestingly, we found that 18% of the place cells remapped during MS stimulation, including two units that were inactive during baseline recording.

A related study showed that inhibition and not excitation of place cells could induce place field remapping by LTP dependent process (Schoenenberger et al., 2016). However, in our results, the remapping occurred in both excited and inhibited place cells. The CA1 pyramidal cells receive projections from several regions that are directly modulated by MS, including CA3 (Amaral and Witter, 1989) and entorhinal cortex pyramidal cells (Steward and Scoville, 1976, Desikan et al., 2018). Disturbing the septohippocampal circuit by MS stimulation can induce an unpredicted effect in all hippocampal and parahippocampal network responsible for spatial and non-spatial processing (Unal et al., 2015, Muller and Remy, 2018). Therefore, this suggests that the remapping could be caused by interactions of the complex hippocampal interneuron network.

We also observed two place cells which were silent in the first half of the recording and were active during the second half when the laser protocol was initialized. Previous data demonstrated that field activity could appear from silent neurons induced by artificial stimulation (Diamantaki et al., 2018). Direct excitatory inputs from MS could cause the appearance of these place field from silent cells.

To analyse the distance between place cells, an arbitrary minimal distance was used. This distance was based on the distribution of distances of non-affected units because the definition of place field position is not precise. To define the position, we used the bin in the field with the maximum number of spikes. However, this number is not the same between recordings, as the animal can walk in a different manner and this position can vary a few centimetres. To ensure that the cells remapped due to the stimulation, we measure the distribution of differences in place cell positions for non-affected cells and used the averaged distances summed to three times the standard deviation of this distribution. The value is restrictive to ensure that there was a remapping and not a natural variation from one recording to another.

5.5.4. Analysis of place fields properties in the linear squared maze

We showed that MS stimulation did not affect place fields properties on the linear maze. Before measuring place fields properties, we separated the place fields by navigation directions in CW and CCW. It has been shown that when animals

navigate in constrained stereotyped trajectories, the place fields representation of both directions can be uncorrelated (McNaughton et al., 1983a, Gothard et al., 1996b). Indeed, we observed that someplace fields only occurred during one direction of the trajectory. Our results showed no differences between baseline and stimulation in neither of the navigation directions. However, we should consider that we did not segregate the place cells by position on the maze. Place fields on the laser area would be more susceptible being affected by MS stimulation than place fields that did not receive laser stimulation. The downside of this approach is that a less restrictive test could include more remapped units to the analysis.

5.5.5. Hippocampal place fields assembly encode reward

Lastly, we demonstrated that the spatial distribution of the place fields could encode reward. Place fields assembly distribution was biased towards the stimulation side of the maze, measured by the shift of the COM angle. The COM angle method used in this study was used to demonstrated that hippocampal place field assembly encodes the position of the reward induced by optogenetic stimulation of the VTA (Mamad et al., 2017). Understanding what type of information is encoded by the hippocampus has been a challenge, since the discovery of the place cells and many studies have focused on how the hippocampus encodes goal and reward (Hollup et al., 2001, Hok et al., 2007, Holscher et al., 2003, Kobayashi et al., 2003). One study showed that place fields were described to accumulate closer to the escape platform in a water maze,

suggesting that place fields can represent the emotional value of spatial cues (Hollup et al., 2001).

In this study, we used optogenetic stimulation of the MS to induce reward to measured how the place fields were organized. The advantage of intracranial optogenetic stimulation is that no external reward has to be introduced to the behaviour test, avoiding that animals encode the spatial representation of the reward instead of the information itself, causing ambiguity.

The COM angle was measured in two distinct ways: considering the firing rate of the place fields and by considering only the number of place fields on each side. We found that in both measures the COM angle was shifted toward the stimulation side of the maze, indicating that the MS stimulation induced new place fields. These results could be explained by the activation of silent neurons caused by MS stimulation as observed in the open field. However, a recent study demonstrated that a dedicated subpopulation of CA1 place cells encode reward. These cells represent about 5% of the place field population and could be biasing the COM angle towards the stimulation side (Gauthier and Tank, 2018). These results showed for the first time that MS has the potential to modulate spatial representations. However, more data is necessary to separate the direct network effect of MS stimulation from reward processing.

Chapter 6

General Discussion and Conclusion

6.1. Introduction

In this thesis, we explored the medial septum using optogenetic in behaving rats. We addressed pertinent questions about the septohippocampal circuit, which is vital for the understanding of memory processing in the brain. We showed for the first time how nonselective optogenetic stimulation affects the intra-septal network and how it reflects on hippocampal interneurons. Likewise, we investigated using state of the art techniques the classically described reward-related behaviour elicited via MS stimulation. Finally, we showed that MS modulates hippocampal spatial processing, a well-described hippocampal function essential to the encoding of episodic memories. Our results reaffirm the critical importance of the medial septum to the hippocampal processing and contribute to the understanding of the septohippocampal system.

6.2. Stimulation of MS neurons and their effect on hippocampal interneurons

We started in chapter 4 by showing for the first time how the nonselective optogenetic MS stimulation affects intra-septal neurons. The MS was chosen due to its crucial importance for hippocampal oscillations and memory. To address our objectives, we first classified septal neurons by their firing patterns, mainly focusing on the bursting and theta modulated neurons which have been described to modulate hippocampal interneurons and pyramidal cells, resulting in hippocampal theta oscillation (Freund, 2003, Toth et al., 1997, Toth et al., 1993).

Our classification was based on propensity to burst and theta modulation. Bursting neurons are found in several brain regions and are close related to theta frequency and spatial processing in the hippocampus (Zeldenrust et al., 2018). In the CA1 region, place cells fire in bursting when the animal enters the place field, these bursts are synchronized to the theta frequency present in the LFP, an interesting phenomenon known as theta precession, which was described in the introduction. A subpopulation of MS neurons was classified into bursting theta neurons, these neurons were suggested to be parvalbumin positive, based on MS electrophysiological classification studies. Using optogenetic manipulation, we successfully stimulated MS neurons and showed that nonselective MS stimulation induced a strong inhibitory effect on most medial septal neurons. This inhibitory effect was most prominent in the fast spiking MS neurons classified as bursting theta. This result was unexpected since ChR2 can only depolarize the neuronal membrane and raised an important question about the anatomical organization of the MS. The answer could be an intrinsic GABAergic - GABAergic network, having a subpopulation of GABAergic neurons more affected by the laser stimulation. However, as we described in the introduction, the MS is composed by cholinergic, GABAergic and glutamatergic neurons which are interconnected, so several intra-septal configurations could be considered. Unfortunately, anatomical intra septal data are scarce to approach a conclusion.

A very interesting result was the excitatory effect observed in CA1 interneurons, mostly on theta modulated interneurons. For example, 76% of the affected MS theta bursting neurons were inhibited by the MS stimulation, in contrast, 64% of hippocampal theta burst interneurons increased their firing rate. It suggests that

disinhibition of fast spiking theta modulated interneurons could be a result of the inhibition of GABAergic parvalbumin positive in MS. However, caution need to be taken when observing these results, because with the methods used in this thesis, we cannot ensure direct connection between these cells, and an in vitro study would be necessary to elucidate this connection. We also recorded MS neurons while animals were running and showed that most neurons were correlated with speed. This correlation was negative for the majority of MS neurons and correlation was stronger for bursting and theta modulated neurons. Interestingly, hippocampal interneurons are known to increase their firing frequency proportionally to animal's speed (Maurer et al., 2005). Our results could be extrapolated to suggest that hippocampal interneurons are speed modulated by disinhibition from MS GABAergic neurons. However, this is a strong conclusion that needs to be examined with more experiments. Recently, a study proposed that CA1 interneurons encode speed in sub-second time scale, and named these interneurons as speed cells (Góis and Tort, 2018). A proof that interneurons are purely modulated by MS neurons would open a wide range of questions about the origin of this modulation.

6.3. Stimulation of the medial septum induced place preference

In chapter 5 we examined how MS stimulation could affect place preference behaviour. The MS area is classically known as a reward area as animals were described to compulsively press a lever to self-stimulate electricity in this region

(Olds and Milner, 1954). To test our hypothesis, we used non-selective optogenetic stimulation. The results showed that stimulation of the MS induced place preference. Animals would spend more time or cross more times the side of the arena were the laser was on. After observing this behaviour, we attempted to understand what type of MS neuron could be mediating this reward effect. To do so, we used two transgenic rat models: Chat-Cre and Gad1-Cre. The first expresses Cre enzyme in cholinergic neurons and the second in GABAergic GAD1 neurons.

Stimulation of cholinergic MS neurons was inconclusive; no effect was observed. In contrast, MS GABAergic neurons induced place preference as strong as non-selective stimulation. We suggested that stimulation of these neurons could be indirectly affecting VTA dopaminergic neurons via two distinct polysynaptic pathways. One possible pathway involves the subiculum, nucleus accumbens, and ventral pallidum (Nazari-Serenjeh et al., 2011), and another via the lateral hypothalamus (Hahn and Swanson, 2012). We attempted to explore this pathway by implanting an optic fibre in the lateral hypothalamus. However, the number of animals was not sufficient for a statistically significant result.

Despite the unknown pathway, this result is important and perhaps the most important in this thesis, as it reises a set of questions about the role of the MS in the memory processing. In both humans and rodents, theta power increased in motivationally significant stimuli (Gruber et al., 2013, Lansink et al., 2016). Is the MS the link between reward expectancy, theta activity and memory encoding? Our results reaffirm the importance of MS not only for the hippocampal modulation,

but as a critical region for the integration of contextual information, behavioural responses, and memory.

6.4. Medial septum modulates hippocampal place cells

In chapter 5, we explored how MS stimulation affects the hippocampal place cells, which are crucial to spatial navigation and memory formation. We started by evaluating the effect of medial septal stimulation on place cells. We showed that the majority of place cells were inhibited. This effect could be consequence of interneuron disinhibition showed in chapter 4, as interneurons are closely connected to pyramidal cells. We suggested that the inhibitory effect on place cells could be caused by a cascade effect starting by the inhibition of MS neurons as showed in chapter three.

To understand the effect of MS stimulation on the place cells, we firstly recorded place cells on the open arena during MS stimulation. The result showed that a percentage of affected place cells remapped during stimulation. This result suggests that MS have strong control over spatial processing, which could be related to the impairment of memory in MS lesion animals.

The MS excitatory effect on pyramidal cells could be directly via inputs from MS cholinergic neurons. Although cholinergic stimulation had no effect on PLV in chapter 4, it is the major excitatory projection from MS to the hippocampus which terminates in both pyramidal cells and interneurons. Another explanation involves the CA3 and entorhinal cortex, the two primary inputs to CA1 pyramidal

cells. Both areas receive MS inputs and are affected by MS stimulation (Mizumori et al., 1992, Joshi et al., 2017), which could induce desynchronization of the circuit resulting in instability of place fields. However, due to the complexity of the circuit, our suggestions are merely speculations, and further experiments are necessary.

We also showed that the MS stimulation restricted to a region of the arena induced place preference and shifted the place field assembly towards this region. These results are in accordance with already described studies that showed that a small proportion of CA1 place cells also encode reward. hippocampus is essential for episodic memory and it is essential for an animal to remember where the emotion relevant places are, for example: water, food and predators. We proposed that the reward-related response from MS stimulation could be recruiting reward cells (Gauthier and Tank, 2018). However, our data showed that MS stimulation could induce place field formation and remapping. Therefore, due to the design of the experiment, we cannot distinguish between the appearing of reward cells from the disinhibition or excitation caused by MS stimulation.

6.5. Future directions

The results from this thesis have raised some questions about the intra-septal network. We recorded more inhibited than excited neurons inside the MS. To explain this phenomenon, we proposed that a subpopulation of GABAergic neurons could be expressing ChR2, consequently inhibiting the majority of MS neurons. To approach this problem, would be necessary to co-localize the already

the expressed YFP by the infected neurons with other colour fluorescence via immunohistochemistry or as proposed before, by in vitro recordings. The result would reveal what types of neurons are being affected by photo stimulation.

We showed that stimulation of MS GABAergic neurons was sufficient to induce place preference. However, our experimental design did not include stimulation of MS glutamatergic neurons as the animal model was not available. To better understand the intraseptal circuit and the effect of MS glutamatergic stimulation on behaviour, a future experiment using a transgenic model that express Cre recombinase in glutamatergic neurons would be interesting. In mice MS glutamatergic stimulation induced movement. Animals that were immobile started to walk when MS glutamatergic neurons were optogenetically stimulated in theta frequency (Muller and Remy, 2018). As far I am concern, no experiment was ever made to test the reward effect of these neurons.

Recently 'speed cells', i.e., interneurons positively correlated to speed, were identified in the CA1 area that encodes speed in sub-second scale. Would be interesting to understand if hippocampal ‘speed cells’ are speed dependent of MS neurons. This experiment is feasible by inhibiting MS neurons during navigation while recording CA1 speed modulated cells.

In this thesis we attempt to investigate the pathways by which MS mediate behaviour. The same experiment using lateral hypothalamic area and transgenic animals could be done using an adequate number of animals.

6.6. Conclusion

A better understanding of the septohippocampal system could result in new approaches for the treatment of memory deficits caused by dementia or another type of hippocampal dysfunction. This work aimed to explore the septohippocampal system regarding electrophysiology and behaviour. We revealed that MS GABAergic neurons could induce reward-related behaviour, suggesting a strong relationship between the hippocampal oscillations and reinforcement learning. Moreover, our data showed that MS projections could affect hippocampal place cells and interneurons. We also showed that place cells assembly encodes reward.

Altogether, our data expanded the understanding of the MS modulation on hippocampus spatial processing and memory formation.

7. Bibliography

ACSADY, L., GORCS, T. J. & FREUND, T. F. 1996. Different populations of vasoactive intestinal polypeptide-immunoreactive interneurons are specialized to control pyramidal cells or interneurons in the hippocampus. *Neuroscience,* 73**,** 317-34.
ADAMANTIDIS, A. R., TSAI, H. C., BOUTREL, B., ZHANG, F., STUBER, G. D., BUDYGIN, E. A., TOURINO, C., BONCI, A., DEISSEROTH, K. & DE LECEA, L. 2011. Optogenetic interrogation of dopaminergic modulation of the multiple phases of reward-seeking behavior. *J Neurosci,* 31**,** 10829-35.
AFIFI, A. K. & BERGMAN, R. A. 2005. *Functional Neuroanatomy: Text and Atlas*.
ALONSO, A., GAZTELU, J. M., BUNO, W., JR. & GARCIA-AUSTT, E. 1987. Cross-correlation analysis of septohippocampal neurons during theta-rhythm. *Brain Res,* 413**,** 135-46.
ALONSO, A. & KÖHLER, C. 1982. Evidence for separate projections of hippocampal pyramidal and non-pyramidal neurons to different parts of the septum in the rat brain. *Neuroscience Letters,* 31**,** 209-214.
AMARAL, D. G. 1978. A Golgi study of cell types in the hilar region of the hippocampus in the rat. *J Comp Neurol,* 182**,** 851-914.
AMARAL, D. G., DOLORFO, C. & ALVAREZ-ROYO, P. 1991. Organization of CA1 projections to the subiculum: a PHA-L analysis in the rat. *Hippocampus,* 1**,** 415-35.
AMARAL, D. G., ISHIZUKA, N. & CLAIBORNE, B. 1990. Neurons, numbers and the hippocampal network. *Prog Brain Res,* 83**,** 1-11.
AMARAL, D. G. & KURZ, J. 1985. An analysis of the origins of the cholinergic and noncholinergic septal projections to the hippocampal formation of the rat. *J Comp Neurol,* 240**,** 37-59.
AMARAL, D. G. & WITTER, M. P. 1989. The three-dimensional organization of the hippocampal formation: a review of anatomical data. *Neuroscience,* 31**,** 571-91.
AMILHON, B., HUH, C. Y., MANSEAU, F., DUCHARME, G., NICHOL, H., ADAMANTIDIS, A. & WILLIAMS, S. 2015. Parvalbumin Interneurons of Hippocampus Tune Population Activity at Theta Frequency. *Neuron,* 86**,** 1277-89.
ANDERSEN, P., BLAND, H. B., MYHRER, T. & SCHWARTZKROIN, P. A. 1979. Septo-hippocampal pathway necessary for dentate theta production. *Brain Res,* 165**,** 13-22.
ANDERSEN, P., BLISS, T. V. & SKREDE, K. K. 1971. Lamellar organization of hippocampal pathways. *Exp Brain Res,* 13**,** 222-38.
ANDERSON, M. I. & JEFFERY, K. J. 2003. Heterogeneous modulation of place cell firing by changes in context. *J Neurosci,* 23**,** 8827-35.
ANDERSON, M. I. & O'MARA, S. M. 2003. Analysis of recordings of single-unit firing and population activity in the dorsal subiculum of unrestrained, freely moving rats. *J Neurophysiol,* 90**,** 655-65.
ARONOV, D., NEVERS, R. & TANK, D. W. 2017. Mapping of a non-spatial dimension by the hippocampal-entorhinal circuit. *Nature,* 543**,** 719-722.
BACKUS, A. R., SCHOFFELEN, J.-M., SZEBÉNYI, S., HANSLMAYR, S. & DOELLER, C. F. 2016. Hippocampal-Prefrontal Theta Oscillations Support Memory Integration. *Current Biology,* 26**,** 450-457.
BALL, G. G. & GRAY, J. A. 1971. Septal self-stimulation and hippocampal activity. *Physiol Behav,* 6**,** 547-9.
BARBANO, M. F., WANG, H. L., MORALES, M. & WISE, R. A. 2016. Feeding and Reward Are Differentially Induced by Activating GABAergic Lateral Hypothalamic Projections to VTA. *J Neurosci,* 36**,** 2975-85.
BARNES, C. A., SUSTER, M. S., SHEN, J. & MCNAUGHTON, B. L. 1997. Multistability of cognitive maps in the hippocampus of old rats. *Nature,* 388**,** 272-5.

BARRY, C., LEVER, C., HAYMAN, R., HARTLEY, T., BURTON, S., O'KEEFE, J., JEFFERY, K. & BURGESS, N. 2006. The boundary vector cell model of place cell firing and spatial memory. *Rev Neurosci,* 17**,** 71-97.
BARTOS, M., VIDA, I. & JONAS, P. 2007. Synaptic mechanisms of synchronized gamma oscillations in inhibitory interneuron networks. *Nat Rev Neurosci,* 8**,** 45-56.
BARTUS, R. T., DEAN, R. L., 3RD, BEER, B. & LIPPA, A. S. 1982. The cholinergic hypothesis of geriatric memory dysfunction. *Science,* 217**,** 408-14.
BASSANT, M. H., SIMON, A., POINDESSOUS-JAZAT, F., CSABA, Z., EPELBAUM, J. & DOURNAUD, P. 2005. Medial septal GABAergic neurons express the somatostatin sst2A receptor: functional consequences on unit firing and hippocampal theta. *J Neurosci,* 25**,** 2032-41.
BENARROCH, E. E. 2012. GABAB receptors: structure, functions, and clinical implications. *Neurology,* 78**,** 578-84.
BENCHENANE, K., PEYRACHE, A., KHAMASSI, M., TIERNEY, P. L., GIOANNI, Y., BATTAGLIA, F. P. & WIENER, S. I. 2010. Coherent theta oscillations and reorganization of spike timing in the hippocampal- prefrontal network upon learning. *Neuron,* 66**,** 921-36.
BENDER, F., GORBATI, M., CADAVIECO, M. C., DENISOVA, N., GAO, X., HOLMAN, C., KOROTKOVA, T. & PONOMARENKO, A. 2015. Theta oscillations regulate the speed of locomotion via a hippocampus to lateral septum pathway. *Nat Commun,* 6**,** 8521.
BERENS, S. C. & HORNER, A. J. 2017. Theta Rhythm: Temporal Glue for Episodic Memory. *Current Biology,* 27**,** R1110-R1112.
BERGER, T. W., SWANSON, G. W., MILNER, T. A., LYNCH, G. S. & THOMPSON, R. F. 1980. Reciprocal anatomical connections between hippocampus and subiculum in the rabbit evidence for subicular innervation of regio superior. *Brain Res,* 183**,** 265-76.
BERK, M. L. & FINKELSTEIN, J. A. 1982. Efferent connections of the lateral hypothalamic area of the rat: an autoradiographic investigation. *Brain Res Bull,* 8**,** 511-26.
BEZAIRE, M. J. & SOLTESZ, I. 2013. Quantitative assessment of CA1 local circuits: knowledge base for interneuron-pyramidal cell connectivity. *Hippocampus,* 23**,** 751-85.
BJERKNES, T. L., MOSER, E. I. & MOSER, M. B. 2014. Representation of geometric borders in the developing rat. *Neuron,* 82**,** 71-8.
BLISS, T. V. & LOMO, T. 1973. Long-lasting potentiation of synaptic transmission in the dentate area of the anaesthetized rabbit following stimulation of the perforant path. *J Physiol,* 232**,** 331-56.
BLUMBERG, B. J., FLYNN, S. P., BARRIERE, S. J., MOUCHATI, P. R., SCOTT, R. C., HOLMES, G. L. & BARRY, J. M. 2016. Efficacy of nonselective optogenetic control of the medial septum over hippocampal oscillations: the influence of speed and implications for cognitive enhancement. *Physiol Rep,* 4.
BOCCARA, C. N., SARGOLINI, F., THORESEN, V. H., SOLSTAD, T., WITTER, M. P., MOSER, E. I. & MOSER, M. B. 2010. Grid cells in pre- and parasubiculum. *Nat Neurosci,* 13**,** 987-94.
BOCCHIO, M., NABAVI, S. & CAPOGNA, M. 2017. Synaptic Plasticity, Engrams, and Network Oscillations in Amygdala Circuits for Storage and Retrieval of Emotional Memories. *Neuron,* 94**,** 731-743.
BORHEGYI, Z., VARGA, V., SZILAGYI, N., FABO, D. & FREUND, T. F. 2004. Phase segregation of medial septal GABAergic neurons during hippocampal theta activity. *J Neurosci,* 24**,** 8470-9.
BORTZ, D. M. & GRACE, A. A. 2018. Medial septum differentially regulates dopamine neuron activity in the rat ventral tegmental area and substantia nigra via distinct pathways. *Neuropsychopharmacology,* 43**,** 2093-2100.

BOSTOCK, E., MULLER, R. U. & KUBIE, J. L. 1991. Experience-dependent modifications of hippocampal place cell firing. *Hippocampus,* 1**,** 193-205.
BOTEZ-MARQUARD, T. & BOTEZ, M. I. 1992. Visual memory deficits after damage to the anterior commissure and right fornix. *Archives of Neurology,* 49**,** 321-324.
BOUWMAN, B. M., VAN LIER, H., NITERT, H. E., DRINKENBURG, W. H., COENEN, A. M. & VAN RIJN, C. M. 2005. The relationship between hippocampal EEG theta activity and locomotor behaviour in freely moving rats: effects of vigabatrin. *Brain Res Bull,* 64**,** 505-9.
BRANDON, M. P., BOGAARD, A. R., LIBBY, C. P., CONNERNEY, M. A., GUPTA, K. & HASSELMO, M. E. 2011. Reduction of theta rhythm dissociates grid cell spatial periodicity from directional tuning. *Science,* 332**,** 595-9.
BRAZHNIK, E. S. & FOX, S. E. 1999. Action potentials and relations to the theta rhythm of medial septal neurons in vivo. *Exp Brain Res,* 127**,** 244-58.
BREESE, C. R., HAMPSON, R. E. & DEADWYLER, S. A. 1989. Hippocampal place cells: stereotypy and plasticity. *J Neurosci,* 9**,** 1097-111.
BUNO, W., JR. & VELLUTI, J. C. 1977. Relationships of hippocampal theta cycles with bar pressing during self-stimulation. *Physiol Behav,* 19**,** 615-21.
BURGESS, N. 2002. The hippocampus, space, and viewpoints in episodic memory. *Q J Exp Psychol A,* 55**,** 1057-80.
BURGESS, N., MAGUIRE, E. A. & O'KEEFE, J. 2002. The human hippocampus and spatial and episodic memory. *Neuron,* 35**,** 625-41.
BURGESS, N. & O'KEEFE, J. 2005. The theta rhythm. *Hippocampus,* 15**,** 825-826.
BURWELL, R. D. & AMARAL, D. G. 1998a. Cortical afferents of the perirhinal, postrhinal, and entorhinal cortices of the rat. *J Comp Neurol,* 398**,** 179-205.
BURWELL, R. D. & AMARAL, D. G. 1998b. Perirhinal and postrhinal cortices of the rat: interconnectivity and connections with the entorhinal cortex. *J Comp Neurol,* 391**,** 293-321.
BUZSAKI, G. 2002. Theta oscillations in the hippocampus. *Neuron,* 33**,** 325-40.
BUZSÁKI, G. 1996. The Hippocampo-Neocortical Dialogue. *Cerebral Cortex,* 6**,** 81-92.
BUZSAKI, G. & WANG, X. J. 2012. Mechanisms of gamma oscillations. *Annu Rev Neurosci,* 35**,** 203-25.
CARLEZON, W. A., JR. & CHARTOFF, E. H. 2007. Intracranial self-stimulation (ICSS) in rodents to study the neurobiology of motivation. *Nat Protoc,* 2**,** 2987-95.
CAZALA, P., GALEY, D. & DURKIN, T. 1988. Electrical self-stimulation in the medial and lateral septum as compared to the lateral hypothalamus: differential intervention of reward and learning processes? *Physiol Behav,* 44**,** 53-9.
CHEE, S.-S. A., MENARD, J. L. & DRINGENBERG, H. C. 2015. The lateral septum as a regulator of hippocampal theta oscillations and defensive behavior in rats. *Journal of neurophysiology,* 113**,** 1831-1841.
CHEN, L. L., LIN, L. H., GREEN, E. J., BARNES, C. A. & MCNAUGHTON, B. L. 1994. Head-direction cells in the rat posterior cortex. I. Anatomical distribution and behavioral modulation. *Exp Brain Res,* 101**,** 8-23.
CHIBA, T. & MURATA, Y. 1985. Afferent and efferent connections of the medial preoptic area in the rat: a WGA-HRP study. *Brain Res Bull,* 14**,** 261-72.
CHOUINARD, M. L., GALLAGHER, M., YASUDA, R. P., WOLFE, B. B. & MCKINNEY, M. 1995. Hippocampal muscarinic receptor function in spatial learning-impaired aged rats. *Neurobiol Aging,* 16**,** 955-63.
CLAYTON, N. S. & DICKINSON, A. 1998. Episodic-like memory during cache recovery by scrub jays. *Nature,* 395**,** 272-4.
CLOUTER, A., SHAPIRO, K. L. & HANSLMAYR, S. 2017. Theta Phase Synchronization Is the Glue that Binds Human Associative Memory. *Curr Biol,* 27**,** 3143-3148 e6.
COBB, S. R. & DAVIES, C. H. 2005. Cholinergic modulation of hippocampal cells and circuits. *J Physiol,* 562**,** 81-8.

COHEN, J. D., BOLSTAD, M. & LEE, A. K. 2017. Experience-dependent shaping of hippocampal CA1 intracellular activity in novel and familiar environments. *Elife,* 6.
COLGIN, L. L., LEUTGEB, S., JEZEK, K., LEUTGEB, J. K., MOSER, E. I., MCNAUGHTON, B. L. & MOSER, M. B. 2010. Attractor-map versus autoassociation based attractor dynamics in the hippocampal network. *J Neurophysiol,* 104**,** 35-50.
COLGIN, L. L., MOSER, E. I. & MOSER, M. B. 2008. Understanding memory through hippocampal remapping. *Trends Neurosci,* 31**,** 469-77.
COLOM, L. V. 2006. Septal networks: relevance to theta rhythm, epilepsy and Alzheimer's disease. *Journal of Neurochemistry,* 96**,** 609-623.
COLOM, L. V., CASTANEDA, M. T., REYNA, T., HERNANDEZ, S. & GARRIDO-SANABRIA, E. 2005. Characterization of medial septal glutamatergic neurons and their projection to the hippocampus. *Synapse,* 58**,** 151-64.
CONNORS, B. W., GUTNICK, M. J. & PRINCE, D. A. 1982. Electrophysiological properties of neocortical neurons in vitro. *J Neurophysiol,* 48**,** 1302-20.
CORKIN, S. 2002. What's new with the amnesic patient H.M.? *Nat Rev Neurosci,* 3**,** 153-60.
CORKIN, S., AMARAL, D. G., GONZALEZ, R. G., JOHNSON, K. A. & HYMAN, B. T. 1997. H. M.'s medial temporal lobe lesion: findings from magnetic resonance imaging. *J Neurosci,* 17**,** 3964-79.
CRYSTAL, J. D. 2009. Elements of episodic-like memory in animal models. *Behav Processes,* 80**,** 269-77.
CZURKÓ, A., HUXTER, J., LI, Y., HANGYA, B. & MULLER, R. U. 2011. Theta phase classification of interneurons in the hippocampal formation of freely moving rats. *The Journal of neuroscience : the official journal of the Society for Neuroscience,* 31**,** 2938-2947.
DANIELSON, N. B., ZAREMBA, J. D., KAIFOSH, P., BOWLER, J., LADOW, M. & LOSONCZY, A. 2016. Sublayer-Specific Coding Dynamics during Spatial Navigation and Learning in Hippocampal Area CA1. *Neuron,* 91**,** 652-65.
DESHMUKH, S. S. & KNIERIM, J. J. 2011. Representation of non-spatial and spatial information in the lateral entorhinal cortex. *Front Behav Neurosci,* 5**,** 69.
DESIKAN, S., KOSER, D. E., NEITZ, A. & MONYER, H. 2018. Target selectivity of septal cholinergic neurons in the medial and lateral entorhinal cortex. *Proc Natl Acad Sci U S A,* 115**,** E2644-E2652.
DIAMANTAKI, M., COLETTA, S., NASR, K., ZERAATI, R., LATURNUS, S., BERENS, P., PRESTON-FERRER, P. & BURGALOSSI, A. 2018. Manipulating Hippocampal Place Cell Activity by Single-Cell Stimulation in Freely Moving Mice. *Cell Rep,* 23**,** 32-38.
DOALLO, S., PATAI, E. Z. & NOBRE, A. C. 2013. Reward associations magnify memory-based biases on perception. *J Cogn Neurosci,* 25**,** 245-57.
DRAGOI, G., CARPI, D., RECCE, M., CSICSVARI, J. & BUZSAKI, G. 1999. Interactions between hippocampus and medial septum during sharp waves and theta oscillation in the behaving rat. *J Neurosci,* 19**,** 6191-9.
DUPRET, D., PLEYDELL-BOUVERIE, B. & CSICSVARI, J. 2010. Rate remapping: when the code goes beyond space. *Neuron,* 68**,** 1015-6.
DUTAR, P., BASSANT, M. H., SENUT, M. C. & LAMOUR, Y. 1995. The septohippocampal pathway: structure and function of a central cholinergic system. *Physiological Reviews,* 75**,** 393-427.
E TULVING, A. & MADIGAN, S. A. 1970. Memory and Verbal Learning. *Annual Review of Psychology,* 21**,** 437-484.
EGO-STENGEL, V. & WILSON, M. A. 2007. Spatial selectivity and theta phase precession in CA1 interneurons. *Hippocampus,* 17**,** 161-74.
EICHENBAUM, H. 2013. Hippocampus: remembering the choices. *Neuron,* 77**,** 999-1001.

EICHENBAUM, H. 2017. The role of the hippocampus in navigation is memory. *J Neurophysiol,* 117**,** 1785-1796.
EKSTROM, A. D., KAHANA, M. J., CAPLAN, J. B., FIELDS, T. A., ISHAM, E. A., NEWMAN, E. L. & FRIED, I. 2003. Cellular networks underlying human spatial navigation. *Nature,* 425**,** 184-8.
EKSTROM, A. D., MELTZER, J., MCNAUGHTON, B. L. & BARNES, C. A. 2001. NMDA Receptor Antagonism Blocks Experience-Dependent Expansion of Hippocampal “Place Fields”. *Neuron,* 31**,** 631-638.
ELVANDER-TOTTIE, E., ERIKSSON, T. M., SANDIN, J. & OGREN, S. O. 2006. N-methyl-D-aspartate receptors in the medial septal area have a role in spatial and emotional learning in the rat. *Neuroscience,* 142**,** 963-78.
ENGELMANN, J. B., DAMARAJU, E., PADMALA, S. & PESSOA, L. 2009. Combined effects of attention and motivation on visual task performance: transient and sustained motivational effects. *Front Hum Neurosci,* 3**,** 4.
ERGORUL, C. & EICHENBAUM, H. 2004. The hippocampus and memory for "what," "where," and "when". *Learn Mem,* 11**,** 397-405.
ERLANDER, M. G., TILLAKARATNE, N. J., FELDBLUM, S., PATEL, N. & TOBIN, A. J. 1991. Two genes encode distinct glutamate decarboxylases. *Neuron,* 7**,** 91-100.
FERBINTEANU, J. & SHAPIRO, M. L. 2003. Prospective and retrospective memory coding in the hippocampus. *Neuron,* 40**,** 1227-39.
FINKELSTEIN, A., DERDIKMAN, D., RUBIN, A., FOERSTER, J. N., LAS, L. & ULANOVSKY, N. 2015. Three-dimensional head-direction coding in the bat brain. *Nature,* 517**,** 159-64.
FISHER, R. S. 2013. Deep brain stimulation for epilepsy. *Handb Clin Neurol,* 116**,** 217-34.
FITZJOHN, S. M., KUENZI, F., MORTON, R. A., ROSAHL, T. W., LEWIS, H., SMITH, D., SEABROOK, G. R. & COLLINGRIDGE, G. L. 2010. A study of long-term potentiation in transgenic mice over-expressing mutant forms of both amyloid precursor protein and presenilin-1. *Mol Brain,* 3**,** 21.
FOSTER, D. J. & WILSON, M. A. 2007. Hippocampal theta sequences. *Hippocampus,* 17**,** 1093-9.
FOURIEZOS, G., HANSSON, P. & WISE, R. A. 1978. Neuroleptic-induced attenuation of brain stimulation reward in rats. *J Comp Physiol Psychol,* 92**,** 661-71.
FRANK, L. M., STANLEY, G. B. & BROWN, E. N. 2004. Hippocampal plasticity across multiple days of exposure to novel environments. *J Neurosci,* 24**,** 7681-9.
FRASER, K. A., POUCET, B., PARTLOW, G. & HERRMANN, T. 1991. Role of the medial and lateral septum in a variable goal spatial problem solving task. *Physiol Behav,* 50**,** 739-44.
FREUND, T. F. 1989. GABAergic septohippocampal neurons contain parvalbumin. *Brain Res,* 478**,** 375-81.
FREUND, T. F. 2003. Interneuron Diversity series: Rhythm and mood in perisomatic inhibition. *Trends Neurosci,* 26**,** 489-95.
FREUND, T. F. & ANTAL, M. 1988. GABA-containing neurons in the septum control inhibitory interneurons in the hippocampus. *Nature,* 336**,** 170-3.
FREUND, T. F. & BUZSAKI, G. 1996. Interneurons of the hippocampus. *Hippocampus,* 6**,** 347-470.
FREUND, T. F. & KATONA, I. 2007. Perisomatic inhibition. *Neuron,* 56**,** 33-42.
FRITSCHY, J. M. & PANZANELLI, P. 2014. GABAA receptors and plasticity of inhibitory neurotransmission in the central nervous system. *Eur J Neurosci,* 39**,** 1845-65.
FROTSCHER, M. & LERANTH, C. 1985. Cholinergic innervation of the rat hippocampus as revealed by choline acetyltransferase immunocytochemistry: a combined light and electron microscopic study. *J Comp Neurol,* 239**,** 237-46.

FUENTEMILLA, L., PENNY, W. D., CASHDOLLAR, N., BUNZECK, N. & DUZEL, E. 2010. Theta-coupled periodic replay in working memory. *Curr Biol,* 20**,** 606-12.
FUHRMANN, F., JUSTUS, D., SOSULINA, L., KANEKO, H., BEUTEL, T., FRIEDRICHS, D., SCHOCH, S., SCHWARZ, MARTIN K., FUHRMANN, M. & REMY, S. 2015. Locomotion, Theta Oscillations, and the Speed-Correlated Firing of Hippocampal Neurons Are Controlled by a Medial Septal Glutamatergic Circuit. *Neuron,* 86**,** 1253-1264.
FUHS, M. C. & TOURETZKY, D. S. 2006. A spin glass model of path integration in rat medial entorhinal cortex. *J Neurosci,* 26**,** 4266-76.
FUHS, M. C., VANRHOADS, S. R., CASALE, A. E., MCNAUGHTON, B. & TOURETZKY, D. S. 2005. Influence of path integration versus environmental orientation on place cell remapping between visually identical environments. *J Neurophysiol,* 94**,** 2603-16.
FYHN, M., MOLDEN, S., WITTER, M. P., MOSER, E. I. & MOSER, M. B. 2004. Spatial representation in the entorhinal cortex. *Science,* 305**,** 1258-64.
GAFFAN, E. A., GAFFAN, D. & HODGES, J. R. 1991. Amnesia following damage to the left fornix and to other sites. A comparative study. *Brain,* 114 (Pt 3)**,** 1297-313.
GAUTHIER, J. L. & TANK, D. W. 2018. A Dedicated Population for Reward Coding in the Hippocampus. *Neuron,* 99**,** 179-193 e7.
GAVELLO-BAUDY, S., LE MERRER, J., DECORTE, L., DAVID, V. & CAZALA, P. 2008. Self-administration of the GABAA agonist muscimol into the medial septum: dependence on dopaminergic mechanisms. *Psychopharmacology (Berl),* 201**,** 219-28.
GAYKEMA, R. P., LUITEN, P. G., NYAKAS, C. & TRABER, J. 1990. Cortical projection patterns of the medial septum-diagonal band complex. *J Comp Neurol,* 293**,** 103-24.
GAZTELU, J. M. & BUNO, W., JR. 1982. Septo-hippocampal relationships during EEG theta rhythm. *Electroencephalogr Clin Neurophysiol,* 54**,** 375-87.
GEILLER, T., FATTAHI, M., CHOI, J. S. & ROYER, S. 2017. Place cells are more strongly tied to landmarks in deep than in superficial CA1. *Nat Commun,* 8**,** 14531.
GEISLER, S. & WISE, R. A. 2008. Functional implications of glutamatergic projections to the ventral tegmental area. *Rev Neurosci,* 19**,** 227-44.
GEISLER, S. & ZAHM, D. S. 2005. Afferents of the ventral tegmental area in the rat-anatomical substratum for integrative functions. *J Comp Neurol,* 490**,** 270-94.
GILL, T. M. & GALLAGHER, M. 1998. Evaluation of muscarinic M2 receptor sites in basal forebrain and brainstem cholinergic systems of behaviorally characterized young and aged Long-Evans rats. *Neurobiol Aging,* 19**,** 217-25.
GIVENS, B. S. & OLTON, D. S. 1990. Cholinergic and GABAergic modulation of medial septal area: effect on working memory. *Behav Neurosci,* 104**,** 849-55.
GOGOLAK, G., STUMPF, C., PETSCHE, H. & STERC, J. 1968. The firing pattern of septal neurons and the form of the hippocampal theta wave. *Brain Res,* 7**,** 201-7.
GÓIS, Z. H. T. D. & TORT, A. B. L. 2018. Characterizing Speed Cells in the Rat Hippocampus. *Cell Reports,* 25**,** 1872-1884.e4.
GOODRIDGE, J. P., DUDCHENKO, P. A., WORBOYS, K. A., GOLOB, E. J. & TAUBE, J. S. 1998. Cue control and head direction cells. *Behav Neurosci,* 112**,** 749-61.
GORDON, J. A., LACEFIELD, C. O., KENTROS, C. G. & HEN, R. 2005. State-dependent alterations in hippocampal oscillations in serotonin 1A receptor-deficient mice. *J Neurosci,* 25**,** 6509-19.
GOTHARD, K. M., SKAGGS, W. E. & MCNAUGHTON, B. L. 1996a. Dynamics of mismatch correction in the hippocampal ensemble code for space: interaction between path integration and environmental cues. *J Neurosci,* 16**,** 8027-40.

GOTHARD, K. M., SKAGGS, W. E., MOORE, K. M. & MCNAUGHTON, B. L. 1996b. Binding of hippocampal CA1 neural activity to multiple reference frames in a landmark-based navigation task. *J Neurosci,* 16**,** 823-35.
GOUTAGNY, R., JACKSON, J. & WILLIAMS, S. 2009. Self-generated theta oscillations in the hippocampus. *Nat Neurosci,* 12**,** 1491-3.
GRAY, J. A. 1971. Medial septal lesions, hippocampal theta rhythm and the control of vibrissal movement in the freely moving rat. *Electroencephalogr Clin Neurophysiol,* 30**,** 189-97.
GREEN, J. D. & ARDUINI, A. A. 1954. Hippocampal electrical activity in arousal. *J Neurophysiol,* 17**,** 533-57.
GRIEVES, R. M. & JEFFERY, K. J. 2017. The representation of space in the brain. *Behav Processes,* 135**,** 113-131.
GRUBER, M. J., WATROUS, A. J., EKSTROM, A. D., RANGANATH, C. & OTTEN, L. J. 2013. Expected reward modulates encoding-related theta activity before an event. *NeuroImage,* 64**,** 68-74.
GULYAS, A. I., HAJOS, N. & FREUND, T. F. 1996. Interneurons containing calretinin are specialized to control other interneurons in the rat hippocampus. *J Neurosci,* 16**,** 3397-411.
GULYAS, A. I., HAJOS, N., KATONA, I. & FREUND, T. F. 2003. Interneurons are the local targets of hippocampal inhibitory cells which project to the medial septum. *Eur J Neurosci,* 17**,** 1861-72.
GULYAS, A. I., SERESS, L., TOTH, K., ACSADY, L., ANTAL, M. & FREUND, T. F. 1991. Septal GABAergic neurons innervate inhibitory interneurons in the hippocampus of the macaque monkey. *Neuroscience,* 41**,** 381-90.
GUPTA, A. S., VAN DER MEER, M. A. A., TOURETZKY, D. S. & REDISH, A. D. 2012. Segmentation of spatial experience by hippocampal θ sequences. *Nature neuroscience,* 15**,** 1032-1039.
HAFTING, T., FYHN, M., BONNEVIE, T., MOSER, M. B. & MOSER, E. I. 2008. Hippocampus-independent phase precession in entorhinal grid cells. *Nature,* 453**,** 1248-52.
HAFTING, T., FYHN, M., MOLDEN, S., MOSER, M. B. & MOSER, E. I. 2005. Microstructure of a spatial map in the entorhinal cortex. *Nature,* 436**,** 801-6.
HAHN, J. D. & SWANSON, L. W. 2012. Connections of the lateral hypothalamic area juxtadorsomedial region in the male rat. *J Comp Neurol,* 520**,** 1831-90.
HAJSZAN, T., ALREJA, M. & LERANTH, C. 2004. Intrinsic vesicular glutamate transporter 2-immunoreactive input to septohippocampal parvalbumin-containing neurons: novel glutamatergic local circuit cells. *Hippocampus,* 14**,** 499-509.
HAMMOND, S. L., LEEK, A. N., RICHMAN, E. H. & TJALKENS, R. B. 2017. Cellular selectivity of AAV serotypes for gene delivery in neurons and astrocytes by neonatal intracerebroventricular injection. *PLOS ONE,* 12**,** e0188830.
HANGYA, B., BORHEGYI, Z., SZILÁGYI, N., FREUND, T. F. & VARGA, V. 2009. GABAergic Neurons of the Medial Septum Lead the Hippocampal Network during Theta Activity. *The Journal of Neuroscience,* 29**,** 8094-8102.
HARRIS, G. C., WIMMER, M. & ASTON-JONES, G. 2005. A role for lateral hypothalamic orexin neurons in reward seeking. *Nature,* 437**,** 556-9.
HARTLEY, T., LEVER, C., BURGESS, N. & O'KEEFE, J. 2014. Space in the brain: how the hippocampal formation supports spatial cognition. *Philos Trans R Soc Lond B Biol Sci,* 369**,** 20120510.
HEBB, D. O. 1938. Studies of the organization of behavior. I. Behavior of the rat in a field orientation. *Journal of Comparative Psychology,* 25**,** 333-353.
HENDERSON, Z., LU, C. B., JANZSO, G., MATTO, N., MCKINLEY, C. E., YANAGAWA, Y. & HALASY, K. 2010. Distribution and role of Kv3.1b in neurons in the medial septum diagonal band complex. *Neuroscience,* 166**,** 952-69.

HENDERSON, Z., MORRIS, N. P., GRIMWOOD, P., FIDDLER, G., YANG, H. W. & APPENTENG, K. 2001. Morphology of local axon collaterals of electrophysiologically characterised neurons in the rat medial septal/ diagonal band complex. *J Comp Neurol,* 430**,** 410-32.
HERZOG, C. D., GANDHI, C., BHATTACHARYA, P. & WALSH, T. J. 2000. Effects of intraseptal zolpidem and chlordiazepoxide on spatial working memory and high-affinity choline uptake in the hippocampus. *Neurobiol Learn Mem,* 73**,** 168-79.
HILL, A. J. 1978. First occurrence of hippocampal spatial firing in a new environment. *Exp Neurol,* 62**,** 282-97.
HOEBEL, B. G. 1979. Hypothalamic self-stimulation and stimulation escape in relation to feeding and mating. *Fed Proc,* 38**,** 2454-61.
HOK, V., LENCK-SANTINI, P. P., ROUX, S., SAVE, E., MULLER, R. U. & POUCET, B. 2007. Goal-related activity in hippocampal place cells. *J Neurosci,* 27**,** 472-82.
HOLLERMAN, J. R. & SCHULTZ, W. 1998. Dopamine neurons report an error in the temporal prediction of reward during learning. *Nat Neurosci,* 1**,** 304-9.
HOLLUP, S. A., MOLDEN, S., DONNETT, J. G., MOSER, M. B. & MOSER, E. I. 2001. Accumulation of hippocampal place fields at the goal location in an annular watermaze task. *J Neurosci,* 21**,** 1635-44.
HOLSCHER, C., JACOB, W. & MALLOT, H. A. 2003. Reward modulates neuronal activity in the hippocampus of the rat. *Behav Brain Res,* 142**,** 181-91.
HU, H., GAN, J. & JONAS, P. 2014. Interneurons. Fast-spiking, parvalbumin(+) GABAergic interneurons: from cellular design to microcircuit function. *Science,* 345**,** 1255263.
HUERTA, P. T. & LISMAN, J. E. 1995. Bidirectional synaptic plasticity induced by a single burst during cholinergic theta oscillation in CA1 in vitro. *Neuron,* 15**,** 1053-63.
HUGUET, G., ALDAVERT-VERA, L., KADAR, E., PENA DE ORTIZ, S., MORGADO-BERNAL, I. & SEGURA-TORRES, P. 2009. Intracranial self-stimulation to the lateral hypothalamus, a memory improving treatment, results in hippocampal changes in gene expression. *Neuroscience,* 162**,** 359-74.
HUH, C. Y. L., GOUTAGNY, R. & WILLIAMS, S. 2010. Glutamatergic Neurons of the Mouse Medial Septum and Diagonal Band of Broca Synaptically Drive Hippocampal Pyramidal Cells: Relevance for Hippocampal Theta Rhythm. *The Journal of Neuroscience,* 30**,** 15951-15961.
HUXTER, J. R., SENIOR, T. J., ALLEN, K. & CSICSVARI, J. 2008. Theta phase-specific codes for two-dimensional position, trajectory and heading in the hippocampus. *Nat Neurosci,* 11**,** 587-94.
HYMAN, J. M., WYBLE, B. P., GOYAL, V., ROSSI, C. A. & HASSELMO, M. E. 2003. Stimulation in hippocampal region CA1 in behaving rats yields long-term potentiation when delivered to the peak of theta and long-term depression when delivered to the trough. *J Neurosci,* 23**,** 11725-31.
ISHIZUKA, N., WEBER, J. & AMARAL, D. G. 1990. Organization of intrahippocampal projections originating from CA3 pyramidal cells in the rat. *J Comp Neurol,* 295**,** 580-623.
JACOB, P. Y., CASALI, G., SPIESER, L., PAGE, H., OVERINGTON, D. & JEFFERY, K. 2017. An independent, landmark-dominated head-direction signal in dysgranular retrosplenial cortex. *Nat Neurosci,* 20**,** 173-175.
JAKAB, R. L. & LERANTH, C. 1993. Presence of somatostatin or neurotensin in lateral septal dopaminergic axon terminals of distinct hypothalamic and midbrain origins: convergence on the somatospiny neurons. *Exp Brain Res,* 92**,** 420-30.
JAKAB, R. L. & LERANTH, C. 1995. *The rat nervous system,* San Diego, Academic Press.
JANG, H. J., PARK, K., LEE, J., KIM, H., HAN, K. H. & KWAG, J. 2015. GABAA receptor-mediated feedforward and feedback inhibition differentially modulate

the gain and the neural code transformation in hippocampal CA1 pyramidal cells. *Neuropharmacology,* 99**,** 177-86.
JANKOWSKI, M. M. & O'MARA, S. M. 2015. Dynamics of place, boundary and object encoding in rat anterior claustrum. *Front Behav Neurosci,* 9**,** 250.
JEANTET, Y. & CHO, Y. H. 2012. Evolution of hippocampal spatial representation over time in mice. *Neurobiol Learn Mem,* 98**,** 354-60.
JEFFERY, K. J., DONNETT, J. G., BURGESS, N. & O'KEEFE, J. M. 1997. Directional control of hippocampal place fields. *Exp Brain Res,* 117**,** 131-42.
JENSEN, O. & LISMAN, J. E. 2000. Position reconstruction from an ensemble of hippocampal place cells: contribution of theta phase coding. *J Neurophysiol,* 83**,** 2602-9.
JEONG, D. U., LEE, J. E., LEE, S. E., CHANG, W. S., KIM, S. J. & CHANG, J. W. 2014. Improvements in memory after medial septum stimulation are associated with changes in hippocampal cholinergic activity and neurogenesis. *Biomed Res Int,* 2014**,** 568587.
JINNO, S. & KOSAKA, T. 2002. Immunocytochemical characterization of hippocamposeptal projecting GABAergic nonprincipal neurons in the mouse brain: a retrograde labeling study. *Brain Res,* 945**,** 219-31.
JOHNSON, A. & REDISH, A. D. 2007. Neural ensembles in CA3 transiently encode paths forward of the animal at a decision point. *J Neurosci,* 27**,** 12176-89.
JOHNSON, S. W. & NORTH, R. A. 1992. Two types of neurone in the rat ventral tegmental area and their synaptic inputs. *J Physiol,* 450**,** 455-68.
JONES, G. A., NORRIS, S. K. & HENDERSON, Z. 1999. Conduction velocities and membrane properties of different classes of rat septohippocampal neurons recorded in vitro. *The Journal of physiology,* 517 (Pt 3)**,** 867-877.
JONES, M. W. & WILSON, M. A. 2005. Theta Rhythms Coordinate Hippocampal–Prefrontal Interactions in a Spatial Memory Task. *PLOS Biology,* 3**,** e402.
JONES, R. 2003. Double code in place cells. *Nature Reviews Neuroscience,* 4**,** 933.
JOSHI, A., SALIB, M., VINEY, T. J., DUPRET, D. & SOMOGYI, P. 2017. Behavior-Dependent Activity and Synaptic Organization of Septo-hippocampal GABAergic Neurons Selectively Targeting the Hippocampal CA3 Area. *Neuron,* 96**,** 1342-1357.e5.
JOUVET, M. 1969. Biogenic Amines and the States of Sleep. *Science,* 163**,** 32-41.
KANG, D., DING, M., TOPCHIY, I., SHIFFLETT, L. & KOCSIS, B. 2015. Theta-rhythmic drive between medial septum and hippocampus in slow-wave sleep and microarousal: a Granger causality analysis. *J Neurophysiol,* 114**,** 2797-803.
KARLSSON, M. P. & FRANK, L. M. 2008. Network dynamics underlying the formation of sparse, informative representations in the hippocampus. *J Neurosci,* 28**,** 14271-81.
KAWAGUCHI, Y. & KUBOTA, Y. 1996. Physiological and morphological identification of somatostatin- or vasoactive intestinal polypeptide-containing cells among GABAergic cell subtypes in rat frontal cortex. *J Neurosci,* 16**,** 2701-15.
KELLEHER, R. J., 3RD, GOVINDARAJAN, A. & TONEGAWA, S. 2004. Translational regulatory mechanisms in persistent forms of synaptic plasticity. *Neuron,* 44**,** 59-73.
KEMPADOO, K. A., MOSHAROV, E. V., CHOI, S. J., SULZER, D. & KANDEL, E. R. 2016. Dopamine release from the locus coeruleus to the dorsal hippocampus promotes spatial learning and memory. *Proc Natl Acad Sci U S A,* 113**,** 14835-14840.
KENTROS, C., HARGREAVES, E., HAWKINS, R. D., KANDEL, E. R., SHAPIRO, M. & MULLER, R. V. 1998. Abolition of long-term stability of new hippocampal place cell maps by NMDA receptor blockade. *Science,* 280**,** 2121-6.
KESNER, R. P., CRUTCHER, K. A. & MEASOM, M. O. 1986. Medial septal and nucleus basalis magnocellularis lesions produce order memory deficits in rats

which mimic symptomatology of Alzheimer's disease. *Neurobiol Aging,* 7**,** 287-95.
KESSELS, R. P., DE HAAN, E. H., KAPPELLE, L. J. & POSTMA, A. 2001. Varieties of human spatial memory: a meta-analysis on the effects of hippocampal lesions. *Brain Res Brain Res Rev,* 35**,** 295-303.
KHAKPAI, F., NASEHI, M., HAERI-ROHANI, A., EIDI, A. & ZARRINDAST, M. R. 2013. Septo-hippocampo-septal loop and memory formation. *Basic and clinical neuroscience,* 4**,** 5-23.
KING, C., RECCE, M. & O'KEEFE, J. 1998. The rhythmicity of cells of the medial septum/diagonal band of Broca in the awake freely moving rat: relationships with behaviour and hippocampal theta. *Eur J Neurosci,* 10**,** 464-77.
KISS, J., PATEL, A. J., BAIMBRIDGE, K. G. & FREUND, T. F. 1990. Topographical localization of neurons containing parvalbumin and choline acetyltransferase in the medial septum-diagonal band region of the rat. *Neuroscience,* 36**,** 61-72.
KJELSTRUP, K. B., SOLSTAD, T., BRUN, V. H., HAFTING, T., LEUTGEB, S., WITTER, M. P., MOSER, E. I. & MOSER, M. B. 2008. Finite scale of spatial representation in the hippocampus. *Science,* 321**,** 140-3.
KLAUSBERGER, T. 2009. GABAergic interneurons targeting dendrites of pyramidal cells in the CA1 area of the hippocampus. *Eur J Neurosci,* 30**,** 947-57.
KLAUSBERGER, T., MAGILL, P. J., MARTON, L. F., ROBERTS, J. D., COBDEN, P. M., BUZSAKI, G. & SOMOGYI, P. 2003. Brain-state- and cell-type-specific firing of hippocampal interneurons in vivo. *Nature,* 421**,** 844-8.
KLAUSBERGER, T. & SOMOGYI, P. 2008. Neuronal Diversity and Temporal Dynamics: The Unity of Hippocampal Circuit Operations. *Science,* 321**,** 53-57.
KLEEN, J. K., WU, E. X., HOLMES, G. L., SCOTT, R. C. & LENCK-SANTINI, P. P. 2011. Enhanced oscillatory activity in the hippocampal-prefrontal network is related to short-term memory function after early-life seizures. *J Neurosci,* 31**,** 15397-406.
KNAPP, J. A., MORRIS, N. P., HENDERSON, Z. & MATTHEWS, R. T. 2000. Electrophysiological characteristics of non-bursting, glutamate decarboxylase messenger RNA-positive neurons of the medial septum/diagonal band nuclei of guinea-pig and rat. *Neuroscience,* 98**,** 661-8.
KNIERIM, J. J., KUDRIMOTI, H. S. & MCNAUGHTON, B. L. 1998. Interactions between idiothetic cues and external landmarks in the control of place cells and head direction cells. *J Neurophysiol,* 80**,** 425-46.
KNIERIM, J. J. & MCNAUGHTON, B. L. 2001. Hippocampal place-cell firing during movement in three-dimensional space. *J Neurophysiol,* 85**,** 105-16.
KOBAYASHI, T., TRAN, A. H., NISHIJO, H., ONO, T. & MATSUMOTO, G. 2003. Contribution of hippocampal place cell activity to learning and formation of goal-directed navigation in rats. *Neuroscience,* 117**,** 1025-35.
KOCSIS, B., BRAGIN, A. & BUZSAKI, G. 1999. Interdependence of multiple theta generators in the hippocampus: a partial coherence analysis. *J Neurosci,* 19**,** 6200-12.
KOENIG, J., LINDER, A. N., LEUTGEB, J. K. & LEUTGEB, S. 2011. The Spatial Periodicity of Grid Cells Is Not Sustained During Reduced Theta Oscillations. *Science,* 332**,** 592-595.
KUGLER, S., KILIC, E. & BAHR, M. 2003. Human synapsin 1 gene promoter confers highly neuron-specific long-term transgene expression from an adenoviral vector in the adult rat brain depending on the transduced area. *Gene Ther,* 10**,** 337-47.
LACAILLE, J. C., MUELLER, A. L., KUNKEL, D. D. & SCHWARTZKROIN, P. A. 1987. Local circuit interactions between oriens/alveus interneurons and CA1 pyramidal cells in hippocampal slices: electrophysiology and morphology. *J Neurosci,* 7**,** 1979-93.

LACHAUX, J.-P., RODRIGUEZ, E., MARTINERIE, J. & VARELA, F. J. 1999. Measuring phase synchrony in brain signals. *Human Brain Mapping,* 8**,** 194-208.
LANSINK, C. S., MEIJER, G. T., LANKELMA, J. V., VINCK, M. A., JACKSON, J. C. & PENNARTZ, C. M. A. 2016. Reward Expectancy Strengthens CA1 Theta and Beta Band Synchronization and Hippocampal-Ventral Striatal Coupling. *The Journal of Neuroscience,* 36**,** 10598-10610.
LASHLEY, K. 1950. In search of the engram. *Society of Experimental Biology Symposium.* Cambridge, England: Cambridge University Press.
LAXPATI, N. G., MAHMOUDI, B., GUTEKUNST, C. A., NEWMAN, J. P., ZELLER-TOWNSON, R. & GROSS, R. E. 2014. Real-time in vivo optogenetic neuromodulation and multielectrode electrophysiologic recording with NeuroRighter. *Front Neuroeng,* 7**,** 40.
LEAO, R. N., MIKULOVIC, S., LEAO, K. E., MUNGUBA, H., GEZELIUS, H., ENJIN, A., PATRA, K., ERIKSSON, A., LOEW, L. M., TORT, A. B. & KULLANDER, K. 2012. OLM interneurons differentially modulate CA3 and entorhinal inputs to hippocampal CA1 neurons. *Nat Neurosci,* 15**,** 1524-30.
LEÃO, R. N., TARGINO, Z. H., COLOM, L. V. & FISAHN, A. 2015. Interconnection and synchronization of neuronal populations in the mouse medial septum/diagonal band of Broca. *Journal of neurophysiology,* 113**,** 971-980.
LEE, D. J., GURKOFF, G. G., IZADI, A., BERMAN, R. F., EKSTROM, A. D., MUIZELAAR, J. P., LYETH, B. G. & SHAHLAIE, K. 2013. Medial septal nucleus theta frequency deep brain stimulation improves spatial working memory after traumatic brain injury. *J Neurotrauma,* 30**,** 131-9.
LEE, D. J., IZADI, A., MELNIK, M., SEIDL, S., ECHEVERRI, A., SHAHLAIE, K. & GURKOFF, G. G. 2017. Stimulation of the medial septum improves performance in spatial learning following pilocarpine-induced status epilepticus. *Epilepsy Res,* 130**,** 53-63.
LENCK-SANTINI, P. P., RIVARD, B., MULLER, R. U. & POUCET, B. 2005. Study of CA1 place cell activity and exploratory behavior following spatial and nonspatial changes in the environment. *Hippocampus,* 15**,** 356-69.
LERANTH, C., DELLER, T. & BUZSAKI, G. 1992. Intraseptal connections redefined: lack of a lateral septum to medial septum path. *Brain Res,* 583**,** 1-11.
LERANTH, C. & FROTSCHER, M. 1987. GABAergic input of cholecystokinin-immunoreactive neurons in the hilar region of the rat hippocampus. An electron microscopic double immunostaining study. *Histochemistry,* 86**,** 287-90.
LERANTH, C. & FROTSCHER, M. 1989. Organization of the septal region in the rat brain: cholinergic-GABAergic interconnections and the termination of hippocampo-septal fibers. *J Comp Neurol,* 289**,** 304-14.
LEUNG, L. W. 1987. Hippocampal electrical activity following local tetanization. I. Afterdischarges. *Brain Res,* 419**,** 173-87.
LEUTGEB, S. & LEUTGEB, J. K. 2007. Pattern separation, pattern completion, and new neuronal codes within a continuous CA3 map. *Learn Mem,* 14**,** 745-57.
LEUTGEB, S., LEUTGEB, J. K., BARNES, C. A., MOSER, E. I., MCNAUGHTON, B. L. & MOSER, M. B. 2005a. Independent codes for spatial and episodic memory in hippocampal neuronal ensembles. *Science,* 309**,** 619-23.
LEUTGEB, S., LEUTGEB, J. K., MOSER, M. B. & MOSER, E. I. 2005b. Place cells, spatial maps and the population code for memory. *Curr Opin Neurobiol,* 15**,** 738-46.
LEUTGEB, S., LEUTGEB, J. K., TREVES, A., MOSER, M. B. & MOSER, E. I. 2004. Distinct ensemble codes in hippocampal areas CA3 and CA1. *Science,* 305**,** 1295-8.
LEUTGEB, S. & MIZUMORI, S. J. 2002. Context-specific spatial representations by lateral septal cells. *Neuroscience,* 112**,** 655-63.

LEVER, C., BURGESS, N., CACUCCI, F., HARTLEY, T. & O'KEEFE, J. 2002. What can the hippocampal representation of environmental geometry tell us about Hebbian learning? *Biol Cybern,* 87**,** 356-72.
LEWIS, S. 2010. Synaptic transmission: A closer look at presynaptic GABA(B) receptors. *Nat Rev Neurosci,* 11**,** 664.
LINDEN, D. J. & ROUTTENBERG, A. 1989. The role of protein kinase C in long-term potentiation: a testable model. *Brain Res Brain Res Rev,* 14**,** 279-96.
LISMAN, J. 2010. Working memory: the importance of theta and gamma oscillations. *Curr Biol,* 20**,** R490-2.
LIU, Z. H., SHIN, R. & IKEMOTO, S. 2008. Dual role of medial A10 dopamine neurons in affective encoding. *Neuropsychopharmacology,* 33**,** 3010-20.
LUBENOV, E. V. & SIAPAS, A. G. 2009. Hippocampal theta oscillations are travelling waves. *Nature,* 459**,** 534-9.
LYNCH, G. 2004. AMPA receptor modulators as cognitive enhancers. *Curr Opin Pharmacol,* 4**,** 4-11.
MA, J. & LEUNG, L. S. 2014. Deep brain stimulation of the medial septum or nucleus accumbens alleviates psychosis-relevant behavior in ketamine-treated rats. *Behav Brain Res,* 266**,** 174-82.
MAMAD, O., MCNAMARA, H. M., REILLY, R. B. & TSANOV, M. 2015. Medial septum regulates the hippocampal spatial representation. *Front Behav Neurosci,* 9**,** 166.
MAMAD, O., STUMPP, L., MCNAMARA, H. M., RAMAKRISHNAN, C., DEISSEROTH, K., REILLY, R. B. & TSANOV, M. 2017. Place field assembly distribution encodes preferred locations. *PLoS Biol,* 15**,** e2002365.
MANSEAU, F., DANIK, M. & WILLIAMS, S. 2005. A functional glutamatergic neurone network in the medial septum and diagonal band area. *The Journal of Physiology,* 566**,** 865-884.
MANSEAU, F., GOUTAGNY, R., DANIK, M. & WILLIAMS, S. 2008. The Hippocamposeptal Pathway Generates Rhythmic Firing of GABAergic Neurons in the Medial Septum and Diagonal Bands: An Investigation Using a Complete Septohippocampal Preparation In Vitro. *The Journal of Neuroscience,* 28**,** 4096-4107.
MARKUS, E. J., QIN, Y. L., LEONARD, B., SKAGGS, W. E., MCNAUGHTON, B. L. & BARNES, C. A. 1995. Interactions between location and task affect the spatial and directional firing of hippocampal neurons. *J Neurosci,* 15**,** 7079-94.
MATTIS, J., BRILL, J., EVANS, S., LERNER, T. N., DAVIDSON, T. J., HYUN, M., RAMAKRISHNAN, C., DEISSEROTH, K. & HUGUENARD, J. R. 2014. Frequency-dependent, cell type-divergent signaling in the hippocamposeptal projection. *J Neurosci,* 34**,** 11769-80.
MAURER, A. P., COWEN, S. L., BURKE, S. N., BARNES, C. A. & MCNAUGHTON, B. L. 2006a. Organization of hippocampal cell assemblies based on theta phase precession. *Hippocampus,* 16**,** 785-94.
MAURER, A. P., COWEN, S. L., BURKE, S. N., BARNES, C. A. & MCNAUGHTON, B. L. 2006b. Phase Precession in Hippocampal Interneurons Showing Strong Functional Coupling to Individual Pyramidal Cells. *The Journal of Neuroscience,* 26**,** 13485-13492.
MAURER, A. P., VANRHOADS, S. R., SUTHERLAND, G. R., LIPA, P. & MCNAUGHTON, B. L. 2005. Self-motion and the origin of differential spatial scaling along the septo-temporal axis of the hippocampus. *Hippocampus,* 15**,** 841-52.
MAURER, S. V. & WILLIAMS, C. L. 2017. The Cholinergic System Modulates Memory and Hippocampal Plasticity via Its Interactions with Non-Neuronal Cells. *Frontiers in immunology,* 8**,** 1489-1489.

MCHUGH, T. J., BLUM, K. I., TSIEN, J. Z., TONEGAWA, S. & WILSON, M. A. 1996. Impaired hippocampal representation of space in CA1-specific NMDAR1 knockout mice. *Cell,* 87**,** 1339-49.
MCKENZIE, S., ROBINSON, N. T., HERRERA, L., CHURCHILL, J. C. & EICHENBAUM, H. 2013. Learning causes reorganization of neuronal firing patterns to represent related experiences within a hippocampal schema. *J Neurosci,* 33**,** 10243-56.
MCNAUGHTON, B. L., BARNES, C. A. & O'KEEFE, J. 1983a. The contributions of position, direction, and velocity to single unit activity in the hippocampus of freely-moving rats. *Exp Brain Res,* 52**,** 41-9.
MCNAUGHTON, B. L., O'KEEFE, J. & BARNES, C. A. 1983b. The stereotrode: a new technique for simultaneous isolation of several single units in the central nervous system from multiple unit records. *J Neurosci Methods,* 8**,** 391-7.
MCNAUGHTON, N. 2006. The role of the subiculum within the behavioural inhibition system. *Behav Brain Res,* 174**,** 232-50.
MCQUISTON, A. R. 2014. Acetylcholine release and inhibitory interneuron activity in hippocampal CA1. *Front Synaptic Neurosci,* 6**,** 20.
MEIBACH, R. C. & SIEGEL, A. 1977. Efferent connections of the septal area in the rat: an analysis utilizing retrograde and anterograde transport methods. *Brain Res,* 119**,** 1-20.
MILES, R., TOTH, K., GULYAS, A. I., HAJOS, N. & FREUND, T. F. 1996. Differences between somatic and dendritic inhibition in the hippocampus. *Neuron,* 16**,** 815-23.
MITOMA, H., ISHIDA, K., SHIZUKA-IKEDA, M. & MIZUSAWA, H. 2003. Dual impairment of GABAA- and GABAB-receptor-mediated synaptic responses by autoantibodies to glutamic acid decarboxylase. *J Neurol Sci,* 208**,** 51-6.
MIYOSHI, G. 2018. Elucidating the developmental trajectories of GABAergic cortical interneuron subtypes. *Neurosci Res*.
MIZUMORI, S. J., PEREZ, G. M., ALVARADO, M. C., BARNES, C. A. & MCNAUGHTON, B. L. 1990. Reversible inactivation of the medial septum differentially affects two forms of learning in rats. *Brain Res,* 528**,** 12-20.
MIZUMORI, S. J., WARD, K. E. & LAVOIE, A. M. 1992. Medial septal modulation of entorhinal single unit activity in anesthetized and freely moving rats. *Brain Res,* 570**,** 188-97.
MIZUSEKI, K., SIROTA, A., PASTALKOVA, E. & BUZSAKI, G. 2009. Theta oscillations provide temporal windows for local circuit computation in the entorhinal-hippocampal loop. *Neuron,* 64**,** 267-80.
MONTAGNESE, C. M., SZÉKELY, A. D., ÁDÁM, Á. & CSILLAG, A. 2004. Efferent connections of septal nuclei of the domestic chick (Gallus domesticus): An anterograde pathway tracing study with a bearing on functional circuits. *Journal of Comparative Neurology,* 469**,** 437-456.
MORRIS, M. K., BOWERS, D., CHATTERJEE, A. & HEILMAN, K. M. 1992. Amnesia following a discrete basal forebrain lesion. *Brain,* 115 (Pt 6)**,** 1827-47.
MORRIS, N. P., HARRIS, S. J. & HENDERSON, Z. 1999. Parvalbumin-immunoreactive, fast-spiking neurons in the medial septum/diagonal band complex of the rat: intracellular recordings in vitro. *Neuroscience,* 92**,** 589-600.
MORRIS, R. G. 2001. Episodic-like memory in animals: psychological criteria, neural mechanisms and the value of episodic-like tasks to investigate animal models of neurodegenerative disease. *Philos Trans R Soc Lond B Biol Sci,* 356**,** 1453-65.
MOSCOVITCH, M., NADEL, L., WINOCUR, G., GILBOA, A. & ROSENBAUM, R. S. 2006. The cognitive neuroscience of remote episodic, semantic and spatial memory. *Curr Opin Neurobiol,* 16**,** 179-90.
MULLER, C. & REMY, S. 2018. Septo-hippocampal interaction. *Cell Tissue Res,* 373**,** 565-575.

MÜLLER, C. & REMY, S. 2014. Dendritic inhibition mediated by O-LM and bistratified interneurons in the hippocampus. *Frontiers in synaptic neuroscience,* 6**,** 23-23.
MULLER, R. U. & KUBIE, J. L. 1987. The effects of changes in the environment on the spatial firing of hippocampal complex-spike cells. *J Neurosci,* 7**,** 1951-68.
MULLER, R. U., KUBIE, J. L. & RANCK, J. B., JR. 1987. Spatial firing patterns of hippocampal complex-spike cells in a fixed environment. *J Neurosci,* 7**,** 1935-50.
NAKASHIBA, T., BUHL, D. L., MCHUGH, T. J. & TONEGAWA, S. 2009. Hippocampal CA3 output is crucial for ripple-associated reactivation and consolidation of memory. *Neuron,* 62**,** 781-7.
NAKASHIBA, T., YOUNG, J. Z., MCHUGH, T. J., BUHL, D. L. & TONEGAWA, S. 2008. Transgenic inhibition of synaptic transmission reveals role of CA3 output in hippocampal learning. *Science,* 319**,** 1260-4.
NAZARI-SERENJEH, F., REZAYOF, A. & ZARRINDAST, M. R. 2011. Functional correlation between GABAergic and dopaminergic systems of dorsal hippocampus and ventral tegmental area in passive avoidance learning in rats. *Neuroscience,* 196**,** 104-14.
NEVES, G., COOKE, S. F. & BLISS, T. V. 2008. Synaptic plasticity, memory and the hippocampus: a neural network approach to causality. *Nat Rev Neurosci,* 9**,** 65-75.
NEWMAN, E. L., GILLET, S. N., CLIMER, J. R. & HASSELMO, M. E. 2013. Cholinergic blockade reduces theta-gamma phase amplitude coupling and speed modulation of theta frequency consistent with behavioral effects on encoding. *The Journal of neuroscience : the official journal of the Society for Neuroscience,* 33**,** 19635-19646.
NIEH, E. H., MATTHEWS, G. A., ALLSOP, S. A., PRESBREY, K. N., LEPPLA, C. A., WICHMANN, R., NEVE, R., WILDES, C. P. & TYE, K. M. 2015. Decoding neural circuits that control compulsive sucrose seeking. *Cell,* 160**,** 528-41.
NIEH, E. H., VANDER WEELE, C. M., MATTHEWS, G. A., PRESBREY, K. N., WICHMANN, R., LEPPLA, C. A., IZADMEHR, E. M. & TYE, K. M. 2016. Inhibitory Input from the Lateral Hypothalamus to the Ventral Tegmental Area Disinhibits Dopamine Neurons and Promotes Behavioral Activation. *Neuron,* 90**,** 1286-1298.
NUMAN, R. & QUARANTA, J. R. 1990. Effects of medial septal lesions on operant delayed alternation in rats. *Brain Research,* 531**,** 232-241.
O'KEEFE, J. 1976. Place units in the hippocampus of the freely moving rat. *Exp Neurol,* 51**,** 78-109.
O'KEEFE, J. 1979. A review of the hippocampal place cells. *Prog Neurobiol,* 13**,** 419-39.
O'KEEFE, J. & BURGESS, N. 1996. Geometric determinants of the place fields of hippocampal neurons. *Nature,* 381**,** 425-8.
O'KEEFE, J. & BURGESS, N. 2005. Dual phase and rate coding in hippocampal place cells: theoretical significance and relationship to entorhinal grid cells. *Hippocampus,* 15**,** 853-66.
O'KEEFE, J. & CONWAY, D. H. 1978. Hippocampal place units in the freely moving rat: why they fire where they fire. *Exp Brain Res,* 31**,** 573-90.
O'KEEFE, J. & DOSTROVSKY, J. 1971. The hippocampus as a spatial map. Preliminary evidence from unit activity in the freely-moving rat. *Brain Res,* 34**,** 171-5.
O'KEEFE, J. & NADEL, L. 1978. *The Hippocampus As a Cognitive Map*, Clarendon Press.
O'KEEFE, J. & RECCE, M. L. 1993. Phase relationship between hippocampal place units and the EEG theta rhythm. *Hippocampus,* 3**,** 317-30.
OADES, R. D. & HALLIDAY, G. M. 1987. Ventral tegmental (A10) system: neurobiology. 1. Anatomy and connectivity. *Brain Res,* 434**,** 117-65.

ODDIE, S. D. & BLAND, B. H. 1998. Hippocampal formation theta activity and movement selection. *Neurosci Biobehav Rev,* 22**,** 221-31.
OGNJANOVSKI, N., SCHAEFFER, S., WU, J., MOFAKHAM, S., MARUYAMA, D., ZOCHOWSKI, M. & ATON, S. J. 2017. Parvalbumin-expressing interneurons coordinate hippocampal network dynamics required for memory consolidation. *Nature communications,* 8**,** 15039-15039.
OH, S. W., HARRIS, J. A., NG, L., WINSLOW, B., CAIN, N., MIHALAS, S., WANG, Q., LAU, C., KUAN, L., HENRY, A. M., MORTRUD, M. T., OUELLETTE, B., NGUYEN, T. N., SORENSEN, S. A., SLAUGHTERBECK, C. R., WAKEMAN, W., LI, Y., FENG, D., HO, A., NICHOLAS, E., HIROKAWA, K. E., BOHN, P., JOINES, K. M., PENG, H., HAWRYLYCZ, M. J., PHILLIPS, J. W., HOHMANN, J. G., WOHNOUTKA, P., GERFEN, C. R., KOCH, C., BERNARD, A., DANG, C., JONES, A. R. & ZENG, H. 2014. A mesoscale connectome of the mouse brain. *Nature,* 508**,** 207-14.
OLDS, J. 1958a. Satiation effects in self-stimulation of the brain. *J Comp Physiol Psychol,* 51**,** 675-8.
OLDS, J. 1958b. Self-stimulation of the brain; its use to study local effects of hunger, sex, and drugs. *Science,* 127**,** 315-24.
OLDS, J. & MILNER, P. 1954. Positive reinforcement produced by electrical stimulation of septal area and other regions of rat brain. *J Comp Physiol Psychol,* 47**,** 419-27.
PATEL, J., FUJISAWA, S., BERÉNYI, A., ROYER, S. & BUZSÁKI, G. 2012. Traveling theta waves along the entire septotemporal axis of the hippocampus. *Neuron,* 75**,** 410-417.
PAXINOS, G. & CHARLES, W. 2007. *The Rat Brain in Stereotaxic Coordinates*, London: Academic Press.
PELKEY, K. A., CHITTAJALLU, R., CRAIG, M. T., TRICOIRE, L., WESTER, J. C. & MCBAIN, C. J. 2017. Hippocampal GABAergic Inhibitory Interneurons. *Physiol Rev,* 97**,** 1619-1747.
PESSOA, L. 2008. On the relationship between emotion and cognition. *Nat Rev Neurosci,* 9**,** 148-58.
PESSOA, L. & ENGELMANN, J. B. 2010. Embedding reward signals into perception and cognition. *Front Neurosci,* 4.
PETSCHE, H. & STUMPF, C. 1962. [The origin of theta-rhytm in the rabbit hippocampus]. *Wien Klin Wochenschr,* 74**,** 696-700.
PETSCHE, H., STUMPF, C. & GOGOLAK, G. 1962. [The significance of the rabbit's septum as a relay station between the midbrain and the hippocampus. I. The control of hippocampus arousal activity by the septum cells]. *Electroencephalogr Clin Neurophysiol,* 14**,** 202-11.
PRESTON, A. R. & EICHENBAUM, H. 2013. Interplay of hippocampus and prefrontal cortex in memory. *Curr Biol,* 23**,** R764-73.
QUIRK, G. J., MULLER, R. U. & KUBIE, J. L. 1990. The firing of hippocampal place cells in the dark depends on the rat's recent experience. *J Neurosci,* 10**,** 2008-17.
RAISMAN, G. 1966. The connexions of the septum. *Brain,* 89**,** 317-48.
RAMCHARAN, E. J., GNADT, J. W. & SHERMAN, S. M. 2005. Higher-order thalamic relays burst more than first-order relays. *Proc Natl Acad Sci U S A,* 102**,** 12236-41.
RANCK, J. B., JR. 1973. Studies on single neurons in dorsal hippocampal formation and septum in unrestrained rats. I. Behavioral correlates and firing repertoires. *Exp Neurol,* 41**,** 461-531.
RAWLINS, J. N. & OLTON, D. S. 1982. The septo-hippocampal system and cognitive mapping. *Behav Brain Res,* 5**,** 331-58.

REIS, D. G., SCOPINHO, A. A., GUIMARAES, F. S., CORREA, F. M. & RESSTEL, L. B. 2010. Involvement of the lateral septal area in the expression of fear conditioning to context. *Learn Mem,* 17**,** 134-8.
RISOLD, P. Y. & SWANSON, L. W. 1996. Structural evidence for functional domains in the rat hippocampus. *Science,* 272**,** 1484-6.
RISOLD, P. Y. & SWANSON, L. W. 1997a. Chemoarchitecture of the rat lateral septal nucleus. *Brain Res Brain Res Rev,* 24**,** 91-113.
RISOLD, P. Y. & SWANSON, L. W. 1997b. Connections of the rat lateral septal complex. *Brain Res Brain Res Rev,* 24**,** 115-95.
ROBERTSON, R. G., ROLLS, E. T., GEORGES-FRANCOIS, P. & PANZERI, S. 1999. Head direction cells in the primate pre-subiculum. *Hippocampus,* 9**,** 206-19.
ROBINSON, J., MANSEAU, F., DUCHARME, G., AMILHON, B., VIGNEAULT, E., EL MESTIKAWY, S. & WILLIAMS, S. 2016. Optogenetic Activation of Septal Glutamatergic Neurons Drive Hippocampal Theta Rhythms. *J Neurosci,* 36**,** 3016-23.
ROYER, S., SIROTA, A., PATEL, J. & BUZSAKI, G. 2010. Distinct representations and theta dynamics in dorsal and ventral hippocampus. *J Neurosci,* 30**,** 1777-87.
ROYER, S., ZEMELMAN, B. V., LOSONCZY, A., KIM, J., CHANCE, F., MAGEE, J. C. & BUZSAKI, G. 2012. Control of timing, rate and bursts of hippocampal place cells by dendritic and somatic inhibition. *Nat Neurosci,* 15**,** 769-75.
SAINSBURY, R. S. & BLAND, B. H. 1981. The effects of selective septal lesions on theta production in CA1 and the dentate gyrus of the hippocampus. *Physiol Behav,* 26**,** 1097-101.
SAREL, A., FINKELSTEIN, A., LAS, L. & ULANOVSKY, N. 2017. Vectorial representation of spatial goals in the hippocampus of bats. *Science,* 355**,** 176-180.
SARGOLINI, F., FYHN, M., HAFTING, T., MCNAUGHTON, B. L., WITTER, M. P., MOSER, M. B. & MOSER, E. I. 2006. Conjunctive representation of position, direction, and velocity in entorhinal cortex. *Science,* 312**,** 758-62.
SAVE, E., NERAD, L. & POUCET, B. 2000. Contribution of multiple sensory information to place field stability in hippocampal place cells. *Hippocampus,* 10**,** 64-76.
SCHMITZ, T. W., MUR, M., AGHOURIAN, M., BEDARD, M. A., SPRENG, R. N. & ALZHEIMER'S DISEASE NEUROIMAGING, I. 2018. Longitudinal Alzheimer's Degeneration Reflects the Spatial Topography of Cholinergic Basal Forebrain Projections. *Cell Rep,* 24**,** 38-46.
SCHOENENBERGER, P., O'NEILL, J. & CSICSVARI, J. 2016. Activity-dependent plasticity of hippocampal place maps. *Nature Communications,* 7**,** 11824.
SCHULTZ, W. 1998. Predictive reward signal of dopamine neurons. *J Neurophysiol,* 80**,** 1-27.
SCHULTZ, W., DAYAN, P. & MONTAGUE, P. R. 1997. A neural substrate of prediction and reward. *Science,* 275**,** 1593-9.
SCOVILLE, W. B. & MILNER, B. 1957. Loss of recent memory after bilateral hippocampal lesions. *J Neurol Neurosurg Psychiatry,* 20**,** 11-21.
SHARPE, M. J., MARCHANT, N. J., WHITAKER, L. R., RICHIE, C. T., ZHANG, Y. J., CAMPBELL, E. J., KOIVULA, P. P., NECARSULMER, J. C., MEJIAS-APONTE, C., MORALES, M., PICKEL, J., SMITH, J. C., NIV, Y., SHAHAM, Y., HARVEY, B. K. & SCHOENBAUM, G. 2017. Lateral Hypothalamic GABAergic Neurons Encode Reward Predictions that Are Relayed to the Ventral Tegmental Area to Regulate Learning. *Curr Biol,* 27**,** 2089-2100 e5.
SHEEHAN, T. P., CHAMBERS, R. A. & RUSSELL, D. S. 2004. Regulation of affect by the lateral septum: implications for neuropsychiatry. *Brain Res Brain Res Rev,* 46**,** 71-117.

SHEN, J., BARNES, C. A., WENK, G. L. & MCNAUGHTON, B. L. 1996. Differential effects of selective immunotoxic lesions of medial septal cholinergic cells on spatial working and reference memory. *Behav Neurosci,* 110**,** 1181-6.
SIMON, A. P., POINDESSOUS-JAZAT, F., DUTAR, P., EPELBAUM, J. & BASSANT, M. H. 2006. Firing properties of anatomically identified neurons in the medial septum of anesthetized and unanesthetized restrained rats. *J Neurosci,* 26**,** 9038-46.
SINGEWALD, G. M., RJABOKON, A., SINGEWALD, N. & EBNER, K. 2011. The modulatory role of the lateral septum on neuroendocrine and behavioral stress responses. *Neuropsychopharmacology,* 36**,** 793-804.
SKAGGS, W. E., MCNAUGHTON, B. & GOTHARD, K. 1993. An Information-Theoretic Approach to Deciphering the Hippocampal Code. *Advances in neural information processing systems,* 5**,** 1030-1037.
SKAGGS, W. E. & MCNAUGHTON, B. L. 1998. Spatial firing properties of hippocampal CA1 populations in an environment containing two visually identical regions. *J Neurosci,* 18**,** 8455-66.
SKAGGS, W. E., MCNAUGHTON, B. L., WILSON, M. A. & BARNES, C. A. 1996. Theta phase precession in hippocampal neuronal populations and the compression of temporal sequences. *Hippocampus,* 6**,** 149-172.
SLUKA, C. M., STANKO, K., CAMPBELL, A., CACERES, J., PANOZ-BROWN, D., WHEELER, A., BRADLEY, J. & ALLEN, C. 2018. Incidental spatial memory in the domestic dog (Canis familiaris). *Learn Behav*.
SMITH, D. M. & MIZUMORI, S. J. 2006a. Hippocampal place cells, context, and episodic memory. *Hippocampus,* 16**,** 716-29.
SMITH, D. M. & MIZUMORI, S. J. 2006b. Learning-related development of context-specific neuronal responses to places and events: the hippocampal role in context processing. *J Neurosci,* 26**,** 3154-63.
SOLSTAD, T., BOCCARA, C. N., KROPFF, E., MOSER, M. B. & MOSER, E. I. 2008. Representation of geometric borders in the entorhinal cortex. *Science,* 322**,** 1865-8.
SOTTY, F., DANIK, M., MANSEAU, F., LAPLANTE, F., QUIRION, R. & WILLIAMS, S. 2003. Distinct electrophysiological properties of glutamatergic, cholinergic and GABAergic rat septohippocampal neurons: novel implications for hippocampal rhythmicity. *The Journal of physiology,* 551**,** 927-943.
SPEED, H. E. & DOBRUNZ, L. E. 2009. Developmental changes in short-term facilitation are opposite at temporoammonic synapses compared to Schaffer collateral synapses onto CA1 pyramidal cells. *Hippocampus,* 19**,** 187-204.
SPRUSTON, N. 2008. Pyramidal neurons: dendritic structure and synaptic integration. *Nat Rev Neurosci,* 9**,** 206-21.
SQUIRE, L. R. 1986. Mechanisms of memory. *Science,* 232**,** 1612-9.
SQUIRE, L. R. & ZOLA, S. M. 1998. Episodic memory, semantic memory, and amnesia. *Hippocampus,* 8**,** 205-11.
STACKMAN, R. W. & TAUBE, J. S. 1998. Firing properties of rat lateral mammillary single units: head direction, head pitch, and angular head velocity. *J Neurosci,* 18**,** 9020-37.
STAIB, J. M., DELLA VALLE, R. & KNOX, D. K. 2018. Disruption of medial septum and diagonal bands of Broca cholinergic projections to the ventral hippocampus disrupt auditory fear memory. *Neurobiology of Learning and Memory,* 152**,** 71-79.
STAIGER, J. F. & NURNBERGER, F. 1991. The efferent connections of the lateral septal nucleus in the guinea pig: projections to the diencephalon and brainstem. *Cell Tissue Res,* 264**,** 391-413.
STAMATAKIS, A. M. & STUBER, G. D. 2012a. Activation of lateral habenula inputs to the ventral midbrain promotes behavioral avoidance. *Nat Neurosci,* 15**,** 1105-7.

STAMATAKIS, A. M. & STUBER, G. D. 2012b. Optogenetic strategies to dissect the neural circuits that underlie reward and addiction. *Cold Spring Harb Perspect Med,* 2.
STENT, G. S. 1973. A physiological mechanism for Hebb's postulate of learning. *Proc Natl Acad Sci U S A,* 70**,** 997-1001.
STEWARD, O. 1976. Topographic organization of the projections from the entorhinal area to the hippocampal formation of the rat. *J Comp Neurol,* 167**,** 285-314.
STEWARD, O. & SCOVILLE, S. A. 1976. Retrograde labeling of central nervous pathways with tritiated or Evans blue-labeled bovine serum albumin. *Neurosci Lett,* 3**,** 191-6.
STEWART, M. & FOX, S. E. 1989a. Firing relations of medial septal neurons to the hippocampal theta rhythm in urethane anesthetized rats. *Exp Brain Res,* 77**,** 507-16.
STEWART, M. & FOX, S. E. 1989b. Two populations of rhythmically bursting neurons in rat medial septum are revealed by atropine. *J Neurophysiol,* 61**,** 982-93.
STEWART, M. & FOX, S. E. 1990. Do septal neurons pace the hippocampal theta rhythm? *Trends Neurosci,* 13**,** 163-8.
STUBER, G. D. & WISE, R. A. 2016. Lateral hypothalamic circuits for feeding and reward. *Nat Neurosci,* 19**,** 198-205.
SUN, Y., NGUYEN, A. Q., NGUYEN, J. P., LE, L., SAUR, D., CHOI, J., CALLAWAY, E. M. & XU, X. 2014. Cell-type-specific circuit connectivity of hippocampal CA1 revealed through Cre-dependent rabies tracing. *Cell Rep,* 7**,** 269-80.
SWANSON, L. W. & COWAN, W. M. 1977. An autoradiographic study of the organization of the efferent connections of the hippocampal formation in the rat. *J Comp Neurol,* 172**,** 49-84.
SWANSON, L. W. & COWAN, W. M. 1979. The connections of the septal region in the rat. *J Comp Neurol,* 186**,** 621-55.
SWEATT, J. D. 2001. Memory mechanisms: the yin and yang of protein phosphorylation. *Curr Biol,* 11**,** R391-4.
SWEENEY, P., LI, C. & YANG, Y. 2017. Appetite suppressive role of medial septal glutamatergic neurons. *Proceedings of the National Academy of Sciences of the United States of America,* 114**,** 13816-13821.
SWEENEY, P. & YANG, Y. 2016. An Inhibitory Septum to Lateral Hypothalamus Circuit That Suppresses Feeding. *J Neurosci,* 36**,** 11185-11195.
SZABO, B., SIEMES, S. & WALLMICHRATH, I. 2002. Inhibition of GABAergic neurotransmission in the ventral tegmental area by cannabinoids. *Eur J Neurosci,* 15**,** 2057-61.
TAKACS, V. T., FREUND, T. F. & GULYAS, A. I. 2008. Types and synaptic connections of hippocampal inhibitory neurons reciprocally connected with the medial septum. *Eur J Neurosci,* 28**,** 148-64.
TAKAMURA, Y., TAMURA, R., ZHOU, T. L., KOBAYASHI, T., TRAN, A. H., EIFUKU, S. & ONO, T. 2006. Spatial firing properties of lateral septal neurons. *Hippocampus,* 16**,** 635-44.
TAN, K. R., YVON, C., TURIAULT, M., MIRZABEKOV, J. J., DOEHNER, J., LABOUEBE, G., DEISSEROTH, K., TYE, K. M. & LUSCHER, C. 2012. GABA neurons of the VTA drive conditioned place aversion. *Neuron,* 73**,** 1173-83.
TAUBE, J. S. 1995. Head direction cells recorded in the anterior thalamic nuclei of freely moving rats. *J Neurosci,* 15**,** 70-86.
TAUBE, J. S., MULLER, R. U. & RANCK, J. B., JR. 1990. Head-direction cells recorded from the postsubiculum in freely moving rats. II. Effects of environmental manipulations. *J Neurosci,* 10**,** 436-47.
TEMPLER, V. L. & HAMPTON, R. R. 2013. Episodic memory in nonhuman animals. *Curr Biol,* 23**,** R801-6.
TOBLER, P. N., FIORILLO, C. D. & SCHULTZ, W. 2005. Adaptive coding of reward value by dopamine neurons. *Science,* 307**,** 1642-5.

TOLLIN, D. J. & YIN, T. C. T. 2002. The Coding of Spatial Location by Single Units in the Lateral Superior Olive of the Cat. I. Spatial Receptive Fields in Azimuth. *The Journal of Neuroscience,* 22**,** 1454-1467.
TOLMAN, E. C. 1948. Cognitive maps in rats and men. *Psychol Rev,* 55**,** 189-208.
TOTH, K., BORHEGYI, Z. & FREUND, T. 1993. Postsynaptic targets of GABAergic hippocampal neurons in the medial septum-diagonal band of broca complex. *The Journal of Neuroscience,* 13**,** 3712-3724.
TÓTH, K. & FREUND, T. F. 1992. Calbindin D28k-containing nonpyramidal cells in the rat hippocampus: Their immunoreactivity for GABA and projection to the medial septum. *Neuroscience,* 49**,** 793-805.
TOTH, K., FREUND, T. F. & MILES, R. 1997. Disinhibition of rat hippocampal pyramidal cells by GABAergic afferents from the septum. *J Physiol,* 500 (Pt 2)**,** 463-74.
TOTTERDELL, S. & HAYES, L. 1987. Non-pyramidal hippocampal projection neurons: a light and electron microscopic study. *J Neurocytol,* 16**,** 477-85.
TREMBLAY, R., LEE, S. & RUDY, B. 2016. GABAergic Interneurons in the Neocortex: From Cellular Properties to Circuits. *Neuron,* 91**,** 260-292.
TSAI, H. C., ZHANG, F., ADAMANTIDIS, A., STUBER, G. D., BONCI, A., DE LECEA, L. & DEISSEROTH, K. 2009. Phasic firing in dopaminergic neurons is sufficient for behavioral conditioning. *Science,* 324**,** 1080-4.
TSANOV, M. 2017. Speed and Oscillations: Medial Septum Integration of Attention and Navigation. *Frontiers in systems neuroscience,* 11**,** 67-67.
TSANOV, M., CHAH, E., REILLY, R. & O'MARA, S. M. 2014. Respiratory cycle entrainment of septal neurons mediates the fast coupling of sniffing rate and hippocampal theta rhythm. *Eur J Neurosci,* 39**,** 957-74.
TSANOV, M., CHAH, E., VANN, S. D., REILLY, R. B., ERICHSEN, J. T., AGGLETON, J. P. & O'MARA, S. M. 2011. Theta-modulated head direction cells in the rat anterior thalamus. *The Journal of neuroscience : the official journal of the Society for Neuroscience,* 31**,** 9489-9502.
TULVING, E. 2002. Episodic memory: from mind to brain. *Annu Rev Psychol,* 53**,** 1-25.
UNAL, G., JOSHI, A., VINEY, T. J., KIS, V. & SOMOGYI, P. 2015. Synaptic Targets of Medial Septal Projections in the Hippocampus and Extrahippocampal Cortices of the Mouse. *J Neurosci,* 35**,** 15812-26.
UNGLESS, M. A., MAGILL, P. J. & BOLAM, J. P. 2004. Uniform inhibition of dopamine neurons in the ventral tegmental area by aversive stimuli. *Science,* 303**,** 2040-2.
VALENSTEIN, E. S., COX, V. C. & KAKOLEWSKI, J. W. 1970. Reexamination of the role of the hypothalamus in motivation. *Psychol Rev,* 77**,** 16-31.
VAN DER MEER, M. A. & REDISH, A. D. 2010. Expectancies in decision making, reinforcement learning, and ventral striatum. *Front Neurosci,* 4**,** 6.
VANDECASTEELE, M., VARGA, V., BERENYI, A., PAPP, E., BARTHO, P., VENANCE, L., FREUND, T. F. & BUZSAKI, G. 2014. Optogenetic activation of septal cholinergic neurons suppresses sharp wave ripples and enhances theta oscillations in the hippocampus. *Proc Natl Acad Sci U S A,* 111**,** 13535-40.
VANDERWOLF, C. H. 1969. Hippocampal electrical activity and voluntary movement in the rat. *Electroencephalogr Clin Neurophysiol,* 26**,** 407-18.
VARGA, V., HANGYA, B., KRANITZ, K., LUDANYI, A., ZEMANKOVICS, R., KATONA, I., SHIGEMOTO, R., FREUND, T. F. & BORHEGYI, Z. 2008. The presence of pacemaker HCN channels identifies theta rhythmic GABAergic neurons in the medial septum. *J Physiol,* 586**,** 3893-915.
VEGA-FLORES, G., RUBIO, S. E., JURADO-PARRAS, M. T., GÓMEZ-CLIMENT, M. Á., HAMPE, C. S., MANTO, M., SORIANO, E., PASCUAL, M., GRUART, A. & DELGADO-GARCÍA, J. M. 2014. The GABAergic septohippocampal pathway is directly involved in internal processes related to operant reward learning. *Cerebral cortex (New York, N.Y. : 1991),* 24**,** 2093-2107.

VERTES, R. P. 1992. PHA-L analysis of projections from the supramammillary nucleus in the rat. *J Comp Neurol,* 326**,** 595-622.
WANG, X. J. 2002. Pacemaker neurons for the theta rhythm and their synchronization in the septohippocampal reciprocal loop. *J Neurophysiol,* 87**,** 889-900.
WATANABE, M. & SAKAGAMI, M. 2007. Integration of cognitive and motivational context information in the primate prefrontal cortex. *Cereb Cortex,* 17 Suppl 1**,** i101-9.
WHITEHOUSE, P. J., PRICE, D. L., STRUBLE, R. G., CLARK, A. W., COYLE, J. T. & DELON, M. R. 1982. Alzheimer's disease and senile dementia: loss of neurons in the basal forebrain. *Science,* 215**,** 1237-9.
WHITTINGTON, M. A., TRAUB, R. D. & JEFFERYS, J. G. 1995. Synchronized oscillations in interneuron networks driven by metabotropic glutamate receptor activation. *Nature,* 373**,** 612-5.
WIESEL, T. N. & HUBEL, D. H. 1965. Comparison of the effects of unilateral and bilateral eye closure on cortical unit responses in kittens. *J Neurophysiol,* 28**,** 1029-40.
WILSON, I. A., IKONEN, S., GALLAGHER, M., EICHENBAUM, H. & TANILA, H. 2005. Age-Associated Alterations of Hippocampal Place Cells Are Subregion Specific. *The Journal of Neuroscience,* 25**,** 6877-6886.
WILSON, M. A. & MCNAUGHTON, B. L. 1993. Dynamics of the hippocampal ensemble code for space. *Science,* 261**,** 1055-8.
WISE, R. A. 2004. Dopamine and food reward: back to the elements. *Am J Physiol Regul Integr Comp Physiol,* 286**,** R13.
WITTEN, I. B., STEINBERG, E. E., LEE, S. Y., DAVIDSON, T. J., ZALOCUSKY, K. A., BRODSKY, M., YIZHAR, O., CHO, S. L., GONG, S., RAMAKRISHNAN, C., STUBER, G. D., TYE, K. M., JANAK, P. H. & DEISSEROTH, K. 2011. Recombinase-driver rat lines: tools, techniques, and optogenetic application to dopamine-mediated reinforcement. *Neuron,* 72**,** 721-33.
WITTER, M. P. & AMARAL, D. G. 1991. Entorhinal cortex of the monkey: V. Projections to the dentate gyrus, hippocampus, and subicular complex. *J Comp Neurol,* 307**,** 437-59.
WITTER, M. P., GRIFFIOEN, A. W., JORRITSMA-BYHAM, B. & KRIJNEN, J. L. 1988. Entorhinal projections to the hippocampal CA1 region in the rat: an underestimated pathway. *Neurosci Lett,* 85**,** 193-8.
WITTER, M. P., NABER, P. A., VAN HAEFTEN, T., MACHIELSEN, W. C., ROMBOUTS, S. A., BARKHOF, F., SCHELTENS, P. & LOPES DA SILVA, F. H. 2000. Cortico-hippocampal communication by way of parallel parahippocampal-subicular pathways. *Hippocampus,* 10**,** 398-410.
WOOD, E. R., DUDCHENKO, P. A. & EICHENBAUM, H. 1999. The global record of memory in hippocampal neuronal activity. *Nature,* 397**,** 613-6.
WOOLF, N. J. 1996. Global and serial neurons form A hierarchically arranged interface proposed to underlie memory and cognition. *Neuroscience,* 74**,** 625-51.
WOZNY, C. & WILLIAMS, S. R. 2011. Specificity of synaptic connectivity between layer 1 inhibitory interneurons and layer 2/3 pyramidal neurons in the rat neocortex. *Cerebral cortex (New York, N.Y. : 1991),* 21**,** 1818-1826.
YAMANO, M. & LUITEN, P. G. M. 1989. Direct synaptic contacts of medial septal efferents with somatostatin immunoreactive neurons in the rat hippocampus. *Brain Research Bulletin,* 22**,** 993-1001.
YODER, R. M. & PANG, K. C. 2005. Involvement of GABAergic and cholinergic medial septal neurons in hippocampal theta rhythm. *Hippocampus,* 15**,** 381-92.
YODER, R. M. & TAUBE, J. S. 2009. Head direction cell activity in mice: robust directional signal depends on intact otolith organs. *J Neurosci,* 29**,** 1061-76.
YOGANARASIMHA, D., RAO, G. & KNIERIM, J. J. 2011. Lateral entorhinal neurons are not spatially selective in cue-rich environments. *Hippocampus,* 21**,** 1363-74.

ZELDENRUST, F., WADMAN, W. J. & ENGLITZ, B. 2018. Neural Coding With Bursts-Current State and Future Perspectives. *Frontiers in computational neuroscience,* 12**,** 48-48.
ZHANG, H., LIN, S. C. & NICOLELIS, M. A. 2010. Spatiotemporal coupling between hippocampal acetylcholine release and theta oscillations in vivo. *J Neurosci,* 30**,** 13431-40.
ZHAO, C., EISINGER, B. E., DRIESSEN, T. M. & GAMMIE, S. C. 2014. Addiction and reward-related genes show altered expression in the postpartum nucleus accumbens. *Frontiers in behavioral neuroscience,* 8**,** 388-388.
ZHOU, T. L., TAMURA, R., KURIWAKI, J. & ONO, T. 1999. Comparison of medial and lateral septal neuron activity during performance of spatial tasks in rats. *Hippocampus,* 9**,** 220-34.
ZUGARO, M. B., ARLEO, A., BERTHOZ, A. & WIENER, S. I. 2003. Rapid spatial reorientation and head direction cells. *J Neurosci,* 23**,** 3478-82.
ZUTSHI, I., BRANDON, M. P., FU, M. L., DONEGAN, M. L., LEUTGEB, J. K. & LEUTGEB, S. 2018. Hippocampal Neural Circuits Respond to Optogenetic Pacing of Theta Frequencies by Generating Accelerated Oscillation Frequencies. *Curr Biol,* 28**,** 1179-1188 e3.